THE UNIVERSITY OF CALGARY

HEAT AND MASS TRANSFER WITHIN GRANULAR BEDS

by

EMAD BOSHRA FAWZY KHALIL

A THESIS

SUBMITTED TO THE FACULTY OF GRADUATE STUDIES

IN PARTIAL FULFILLMENT OF THE REQUIREMENTS FOR THE

DEGREE OF MASTER OF SCIENCE

DEPARTMENT OF MECHANICAL ENGINEERING

CALGARY, ALBERTA

MARCH, 1993

Canada

◄ Name __EMAD BOSHRA FAWZY KHALIL__

Dissertation Abstracts International is arranged by broad, general subject categories. Please select the one subject which most nearly describes the content of your dissertation. Enter the corresponding four-digit code in the spaces provided.

__MECHANICAL ENGINEERING__ · | 0 | 5 | 4 | 8 | **U·M·I**

SUBJECT TERM   SUBJECT CODE

Subject Categories

THE HUMANITIES AND SOCIAL SCIENCES

COMMUNICATIONS AND THE ARTS
Architecture 0729
Art History 0377
Cinema 0900
Dance 0378
Fine Arts 0357
Information Science 0723
Journalism 0391
Library Science 0399
Mass Communications 0708
Music 0413
Speech Communication 0459
Theater 0465

EDUCATION
General 0515
Administration 0514
Adult and Continuing 0516
Agricultural 0517
Art 0273
Bilingual and Multicultural 0282
Business 0688
Community College 0275
Curriculum and Instruction 0727
Early Childhood 0518
Elementary 0524
Finance 0277
Guidance and Counseling 0519
Health 0680
Higher 0745
History of 0520
Home Economics 0278
Industrial 0521
Language and Literature 0279
Mathematics 0280
Music 0522
Philosophy of 0998
Physical 0523

Psychology 0525
Reading 0535
Religious 0527
Sciences 0714
Secondary 0533
Social Sciences .... 0534·
Sociology of 0340
Special 0529
Teacher Training 0530
Technology 0710
Tests and Measurements 0288
Vocational 0747

LANGUAGE, LITERATURE AND LINGUISTICS
Language
  General 0679
  Ancient 0289
  Linguistics 0290
  Modern 0291
Literature·
  General 0401
  Classical 0294
  Comparative 0295
  Medieval 0297
  Modern 0298
  African 0316
  American 0591
  Asian 0305
  Canadian (English) 0352
  Canadian (French) 0355
  English 0593
  Germanic 0311
  Latin American 0312
  Middle Eastern 0315
  Romance 0313
  Slavic and East European 0314

PHILOSOPHY, RELIGION AND THEOLOGY
Philosophy 0422
Religion
  General 0318
  Biblical Studies 0321
  Clergy 0319
  History of 0320
  Philosophy of 0322
Theology 0469

SOCIAL SCIENCES
American Studies 0323
Anthropology
  Archaeology 0324
  Cultural 0326
  Physical 0327
Business Administration
  General 0310
  Accounting 0272
  Banking 0770
  Management 0454
  Marketing 0338
Canadian Studies 0385
Economics
  General 0501
  Agricultural 0503
  Commerce-Business 0505
  Finance 0508
  History 0509
  Labor 0510
  Theory 0511
Folklore 0358
Geography 0366
Gerontology 0351
History
  General 0578

Ancient 0579
Medieval 0581
Modern 0582
Black 0328
African 0331
Asia, Australia and Oceania 0332
Canadian 0334
European 0335
Latin American 0336
Middle Eastern 0333
United States 0337
History of Science 0585
Law 0398
Political Science
  General 0615
  International Law and
    Relations 0616
  Public Administration 0617
Recreation 0814
Social Work 0452
Sociology
  General 0626
  Criminology and Penology ... 0627
  Demography 0938
  Ethnic and Racial Studies 0631
  Individual and Family
    Studies 0628
  Industrial and Labor
    Relations 0629
  Public and Social Welfare 0630
  Social Structure and
    Development 0700
  Theory and Methods 0344
Transportation 0709
Urban and Regional Planning 0999
Women's Studies 0453

THE SCIENCES AND ENGINEERING

BIOLOGICAL SCIENCES
Agriculture
  General 0473
  Agronomy 0285
  Animal Culture and
    Nutrition 0475
  Animal Pathology 0476
  Food Science and
    Technology 0359
  Forestry and Wildlife 0478
  Plant Culture 0479
  Plant Pathology 0480
  Plant Physiology 0817
  Range Management 0777
  Wood Technology 0746
Biology
  General 0306
  Anatomy 0287
  Biostatistics 0308
  Botany 0309
  Cell 0379
  Ecology 0329
  Entomology 0353
  Genetics 0369
  Limnology 0793
  Microbiology 0410
  Molecular 0307
  Neuroscience 0317
  Oceanography 0416
  Physiology 0433
  Radiation 0821
  Veterinary Science 0778
  Zoology 0472
Biophysics
  General 0786
  Medical 0760

EARTH SCIENCES
Biogeochemistry 0425
Geochemistry 0996

Geodesy 0370
Geology 0372
Geophysics 0373
Hydrology 0388
Mineralogy 0411
Paleobotany 0345
Paleoecology 0426
Paleontology 0418
Paleozoology 0985
Palynology 0427
Physical Geography 0368
Physical Oceanography 0415

HEALTH AND ENVIRONMENTAL SCIENCES
Environmental Sciences 0768
Health Sciences
  General 0566
  Audiology 0300
  Chemotherapy 0992
  Dentistry 0567
  Education 0350
  Hospital Management 0769
  Human Development 0758
  Immunology 0982
  Medicine and Surgery 0564
  Mental Health 0347
  Nursing 0569
  Nutrition 0570
  Obstetrics and Gynecology .. 0380
  Occupational Health and
    Therapy 0354
  Ophthalmology 0381
  Pathology 0571
  Pharmacology 0419
  Pharmacy 0572
  Physical Therapy 0382
  Public Health 0573
  Radiology 0574
  Recreation 0575

Speech Pathology 0460
Toxicology 0383
Home Economics 0386

PHYSICAL SCIENCES
Pure Sciences
Chemistry
  General 0485
  Agricultural 0749
  Analytical 0486
  Biochemistry 0487
  Inorganic 0488
  Nuclear 0738
  Organic 0490
  Pharmaceutical 0491
  Physical 0494
  Polymer 0495
  Radiation 0754
Mathematics 0405
Physics
  General 0605
  Acoustics 0986
  Astronomy and
    Astrophysics 0606
  Atmospheric Science 0608
  Atomic 0748
  Electronics and Electricity 0607
  Elementary Particles and
    High Energy 0798
  Fluid and Plasma 0759
  Molecular 0609
  Nuclear 0610
  Optics 0752
  Radiation 0756
  Solid State 0611
Statistics 0463

Applied Sciences
Applied Mechanics 0346
Computer Science 0984

Engineering
  General 0537
  Aerospace 0538
  Agricultural 0539
  Automotive 0540
  Biomedical 0541
  Chemical 0542
  Civil 0543
  Electronics and Electrical 0544
  Heat and Thermodynamics.... 0348
  Hydraulic 0545
  Industrial 0546
  Marine 0547
  Materials Science 0794
  Mechanical 0548
  Metallurgy 0743
  Mining 0551
  Nuclear 0552
  Packaging 0549
  Petroleum 0765
  Sanitary and Municipal 0554
  System Science 0790
Geotechnology 0428
Operations Research 0796
Plastics Technology 0795
Textile Technology 0994

PSYCHOLOGY
General 0621
Behavioral 0384
Clinical 0622
Developmental 0620
Experimental 0623
Industrial 0624
Personality 0625
Physiological 0989
Psychobiology 0349
Psychometrics 0632
Social 0451

⊕

Nom _____

Dissertation Abstracts International est organisé en catégories de sujets. Veuillez s.v.p. choisir le sujet qui décrit le mieux votre thèse et inscrivez le code numérique approprié dans l'espace réservé ci-dessous.

SUJET

☐☐☐☐ U·M·I
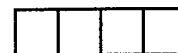
CODE DE SUJET

Catégories par sujets

HUMANITÉS ET SCIENCES SOCIALES

COMMUNICATIONS ET LES ARTS
Architecture 0729
Beaux-arts 0357
Bibliothéconomie 0399
Cinéma 0900
Communication verbale 0459
Communications 0708
Danse 0378
Histoire de l'art 0377
Journalisme 0391
Musique 0413
Sciences de l'information 0723
Théâtre 0465

ÉDUCATION
Généralités 515
Administration 0514
Art 0273
Collèges communautaires 0275
Commerce 0688
Économie domestique 0278
Éducation permanente 0516
Éducation préscolaire 0518
Éducation sanitaire 0680
Enseignement agricole 0517
Enseignement bilingue et
  multiculturel 0282
Enseignement industriel 0521
Enseignement primaire. 0524
Enseignement professionnel 0747
Enseignement religieux 0527
Enseignement secondaire 0533
Enseignement spécial 0529
Enseignement supérieur 0745
Évaluation 0288
Finances 0277
Formation des enseignants 0530
Histoire de l'éducation 0520
Langues et littérature 0279

Lecture 0535
Mathématiques 0280
Musique 0522
Orientation et consultation 0519
Philosophie de l'éducation 0998
Physique 0523
Programmes d'études et
  enseignement 0727
Psychologie 0525
Sciences 0714
Sciences sociales 0534
Sociologie de l'éducation 0340
Technologie 0710

LANGUE, LITTÉRATURE ET LINGUISTIQUE
Langues
  Généralités 0679
  Anciennes 0289
  Linguistique 0290
  Modernes 0291
Littérature
  Généralités 0401
  Anciennes 0294
  Comparée 0295
  Médiévale 0297
  Moderne 0298
  Africaine 0316
  Américaine 0591
  Anglaise 0593
  Asiatique 0305
  Canadienne (Anglaise) 0352
  Canadienne (Française) 0355
  Germanique 0311
  Latino-américaine 0312
  Moyen-orientale 0315
  Romane 0313
  Slave et est-européenne 0314

PHILOSOPHIE, RELIGION ET THÉOLOGIE
Philosophie 0422
Religion
  Généralités 0318
  Clergé 0319
  Études bibliques 0321
  Histoire des religions 0320
  Philosophie de la religion 0322
Théologie 0469

SCIENCES SOCIALES
Anthropologie
  Archéologie 0324
  Culturelle 0326
  Physique 0327
Droit 0398
Économie
  Généralités 0501
  Commerce-Affaires 0505
  Économie agricole 0503
  Économie du travail 0510
  Finances 0508
  Histoire 0509
  Théorie 0511
Études américaines 0323
Études canadiennes 0385
Études féministes 0453
Folklore 0358
Géographie 0366
Gérontologie 0351
Gestion des affaires
  Généralités 0310
  Administration 0454
  Banques 0770
  Comptabilité 0272
  Marketing 0338
Histoire
  Histoire générale 0578

Ancienne 0579
Médiévale 0581
Moderne 0582
Histoire des noirs 0328
Africaine 0331
Canadienne 0334
États-Unis 0337
Européenne 0335
Moyen-orientale 0333
Latino-américaine 0336
Asie, Australie et Océanie 0332
Histoire des sciences 0585
Loisirs 0814
Planification urbaine et
  régionale 0999
Science politique
  Généralités 0615
  Administration publique 0617
  Droit et relations
    internationales 0616
Sociologie
  Généralités 0626
  Aide et bien-être social 0630
  Criminologie et
    établissements
    pénitentiaires 0627
  Démographie 0938
  Études de l'individu et
    de la famille 0628
  Études des relations
    interethniques et
    des relations raciales 0631
  Structure et développement
    social 0700
  Théorie et méthodes. 0344
  Travail et relations
    industrielles 0629
Transports 0709
Travail social 0452

SCIENCES ET INGÉNIERIE

SCIENCES BIOLOGIQUES
Agriculture
  Généralités 0473
  Agronomie. 0285
  Alimentation et technologie
    alimentaire 0359
  Culture 0479
  Élevage et alimentation 0475
  Exploitation des péturages ... 0777
  Pathologie animale 0476
  Pathologie végétale 0480
  Physiologie végétale 0817
  Sylviculture et faune 0478
  Technologie du bois 0746
Biologie
  Généralités 0306
  Anatomie 0287
  Biologie (Statistiques) 0308
  Biologie moléculaire 0307
  Botanique 0309
  Cellule 0379
  Écologie 0329
  Entomologie 0353
  Génétique 0369
  Limnologie 0793
  Microbiologie 0410
  Neurologie 0317
  Océanographie 0416
  Physiologie 0433
  Radiation 0821
  Science vétérinaire 0778
  Zoologie 0472
Biophysique
  Généralités 0786
  Médicale 0760

SCIENCES DE LA TERRE
Biogéochimie 0425
Géochimie 0996
Géodésie 0370
Géographie physique 0368

Géologie 0372
Géophysique 0373
Hydrologie 0388
Minéralogie 0411
Océanographie physique 0415
Paléobotanique 0345
Paléoécologie 0426
Paléontologie 0418
Paléozoologie 0985
Palynologie 0427

SCIENCES DE LA SANTÉ ET DE L'ENVIRONNEMENT
Économie domestique 0386
Sciences de l'environnement 0768
Sciences de la santé
  Généralités 0566
  Administration des hipitaux .. 0769
  Alimentation et nutrition 0570
  Audiologie 0300
  Chimiothérapie 0992
  Dentisterie 0567
  Développement humain 0758
  Enseignement 0350
  Immunologie 0982
  Loisirs 0575
  Médecine du travail et
    thérapie 0354
  Médecine et chirurgie 0564
  Obstétrique et gynécologie ... 0380
  Ophtalmologie 0381
  Orthophonie 0460
  Pathologie 0571
  Pharmacie 0572
  Pharmacologie 0419
  Physiothérapie 0382
  Radiologie 0574
  Santé mentale 0347
  Santé publique 0573
  Soins infirmiers 0569
  Toxicologie 0383

SCIENCES PHYSIQUES

Sciences Pures
Chimie
  Generalités 0485
  Biochimie 487
  Chimie agricole 0749
  Chimie analytique 0486
  Chimie minérale 0488
  Chimie nucléaire 0738
  Chimie organique 0490
  Chimie pharmaceutique 0491
  Physique 0494
  PolymÇres 0495
  Radiation 0754
Mathématiques 0405
Physique
  Généralités 0605
  Acoustique 0986
  Astronomie et
    astrophysique 0606
  Electronique et électricité 0607
  Fluides et plasma 0759
  Météorologie 0608
  Optique 0752
  Particules (Physique
    nucléaire) 0798
  Physique atomique 0748
  Physique de l'état solide 0611
  Physique moléculaire 0609
  Physique nucléaire 0610
  Radiation 0756
Statistiques 0463

Sciences Appliqués Et Technologie
Informatique 0984
Ingénierie
  Généralités 0537
  Agricole 0539
  Automobile 0540

Biomédicale 0541
Chaleur et ther
  modynamique 0348
Conditionnement
  (Emballage) 0549
Génie aérospatial 0538
Génie chimique 0542
Génie civil 0543
Génie électronique et
  électrique 0544
Génie industriel 0546
Génie mécanique 0548
Génie nucléaire 0552
Ingénierie des systámes 0790
Mécanique navale 0547
Métallurgie 0743
Science des matériaux 0794
Technique du pétrole 0765
Technique minière 0551
Techniques sanitaires et
  municipales 0554
Technologie hydraulique 0545
Mécanique appliquée 0346
Géotechnologie 0428
Matières plastiques
  (Technologie) 0795
Recherche opérationnelle 0796
Textiles et tissus (Technologie) .. 0794
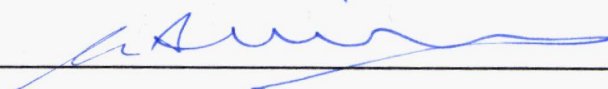
PSYCHOLOGIE
Généralités 0621
Personnalité 0625
Psychobiologie 0349
Psychologie clinique 0622
Psychologie du comportement ... 0384
Psychologie du développement .. 0620
Psychologie expérimentale 0623
Psychologie industrielle 0624
Psychologie physiologique 0989
Psychologie sociale 0451
Psychométrie 0632

♻

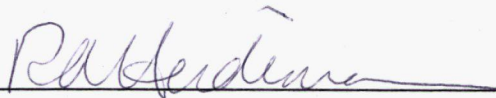# THE UNIVERSITY OF CALGARY

FACULTY OF GRADUATE STUDIES

The undersigned certify that they have read, and recommend to the Faculty of Graduate Studies for acceptance, a thesis entitled "Heat and Mass Transfer Within Granular Beds" submitted by Emad Boshra Fawzy Khalil in partial fulfillment of the requirements for the degree of Master of Science.

Supervisor and Chairperson, Dr. G.A. Karim
Department of Mechanical Engineering

Dr. I. Wierzba
Department of Mechanical Engineering

Dr. R.A. Heidemann
Department of Chemical and Petroleum Engineering

March, 24ᵗʰ 1993

ii

ABSTRACT

Heat and mass transfer processes within dry and partially wetted granular beds were investigated experimentally and theoretically when these beds were subjected to convective streams of heated air. The beds were cylindrical in shape with a central channel. The channel was either left empty for the flow of heated air or packed with beads of different sizes. The experimental study investigated the effects of the different parameters that govern the transport processes within these beds. This investigation showed that the packed channel brought about higher heat transfer rates. This was attributed to the higher heat transfer coefficients and the dispersion of some of the heated air into the bed.

Three theoretical models were attempted to simulate the characteristic transport processes associated with the different cases. The predicted results were in good agreement with the relevant experimental results for dry beds and for drying wetted beds at low temperature levels.

ACKNOWLEDGEMENT

To my dear late Father, my Mother and my Brother

TABLE OF CONTENTS

LIST OF FIGURES

xi

xiii

NOMENCLATURE

A_c	surface area of the equivalent insulation surface (m^2)
A_p	area of a plate of the insulation box (m^2)
c	moisture content defined by Sherwood in equation 2.4
c_p	specific heat at constant pressure (J/kg K)
d	diameter of the channel (m)
D	total effective thermal diffusivity tensor (m^2/s)
D_1	constant defined by Sherwood in equation 2.5
d_b	diameter of glass beads used in the beds (m)
D_d	dispersion tensor (m^2/s)
d_p	channel glass beads diameter (m)
D_v	binary mass diffusion coefficient (m^2/s)
D_{ve}	total effective binary mass diffusion coefficient (m^2/s)
g	gravitational acceleration (m/s^2)
Gr	Grashoff number
h	convective heat transfer coefficient (W/m^2 K)
h_c	average convective heat transfer coefficient at the channel surface (W/m^2 K)
h_m	average convective mass transfer coefficient (m/s)
h_N	average convective heat transfer coefficient at the insulation surface (W/m^2 K)

k	thermal conductivity (W/m K)
L	length of the bed (m)
m	mass flow rate of air (kg/s)
$\langle \dot{m} \rangle$	mass rate of evaporation per unit volume (kg/s m^3)
M	molecular weight (kg/kmol)
m_{lost}	mass lost (kg)
m_o	initial mass of water (kg)
Nu_d	Nusselt number based on the diameter d of the channel
Nu_l	Nusselt number based on the outer insulation surface length
P	pressure (Pa)
P^*	equilibrium vapour pressure at the corresponding temperature (Pa)
Pe	Peclet number (Re Pr = u_D d_t/α)
Pr	Prandtl number
P_u	upstream pressure of the chocked nozzle (Pa)
r	radial distance (m)
R	characteristic gas constant (J/kg K)
r_1	inner radius of the bed (m)
r_2	outer radius of the bed (m)
r_3	radius of the insulation surface (m)
Re_d	Reynolds number based on the diameter of the channel
S	saturation (volume of liquid phase/V_{void})

Sc	Schmidt number (v_f/D_{12}), (v_f/D_v)
Sh	Sherwood number $(h_m\ d/D_{12})$, $(h_m\ d/D_v)$
t	time (s)
T	temperature (K)
T_1–T_6	temperatures measured along the length of the bed at the mid radius
T_{am}	ambient temperature (K)
T_c	average temperature of the air stream (K)
T_i	temperature of the air stream at the inlet of the reactor (K)
T_m	mean film temperature (K)
T_o	temperature of the air stream at the outlet of the reactor (K)
T_{su}	surface temperature (K)
T_u	upstream temperature of the choked nozzle (Pa)
u	average air stream velocity (m/s)
u_D	Darcean velocity or dispersion velocity (m/s)
u_s	shear velocity (m/s)
V	volume (m^3)
v_v	velocity of the vapour phase (m/s)
w	water content (mass of water / mass of dry bed)
x	linear distance (m)
z	distance in the axial direction (m)
B	coefficient of volumetric expansion (K^{-1})

$\langle \Delta h_v \rangle$	enthalpy of vaporization per unit mass (kJ/kg)
ε	porosity of dry beds
ε_i	volume fraction of the ith phase (V_i/V)
ε_{lo}	initial water volume fraction (V_{lo}/V)
σ_{12}	collision diameter (Å)
μ	dynamic viscosity (N s/m^2)
μ_{su}	dynamic viscosity calculated at the surface temperature (N s/m^2)
ν	kinematic viscosity (m^2/s)
τ_s	shear stress at the surface (N/m^2)
Ω	collision integral for diffusion

Suffices

a	air
e	effective
exp	experimental
f	fluid
g	gaseous
i	phase number
ins	insulation
l	liquid
s	solid
v	vapour

CHAPTER 1

INTRODUCTION

1.1 GENERAL

Transport processes within porous media have been subject to numerous investigations in recent years. The interest in this field is motivated by the wide range of engineering applications, for example, geophysics, in situ oil recovery techniques, thermal insulation engineering, drying processes,..etc. The present work originally stemmed from the work of Mehta (26) who examined experimentally the combustion and transport processes within oil sand beds. In his work, the bed was simulated as a cylindrical porous solid medium with a relatively high permeability circular central channel (fracture). In his study, combustion, low temperature oxidation and coke formation were the major items investigated. Though the physical transport processes, such as heat and mass transfer were acknowledged, a close investigation of these processes was not feasible due to the high complexity encountered when considering oil sands. For this reason, a closer examination was decided to be carried out to investigate the physical transport processes in such configurations. In order to make this possible, beds of the same configurations with well-known properties were subjected to controlled hot streams of air through the central channels. The two configurations studied are :

1)   Open Central Channel, where the central channel was left empty for the

flow of the hot stream of air (figure 1.1-a).

2)   Packed Central Channel, where the central channel was filled by glass beads of different sizes (figure 1.1-b).

Moreover, a theoretical analysis was attempted in this study. Apart from the relevance of this study to the previous work of Mehta, since the present study involves several combinations of heat transfer, mass transfer, fluid flow and phase change both experimentally and theoretically, it contributes to the general knowledge of this field.

1.2 ORGANIZATION OF THE THESIS

The text is divided into 7 chapters. Chapter 2 presents a brief review of the evolutionary path of the modelling of heat and mass transfer in porous media. It also presents recent developments using volume-averaged techniques. Chapter 3 describes the apparatus used, preparation procedures and measurement techniques employed throughout the experimental study. Chapter 4 describes the theoretical basis of the three models developed in this work. Chapter 5 and 6 gives qualitative and quantitative results obtained both experimentally and theoretically. A discussion of the experimental results and evaluation of the theoretical models, via comparison of the theoretical and the corresponding experimental results are included. Chapter 5 is limited to the results of dry bed runs while chapter 6 is devoted to those of the wet beds. The last chapter summarizes the most important results and conclusions.

Recommendations for future study are also suggested in this chapter.
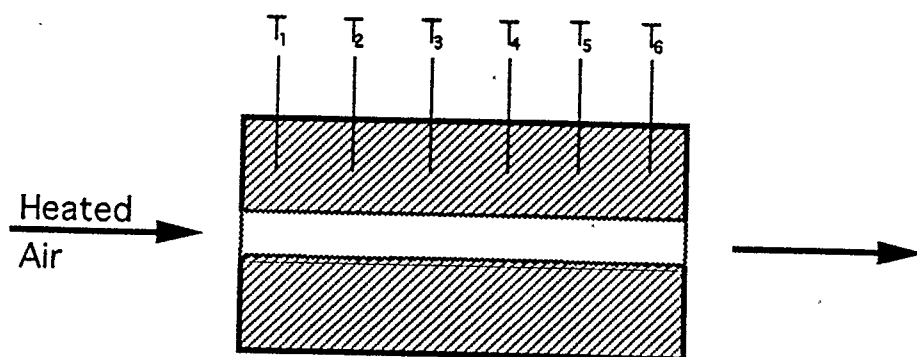
(a) Open Channel Configuration
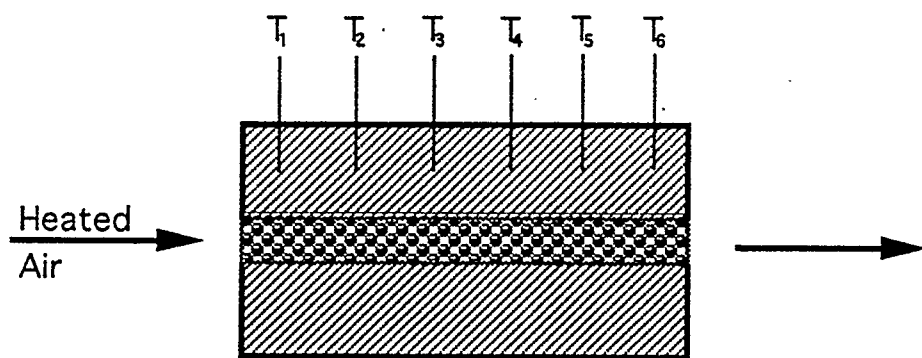
(b) Packed Channel Configuration

Figure 1.1 Schematic diagrams of the Open and Packed Channel configurations.

CHAPTER 2

BACKGROUND AND LITERATURE REVIEW

2.1 CONDUCTION HEAT TRANSFER

Analysis of macroscopic heat transfer in porous media is often described by homogenized equations. These equations resemble the equations of heat transfer in single phase homogeneous media. In order to use these simplified equations, effective properties such as effective thermal conductivity, effective thermal capacity,...etc, have to be determined. In contrast to the effective thermal capacity, the effective thermal conductivity cannot be obtained by simple volume averaging of phases. The most difficult aspect in the calculation of the effective thermal conductivity is the fact that it depends on the structure of the media which varies widely from one medium to another. The complexity of the structure ranges from the relatively simple system of packed nonconsolidated spherical particles to complicated fibrous structures. Even when dealing with nonconsolidated particles, the contact between the particles plays a significant role in determining the final value.

Early investigations were done by Maxwell (24) who studied two cases: the first is a dilute suspension of spherical particles in infinite uniform fluid (designated as Maxwell lower bound) and the second of a solid body containing dilute suspension of fluid filled voids (Maxwell upper bound). These cases represent the two extreme bounds for a homogeneous, isotropic two-phase

mixture. Several approaches since then have been tried to predict the effective thermal conductivity of porous media. A comprehensive review of these approaches is given by Kaviany (13). A brief review is presented with emphasis on the recent approaches. Hashine and Shtrikman (9) used simple statistical analysis to study the effective thermal conductivity of uniform and isotropic multiphase media. Their analysis established bounds which are identical to Maxwell's bounds. As Hashine and Shtrikman did not consider the effect of the structure, their formula did not give realistic predictions. Miller (27) took into consideration the effect of microstructure to derive improved bounds. Nayak and Tien (29) applied the principle of statistical thermodynamics to determine the effective thermal conductivity of random and regular arrangements of spherical particles. Batchelor and O'Brien (1) modeled granular systems of touching particles by applying ensemble average over a large volume while considering the contact contribution to obtain the total thermal conductivity formula.

2.1.1 Recent Approaches

The introduction of volume-averaging techniques by Slattery (38) and Carbonell and Whitaker (4) is one of the approaches that influenced the study of heat transfer in porous media. Slattery applied his averaging theorems without making any assumptions about the structure to obtain a differential local-averaged equation. The equation includes the effective thermal

conductivity k_e which depends on the phase conductivities and the structure through a function that has to be determined empirically. Using this theory, Carbonell and Whitaker (4) limited their work to periodic structures. Hence, they related the previous function to the geometry of the unit cell. The unit cell has to define the solid phase distribution as well as particle contact. In other words, by choosing a representative unit cell, the derivation of the effective thermal conductivity is possible by solving the closure problem. The general equation for heat conduction is expressed as follows:

$$[\epsilon(\rho c_p)_f + (1-\epsilon)(\rho c_p)_s] \frac{\partial \langle T \rangle}{\partial t} = \nabla \cdot [k_e \cdot \nabla \langle T \rangle] \qquad (2.1)$$

where

ρ : density (kg/m^3)

c_p : specific heat (J/kg K)

ϵ : porosity

$\langle T \rangle$: spacial average temperature (K)

t : time (s)

k_e : effective thermal conductivity tensor (W/m K)

and the subscripts are:

f : fluid phase

s : solid phase

Nozad et al.(32) proposed a two dimensional unit cell to solve the closure problem. Two predictions were considered; one with continious fluid phase and

the other with the fluid phases discontinuous (i.e particle-particle contact). Their results for the discontinuous fluid phase case showed that only 2% contact area gives theoretical results that are in excellent agreement with the experimental data of various sources. They concluded that the theory is satisfactory provided there is a reasonably good contact between the particles. Hadley (8) used a semi-empirical approach by combining the Maxwell upper bound with an expression appropriate for a suspension of particles through an adjustable function "$f_o(\varepsilon)$" and another weighing function "$\alpha_o(\varepsilon)$", which are determined experimentally. Their work yields a generalized correlation for media of different consolidation. Moreover, their predictions showed good agreement with two phase results from a variety of sources. In addition to the previous techniques many empirical formulas are available (e.g. 19,20). Finally, Kaviany (13) made an assessment of the previous results and approaches for different values of phase conductivity ratios.

2.2 CONVECTION AND CONDUCTION

In the course of the present study, a fluid phase was not injected into the porous bed as will be explained later. However, in the case of a bed with a central channel filled with glass beads, the radial penetration of the fluid phase through the bed was expected to occur. Accordingly, a background on simultaneous fluid flow and heat transfer in porous media was needed for this investigation. In general when considering simultaneous fluid flow and heat

transfer in porous media, both Darcean and pore level velocities influence the temperature field. Inclusion of the effect of the pore level velocity nonuniformity on the temperature distribution is called the dispersion effect. Hydrodynamic dispersion in tubes was examined by many researchers such as Taylor (40,41). Taylor found that velocity nonuniformities lead to enhancement of the diffusion of heat. He related the dispersion component to a Peclet number. As for conduction, Carbonell and Whitaker (4) developed the volume averaged equations with the inclusion of dispersion effect. The general equation is given as follows:

$$(\rho c_p)_e \, \frac{\partial \langle T \rangle}{\partial t} + (\rho c_p)_f \, u_D \cdot \nabla \langle T \rangle = (\rho c_p)_f \, \nabla \cdot (D \cdot \nabla \langle T \rangle) \qquad (2.2)$$

where:

$$(\rho c_p)_e = [\, \varepsilon (\rho c_p)_f + (1-\varepsilon)(\rho c_p)_s \,]$$

$$D = \frac{k_e}{(\rho c_p)_f} + \varepsilon D_d$$

u_D = Darcean velocity vector (m/s)

D = total effective thermal diffusivity tensor (m²/s)

D_d = Dispersion tensor (m²/s)

Determination of D_d requires assuming a certain unit cell and solving the Navier Stokes equations over the cell. A review of solutions of dispersion tensor is given in Kaviany (13) for ordered and disordered media. He

recommended the closed form solution of Koch and Brady(16) for random arrangements of spherical particles.

2.3 DRYING

The first half of this century saw several theories put forward to explain the various stages of moisture migration in porous media. A good review for the work before 1977 is given in Whitaker (42). The first engineering analysis for drying was done by Lewis (21) who postulated that the drying process involved two independent processes: first the evaporation of the moisture from the surface of the solid and second the diffusion of the moisture from the interior of the solids out to the surface. The term moisture referred to the liquid state (42). The diffusion idea was adopted by Sherwood (37) who formulated a complete theory for drying based on the diffusion equation only which took the form:

$$\frac{\partial c}{\partial t} = D_1 \frac{\partial^2 c}{\partial x^2} \tag{2.3}$$

where "c" represented a vaguely defined moisture content and D_1 represented a parameter which is determined experimentally. Hougen et al (11) discussed the limitations of the diffusion equation in drying after investigating the drying of granular solids. They pointed out that the capillary action can play a dominant role in the movement of moisture. Their experimental results when compared with the solutions based on diffusion theory and those based on capillary action favoured the capillary theory. Krischer (18) was the first

to consider the role that the transport of energy plays in the drying process. During the later part of the century more comprehensive theories of simultaneous heat and mass transfer processes have been introduced. De Vries (7) considered capillary flow and vapour transport and included the thermal energy equation in their analysis. Similar equations for heat and mass transfer in porous media were also used by Luikov (23) and Berger and Pei (3). Starting with Whitaker (42,43) a new approach for the analysis of drying is used, namely volume-averaged equations. A summary of the theory is presented in appendix (A). The latter theory was also used in the model developed in the present work. Whitaker's theory was adopted by many researchers. Ben Nasrallah and Pierre (2) used a model which is deduced from Whitaker's theory to study heat and mass transfer during convective drying of flat porous slabs. The model comprises a comprehensive set of equations that takes the effect of the total gaseous pressure into consideration. Insight into the effect of gaseous pressure was obtained by comparing the results of two porous media ,namely, brick and wood. They concluded that when the gaseous permeability is low, the pressure gradient generated by the diffusive flux is too great to be neglected. Therefore, they introduced a correcting factor for the vapour diffusivity in order to carry the calculation at constant pressure. On the other hand, for higher permeabilities, such as in the case of brick, the total pressure of the gaseous phase could be taken equal to the atmospheric pressure without any noticeable error (less than 1%) . They also introduced

a parameter which is a function of the physical characteristics of the system as a criterion for using a simplified model which assumes a constant total gaseous pressure. Ilic and Turner (12) studied the convective drying of consolidated slabs of wet porous materials. They formulated a model which has the form of Luikov equations but uses the averaging technique of Whitaker. They studied the same case of Ben Nassrallah and Pierre (2) and used the same controlling input for comparison. Their results for dry brick agree with the available experimental results of Ben Nassrallah (2). Moreover the authors claim that their formulation could be extended to include non-equilibrium processes such as problems where stress development is of interest.

Finally, in the present study the volume-averaged equations are used for modelling three cases which are:

a) Dry granular beds of open central channel configuration.

b) Dry granular beds of packed central channel configuration.

c) Wetted granular beds of open central channel configuration.

CHAPTER 3

EXPERIMENTAL STUDY

3.1 INTRODUCTION

The main objective of this investigation was to study the effects of some of the main parameters which govern the processes of heat and mass transfer in dry and partially wet porous granular beds when exposed to a controlled stream of heated air. In order to carry out a parametric study of the processes involved, beds of small uniform diameter beads were used to reduce the uncertainty usually associated with nonuniform beds. For this purpose glass beads of different sizes were employed in turn as test materials. The bed configuration was cylindrical with a central channel. As mentioned in chapter 1, two cases were studied which are:

1. Open channel configuration, where the central channel was left empty for the hot stream of air.

2. Packed channel configuration, where the central channel was filled by glass beads of different uniform sizes.

All beds dimensions were 63 mm outer diameter, 12 mm inner diameter and 120 mm long. In order to retain the glass beads in position, a thin stainless steel cylindrical wire mesh (#70) was used so as to form the channel. The ranges of stream temperature, stream mass flow rate, glass bead size and water content (w) covered in this investigation was 100°C - 200°C, 1.6 kg/h -

2.4 kg/h, 0.27 mm - 1.3 mm, 2% - 4% by weight, respectively.

In this chapter, the apparatus used, experimental methods employed and measurements techniques adopted are presented.

3.2 MAIN EXPERIMENTAL APPARATUS

The apparatus used in the present study was originally designed by Mehta (21) for studying the combustion and transport processes within fractured oil sands beds. A schematic layout of the apparatus is presented in fig (3.1). It consists mainly of two horizontal reactors in parallel. Electrically heated air was introduced to the reactors through flow manifolds. A central flow bypass line was provided to allow time for achieving a prescribed flow condition prior to the introduction of the heated air to the reactors. The flow of air was controlled by several valves and was metered by means of pre-calibrated choked nozzles. Air was then heated in an electric heating furnace to raise its temperature to the prescribed value before conveying it to the main flow manifold. All flow manifold lines were covered by ceramic insulation to minimize the heat losses to the surroundings. The apparatus was designed to have also provisions for the following systems:

1. fuel injection

2. electric ignition

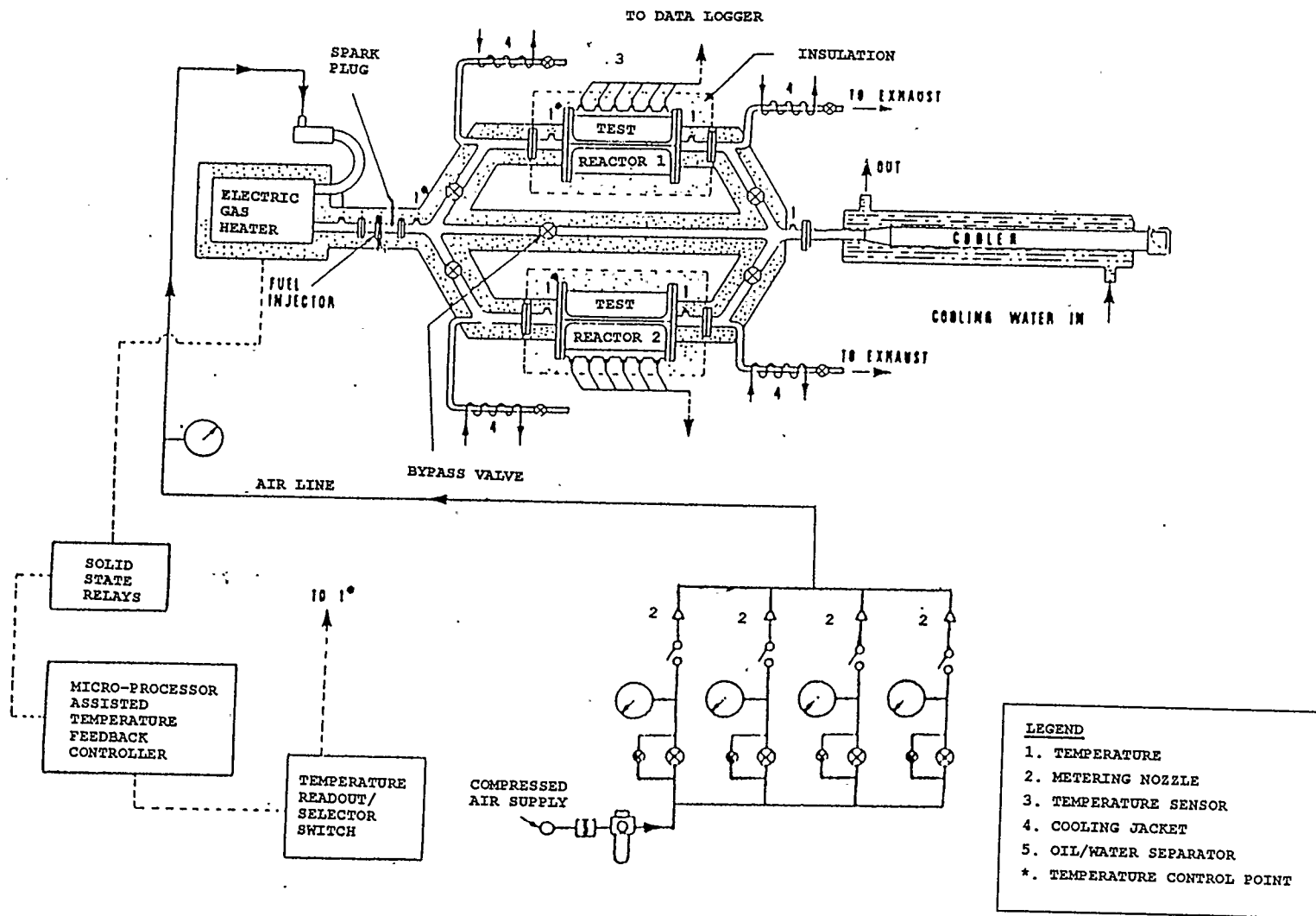3. liquid fuel evaporator

4. exhaust gas sampling

Figure 3.1   Schematic layout of the main test rig.

5. reactor quenching

6. exhaust gas conditioning

In the present study the above systems were isolated from the main apparatus because they were not used. Hence, they will not be described further in this chapter. The features of the main apparatus are explained in more detail in the next sections.

3.2.1 TEST REACTORS

The apparatus was provided with two stainless steel reactors made up of two halves. Each reactor can accommodate a cylindrical sample bed (63 mm diameter, 120 mm long). The upper half of the reactor was equipped with a thermocouple bank having connections for six chromel/alumel (ISA type K) thermocouple. The thermocouple connections were placed at equal intervals along the length of the reactor. This thermocouple connector design provided flexibility in placing six 0.25 mm diameter thermocouple probes at any desired radial position within the beds. The apparatus was fitted with two matching flanges to accommodate the reactor after assembly. In the present study, only one reactor was used for all the runs to provide for better repeatability of readings and reduce the errors that may arise due to any differences in the thermal behaviour of the two similar reactors.

3.2.2 FLOW SYSTEM

The main purpose of the flow system was to provide the heater box and in turn the reactor with a precisely metered supply of air. Air flow was measured by means of four pre-calibrated choked nozzles of different sizes. The nozzles were calibrated using a wet test meter and calibration curves are given in Appendix (B) for mass flow rate versus $(P_u/\sqrt{T_u})$, where P_u and T_u are the upstream pressure and temperature of the nozzle, respectively. Each nozzle was provided with two regulating valves for coarse and fine adjustments of the upstream pressure and flow. High precision stainless steel Bourdon tube gauges and thermocouple were employed to monitor the pressure and temperature mentioned above.

3.2.3 AIR HEATING SYSTEM

The gas flow heating system consists mainly of an electric furnace of six heating elements connected to a 208 V, 30 A power supply through ON-OFF solid state relays. A microprocessor assisted temperature feedback controller was provided to control the relays. It was capable of maintaining any preset temperature within 1°C for the entire air flow and temperature ranges. The safe upper limit for the temperature of the air leaving the heater box was 550°C, approximately. Three temperature control points were provided, one in the main flow manifold and two at the inlet of the reactors.

3.2.4 TEMPERATURE MEASUREMENTS

The air stream temperature at the inlet of the reactor was continuously monitored using Inconnel sheathed chromel/alumel (ISA type K) thermocouple probes. Since the transient temperature within the bed was the main criterion for comparison of different cases, it was found ultimately important to investigate the time taken by the air stream to reach the prescribed temperature. This "warm up" period had been observed to vary from 20 minutes for a stream temperature of 200°C to 10 minutes for a stream temperature of 100°C. Consequently, a temperature-time schedule was established for every temperature level so that the comparison of different cases would be at the same flow conditions.

The temperatures within the beds were monitored using six chromel / alumel (ISA type K) thermocouple probes with 1.6 mm O.D. The probes were connected to the thermocouple bank located in the upper half of the reactor. The thermocouples were connected to a Fluke, 60 channel "Model 2240 B Data Logger" for displaying and recording the readings of the thermocouple simultaneously with the corresponding time during the run.

Two different techniques were tried for holding the thermocouple probes in place within the bed. They are as follows:

i.   The thermocouple probes, suspended from the upper half, were inserted into the bed through holes drilled in sample holders to the required depth. The upper half was then closed carefully and the two halves

tightened together. It was found that the thermocouple were so loose that the position of the junction was altered completely upon assembly of the reactor which led to false measurements corresponding to temperatures at the wrong locations. Hence this technique was discarded.

ii. It was required to find a way to make the inserted portion of the probe an integral part with the sample holder so that it would not be affected by the assembly process. It was found inconvenient to design a clamp to hold the thermocouple in place due to the small space available. An alternative technique was to fix the thermocouple to the wall by means of epoxy resin. A bead was used to support the thermocouple and to provide the required contact surface area for adhesion (fig. 3.2). This assembly was left for six hours until the epoxy attained its full strength then the top cover of the rector was placed. This technique proved to be successful in keeping the thermocouple in place and was adopted during the whole experimental program. The apparatus was then left
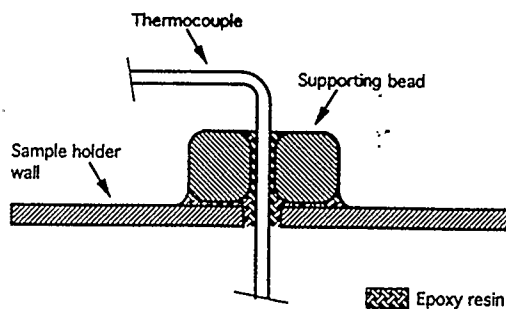

Figure 3.2 Schematic diagram of the thermocouple fixture

to be heated for twelve hours to check any effects that might occur due to the heating of the epoxy. The previous procedure was repeated for every new setting.

3.3 SAMPLE PREPARATION AND REACTOR PACKING

The preparation of the bed and packing of the reactor could be described as follows:

i.   The sample holder was placed in the bottom half of the reactor. The thermocouple probes were connected to the thermocouple bank located in the top half and inserted into the sample holder according to the procedure mentioned in the previous section.

ii.   Glass beads of the required size were poured into the annular portion of the holder. For wet beds, glass beads and distilled water were first thoroughly mixed in the desired proportion .

iii. The central channel was either left empty for open channel runs or filled with glass beads of the required size for the packed channel configuration.

iv.   The sample with the reactor were subjected to an ultrasonic shaker to achieve uniform distribution of the bed.

v.   Lids were placed on top of the sample holder and were sealed using nylon tape.

vi.   The reactor was then placed between the two matching flanges, the

gaskets placed and all the bolts were tightened.

vii.   The reactor was insulated with high temperature ceramic insulation by using an insulation box around the reactor.

3.4 EXPERIMENTAL APPROACH

In light of the main objective mentioned in section 2.1, the experiments carried out in this study were aimed at finding out the effects of the following parameters on heat and mass transfer in open and packed channel configurations for dry and partially saturated cases:

a. glass bead size of the bed

b. glass bead size in the channel

c. mass flow rate of air

d. water content of the bed

e. temperature level

To investigate the effects of the different parameters, the respective parameter was varied, keeping everything else unchanged. The general procedure in operating the apparatus for any run can be summarized as follows:

1.   The apparatus was tested for leaks.

2.   The filter in the compressed air line was replaced.

3.   The bypass line was opened while the reactor line was closed.

4.   The desired air flow rate was set by adjusting the upstream pressure to

the required number of choked nozzles.

5. The heater controller was connected to the thermocouple located at the outlet of the heater box (i.e, the latter thermocouple acts as a temperature control point), programmed for the required temperature and the heaters were switched on. For high temperatures the final required temperature was reached in several steps to avoid burn out of the heater elements.

6. The sample was prepared and the reactor was packed according to the procedure described in section 3.3.

7. Once the required temperature of the air flow was stabilized in the main flow manifold, the Data logger was switched on to monitor the temperatures within the beds, the bypass line was closed while the reactor line was opened. The temperature control point was switched to the thermocouple located at the inlet of the reactor.

8. Readings for the temperatures within the bed were recorded at prescribed time intervals for further analysis.

CHAPTER 4

THEORETICAL STUDY

4.1 INTRODUCTION

The present chapter considers theoretically the problem of heat and mass transfer within granular porous media. Three models were formulated. The first model analyzes the heat transfer process in dry granular beds of open channel configuration. The second model describes the heat transfer process within dry granular bed of the packed channel configuration. The Third model analyzes the simultaneous processes of heat and mass transfer within partially water saturated beds of open channel configuration. These three models were formulated primarily to simulate the transport processes that occurred within the scope of the present study so as to serve the purpose of comparison and extension the experimental findings.

4.2 OPEN CHANNEL DRY BEDS

4.2.1 PHYSICAL MODEL

The bed was represented by a finite circular cylinder subjected to a convective stream of hot air passing through a concentric axial channel. The outer and end surfaces of the cylinder were assumed to be impermeable to flow and were insulated. In order to simulate more realistically the operating conditions, the insulation was assumed not to be perfect but heat losses were

taken into consideration. The governing equations were deduced and solved for a range of operating conditions and for beds of varying properties simulating beds of different porosity and bead sizes.

4.2.2 SIMPLIFYING ASSUMPTIONS

i.   The heat transfer was solely due to conduction, i.e there was no convection within the bed. The latter condition was confirmed experimentally. By comparing the temperature transients obtained for runs with permeable and impermeable central channel, the profiles were found to be effectively identical.

ii.   Heat transfer by radiation was neglected. This assumption was considered to be valid due to the relatively low temperatures encountered in this study.

iii. There is a local thermal equilibrium between the solid and gas phases. This assumption was based on the fact that there was no heat generation within the solid or gas phases and relatively very fast transients were not encountered in this study.

iv.   Circumferential heat transfer was assumed to be negligible within the axially symmetrical bed.

v.   Heat transfer in the axial direction relative to that in the radial direction was assumed small and was neglected. This assumption was supported by the experimental observation that the temperature

variation in the axial direction was effectively negligible.

vi.   To formulate a model that include the insulation region, the insulation
box was replaced by an equivalent cylindrical surface. In order to make
both configurations equivalent, first, a mean thickness for the insulation
was used. Secondly, an equivalent convective heat transfer coefficient
at the insulation surface was derived by equating the heat losses of both
systems. Details are presented in section 4.2.6.

4.2.3 GOVERNING EQUATIONS

The simplifying assumptions made in the previous section reduce the
model to that of a simple transient one dimensional heat conduction problem.
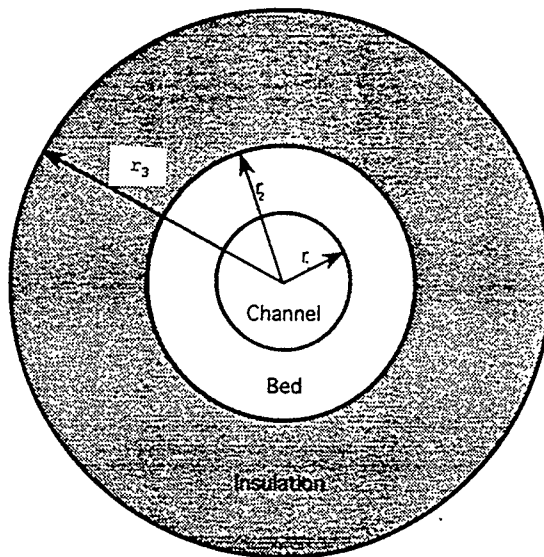Figure (4.1) shows the geometrical configuration schematically.

Figure 4.1 Geometrical configuration of the bed.

The local-averaged energy equation (2.1) for the bed could be represented as follows:

$$(\rho c_p)_e \frac{\partial \langle T \rangle}{\partial t} = \frac{1}{r} \frac{\partial}{\partial r} \left[r \, k_e \frac{\partial \langle T \rangle}{\partial r} \right] \qquad (4.1)$$

where:

$\langle T \rangle$ = local spacial average temperature within the bed (K)

t = time (s)

$(\rho c_p)_e$ = effective volumetric heat capacity (J/m^3 K)

k_e = effective thermal conductivity of the bed (W/m K)

r = radial distance (m)

As mentioned earlier external heat losses were taken into consideration, hence a similar equation has to be introduced for heat conduction within the insulation region. The equation could be written as follows:

$$\rho_{ins} \, c_{p_{ins}} \frac{\partial T}{\partial t} = \frac{1}{r} \frac{\partial}{\partial r} \left[r \, k_{ins} \frac{\partial T}{\partial r} \right] \qquad (4.2)$$

where subscript "ins" refers to the insulation.

4.2.4 INITIAL AND BOUNDARY CONDITIONS

a) Initial conditions:

$$T (r,0) = T_{am} \qquad \text{for} \qquad r_1 \leq r \leq r_3$$

b) Boundary conditions:

1) Central channel Boundary ($r = r_1$)

The balance of heat transfer rates on the channel surface due to convective stream leads to:

$$- (k_e \frac{\partial \langle T \rangle}{\partial r}) = h_c [T_c - \langle T(r_1,t) \rangle] \qquad (4.3)$$

where:

h_c = average convective heat transfer coefficient (W/m^2 K)

T_c = average temperature of the convective stream of air (K)

2) Convective boundary at the insulation surface ($r = r_3$)

$$- (k_{ins} \frac{\partial T}{\partial r}) = h_N (T(r_3,t) - T_{am}) \qquad (4.4)$$

where:

T_{am} = ambient temperature (K)

h_N = average heat transfer coefficient of natural convection over the insulation surface (W/m^2 K)

4.2.5 SOLUTION OF GOVERNING EQUATION

Solution of the second order partial differential equations can be carried out using either analytical or numerical techniques. Although analytical solutions are available for solving transient heat transfer problems similar to

that of the present model (22), the solution would be very complicated for the case of wet beds. Hence, the finite difference numerical technique was employed in solving the present problem. In order to get an unconditionally stable numerical solution, the "Crank-Nicolson" (5,33) method was chosen to formulate the finite difference equations. A problem associated with such an approach was that the results may become oscillatory around the exact solution. Smith(39) suggested the arithmetic average of each two consecutive values to be used to suppress the oscillatory effects. This method was tried in this investigation and found to be successful. Appendix (C) lists the computer program developed to solve the present problem.

4.2.6 PHYSICAL PROPERTIES AND HEAT TRANSFER COEFFICIENTS

A) Volumetric heat capacity

The volumetric heat capacity (density x specific heat) of the bed was obtained by simple value averaging of phases using the following formula (13):

$$\langle \rho c_p \rangle_e = (1 - \varepsilon) \langle \rho c_p \rangle_s + \varepsilon \langle \rho c_p \rangle_g \qquad (4.5)$$

where:

ε = porosity of the bed

and the suffixes:

s = solid phase

g = gaseous phase (air)

Since the heat capacity of air is much smaller than that of the solid matrix, equation (4.5) could be approximated to:

$$\langle \rho c_p \rangle_e = (1 - \varepsilon) \langle \rho c_p \rangle_s$$

B) Effective thermal conductivity

In contrast to the volumetric heat capacity, the effective thermal conductivity of porous or granular porous media cannot be calculated using a simple value averaging of phases (13). In general the effective thermal conductivity depends on:

1.   The thermal conductivity of each phase (relative magnitude of (k_s/k_g).

2.   The structure of the solid matrix and the extent of continuity of the solid phase.

3.   The contact resistance between the nonconsolidated particles for granular porous beds.

In spite of much research in the area of effective thermal conductivity of porous beds, yet there is a lot of discrepancy and uncertainty due to the different nature and systems involved in every study. Furthermore, the sensitivity of the value of the thermal conductivity to the structure and contact area of particles enhances the errors due to different preparation of beds. As mentioned earlier in section 1.2, Kaviany (13) has investigated the various formulas which were proposed by many researchers whether empirical or

theoretical. The latter investigation showed that for low values of relative thermal conductivities of the solid to the fluid phases (less than a value of 25), the following mean relation could be used for estimating the effective thermal conductivity of the porous media:

$$k_e = (k_s)^{(1-\varepsilon)} (k_g)^{\varepsilon} \qquad (4.7)$$

Since the relative thermal conductivities of phases encountered in the present study lie in above region, equation (4.7) was used.

C) Thermal and physical properties of the insulating material

The values of the thermal conductivity and density of the ceramic insulation were obtained from data sheets provided by the supplier. The values are as follows:

$$k_{ins} = 0.07 \ (W/m \ K)$$

$$\rho_{ins} = 96.0 \ (kg/m^3)$$

D) Coefficient of convective heat transfer on the channel surface h_c

The present problem involved laminar to slightly transient forced convection in a circular channel. Accordingly, the average coefficient of heat transfer could be estimated using the following relation (10,17,25):

$$Nu_d = 1.86\ Re^{(1/3)}\ Pr^{(1/3)}\ \left(\frac{d}{L}\right)^{(1/3)} \left(\frac{\mu_f}{\mu_{su}}\right)^{0.14} \tag{4.8}$$

where:

Nu_d	=	Nusselt number based on the diameter of the circular channel ($h_f d/k_f$)
h_f	=	average coefficient of heat transfer by convection (W/m^2 K)
k_f	=	average thermal conductivity of the flowing fluid (W/m K)
d	=	diameter of the circular channel (m)
L	=	length of the circular channel (m)
Re	=	average flow Reynolds number ($u.d/v_f$)
v_f	=	kinematic viscosity of the flowing fluid (m^2/s)
u	=	average free stream velocity of the flowing fluid (m/s)
Pr	=	Prandtl number of the flowing fluid $\{(c_p\mu/k)_f\}$
μ_f	=	average absolute viscosity of the flowing fluid (kg/m s)

Properties of the convective air stream were obtained from standard tables, and evaluated at the mean film temperature except for μ_{su} which was evaluated at the surface temperature. The mean film temperature was defined as:

$$T_m = 0.5\ (T_{su} + T_c)$$

where:

T_m	=	mean film temperature (K)

$$T_{su} \quad = \quad \text{surface temperature (K)}$$

E) Coefficient of convective heat transfer at the insulation surface(h_N)

The insulation was packed in a square box around the reactor. Hence, this represented a situation that involves heat transfer by natural convection over a box composed of two hot vertical plates and two hot horizontal plates. The heat transfer coefficient for natural convection over plates could be estimated using the following relation (9,16,25):

$$Nu_l = a \ (\ Gr \ Pr \ )^b \qquad (4.9)$$

where

Nu_l = Nusselt number based on the length of the plate (hl/k_f)

h = average coefficient of heat transfer by convection (W/m^2 K)

l = length of the plate (m)

Gr = Grashof number based on the plate length

$[g\beta(T_{su}-T_{am})l^3/\nu^2]$

g = gravitational acceleration (m/s^2)

β = Coefficient of volumetric expansion (K^{-1})

a = 0.54 for vertical plate and horizontal hot plate facing upward

= 0.27 for horizontal hot plate facing downwards

b   =   0.25

Properties of the convective air were obtained from standard tables, and calculated at the mean film temperature.

Finally, to calculate the equivalent heat transfer coefficient over the cylindrical surface, the heat losses from the box and the cylindrical were equated using the following equation:

$$\sum_{i=1}^{4} h_i \, A_p \, \Delta t = h_N \, A_c \, \Delta t \qquad (4.10)$$

where:

h_i =   convective heat transfer coefficient over the ith plate (W/m^2 K)

A_p =   Area of a plate (m^2)

Δt =   temperature difference (T_{su}-T_{am}) (K)

A_c =   surface area of the equivalent surface (m^2)

4.3 PACKED CHANNEL DRY BED

4.3.1 FORMULATION OF THE PROBLEM

In case of packed channel configuration, a radial penetration of the flow was expected to occur within the bed. Since velocities could not be measured within the bed, the use of a model to predict the effect of radial dispersion of flow was needed to estimate the relative magnitude of the dispersion compared to that of only conduction. The first problem arises from the multi-dimensionality of the problem in addition to the complexity of the flow pattern within the bed. The initial approach was to use the conduction model to predict the temperature history within the bed. To overcome the problem of multi-dimensionality, an approximate, yet adequate method was employed that assumed the bed to be made up of six segments in the axial direction. It was also assumed that heat transfer occurs radially within each segment. For each segment, the corresponding experimentally measured surface temperature was used as an input to the conduction model to predict the temperature histories at various radial locations. In order to check the validity of this approach, a comparison between the predicted temperature history using the model and the experimentally measured counterpart was done for a set of runs carried out. The results of the comparison showed that the predicted temperatures are consistently lower than their corresponding measured ones even at the steady state. This emphasizes that the effect of dispersion needs to be included in the modelling process of packed bed configuration.

4.3.2 DISPERSION MODEL

To include the effect of dispersion, the general volume-averaged conduction-convection energy equation for dispersion in porous media (2.2) has to be used instead of equation (2.1).

$$(\rho c_p)_e \, \frac{\partial \langle T \rangle}{\partial t} + (\rho c_p)_f \, u_D \cdot \nabla \langle T \rangle = (\rho c_p)_f \, \nabla \cdot (D \cdot \nabla \langle T \rangle) \tag{4.11}$$

Where:

$$(\rho c_p)_e = [\; \varepsilon (\rho c_p)_f + (1-\varepsilon)(\rho c_p)_s \;]$$

$$D = \frac{k_e}{(\rho c_p)_f} + \varepsilon \, D_d$$

u_D =   Darcean velocity vector (m/s)

D =   total effective thermal diffusivity tensor (m^2/s)

D_d =   dispersion tensor (m^2/s)

The rest of the symbols were defined earlier.

4.3.3 SIMPLIFYING ASSUMPTIONS

i.   The assumptions (ii) through (iv) of section 4.2.2 were assumed to be valid for this model also.

ii.   The net Darcean velocity was assumed to be radial everywhere within the bed ($[u_D x r]_{r_1} = [u_D x r]_r$).

Finally, the approximate method described in section 4.3.1 was

employed. Hence, the heat transfer and flow within each segment was assumed to be in the radial direction.

4.3.4 GOVERNING EQUATIONS

The assumptions made in the previous section reduce the general equation (4.10) to the following form:

$$(\rho c_p)_e \frac{\partial \langle T \rangle}{\partial t} + (\rho c_p)_f u_D \frac{\partial \langle T \rangle}{\partial r} = (\rho c_p)_f \frac{1}{r} [\frac{\partial}{\partial r}(D\ r\ \frac{\partial \langle T \rangle}{\partial r})] \qquad (4.12)$$

The heat conduction equation for the insulation region ($r_2 \leq r \leq r_3$) was assumed as in equation (4.2).

4.3.5 INITIAL BOUNDARY CONDITIONS

The initial and the convective boundary condition at the insulation surface were assumed to be the same as those of the conduction model. In addition, the experimentally measured surface temperature was used as input for the model. Hence:

$$T(r_1,t) = T_{exp}(r_1,t)$$

where T_{exp} is the experimentally measured temperature.

4.3.6 PHYSICAL PROPERTIES AND HEAT TRANSFER COEFFICIENTS

The relevant physical properties and heat transfer coefficients were

assumed to be the same as that for the conduction model. Finally, discussions of the results of this model are presented in section (5.3). Moreover, the temperature histories predicted by this model were compared to the corresponding experimental temperature histories to check the validity of this approach. Also, a comparison between these results and those using the conduction model are presented in the same section.

4.4 OPEN CHANNEL WET BEDS

4.4.1 FORMULATION OF THE PROBLEM

The configuration is that of a hollow cylinder constituted of a solid phase, liquid phase(water) and a gaseous phase composed of air and vapour(water vapour). The cylinder is exposed to a stream of hot air of known properties through the inner channel while the outer surface was impervious and insulated. As a result of the convective flow of air, heat will be transported to the bed, water will vaporize and diffuse towards the central channel. Heat losses from the bed were taken into consideration using the same method of the previous models. Though the rate of evaporation was not measured experimentally, the present model was formulated as a complementary part to the experimental study to help in understanding the role of different parameters. Furthermore, the experimental transient temperature profile will be compared with those predicted by this model to check the validity of the model.

4.4.2 THEORETICAL BACKGROUND

The theoretical formulation of the equations was drawn from Whitaker's theoretical approach(42,43). Whitaker used the local volume averaging technique to develop a rigorous set of governing equations for the transport processes in porous media. He defined two different averages of a quantity; these are spacial average (local volume average) and the intrinsic phase average. The local volume average of a function Ψ is represented by $\langle\Psi\rangle$ and is defined by:

$$\langle\psi\rangle = \frac{1}{V} \int_V \psi \, dV \tag{4.13}$$

while, the intrinsic phase average of a function Ψ over the phase i is represented by $\langle\Psi\rangle^i$ and is defined by:

$$\langle\psi\rangle^i = \frac{1}{V_i} \int_V \psi \, dV \tag{4.14}$$

Appendix (A) shows the final set of equations derived by Whitaker in their general form along with the main assumptions of his theoretical approach.

4.4.3 MAIN ASSUMPTIONS OF THE THEORY OF WHITAKER

1. The enthalpy of solid, liquid and gaseous phases is a linear function of temperature

2. The solid phase is a rigid matrix fixed in an inertial frame.

3.   Liquid phase density is constant.

4.   The three phase system is in local equilibrium.

5.   The gas phase is ideal in the thermodynamic sense.

6.   The gas phase is continuous.

7.   There is no chemical reaction in the gaseous phase.

4.4.4 SIMPLIFYING ASSUMPTIONS

1.   The liquid phase is not continuous, and there is no transport of moisture due to liquid motion. Initially the bed could be considered in the pendular state* where moisture migration is in the vapour state only.

2.   The total pressure is constant everywhere and equal to the atmospheric pressure.

3.   Transport processes occur along the radial direction only.

4.   The partial pressure of the vapour in the wet region is equal to its equilibrium pressure at the corresponding temperature.

5.   There is no chemical reactions in any of the phases.

---

*According to ref. 13 the Pendular state is the phase distribution at very low saturations (wetting phase), where the wetting phase is distributed in the pores as discrete masses. Each mass is a ring of liquid wrapped around the contact point of adjacent elements of the solid matrix.

4.4.5 GOVERNING EQUATIONS OF THE PRESENT MODEL (DRYING MODEL)

The assumptions made in the previous section reduce the set of equations to the following:

a) Total thermal energy equation

$$\frac{\partial}{\partial t}\langle \rho c_p T \rangle + (\langle \rho_v \rangle^g \langle v_v \rangle \langle (c_p)_v \rangle^g) \frac{\partial \langle T \rangle}{\partial r} + \langle \dot{m} \rangle \Delta h_v$$

$$= \frac{1}{r} \frac{\partial}{\partial r} \left(r \, k_e \, \frac{\partial T}{\partial r} \right) \qquad (4.15)$$

where:

$\langle \dot{m} \rangle$ = mass rate of evaporation per unit volume (kg/s m³)

Δh = enthalpy of vaporization per unit mass (J/kg)

v_v = velocity of the vapour phase (m/s)

and for the subscripts:

g = gaseous phase

v = vapour

b) Liquid phase continuity equation

$$\frac{\partial}{\partial t}(\rho_l \varepsilon_l) + \langle \dot{m} \rangle = 0 \qquad (4.16)$$

where l stands for the liquid phase

c) Gas phase diffusion equation

where:

$$\frac{\partial}{\partial t}(\varepsilon_g \langle \rho_v \rangle^g) + \frac{1}{r}\frac{\partial}{\partial r}[\ r \ (\langle \rho_v \rangle^g \langle v_v \rangle) \ ] - \langle \dot{m} \rangle = 0 \qquad (4.17)$$

$$\langle \rho_v \rangle^g \langle v_v \rangle = - \ \frac{\langle \rho_g \rangle^g D_{ve}}{1 - \langle \rho_v \rangle^g / \langle \rho_g \rangle^g} \ \frac{\partial}{\partial r}(\frac{\langle \rho_v \rangle^g}{\langle \rho_g \rangle^g}) \qquad (4.18)$$

where D_{ve} is the vapour phase effective diffusivity

d) Volume constraint

$$\varepsilon_s + \varepsilon_l(t) + \varepsilon_g(t) = 1 \qquad (4.19)$$

where the subscript "s" stands for the solid phase.

e) Thermodynamic relations

$$\langle P_v \rangle^g = \langle \rho_v \rangle^g \ R_v \ \langle T \rangle \qquad (4.20)$$

$$\langle P_a \rangle^g = \langle \rho_a \rangle^g \ R_a \ \langle T \rangle \qquad (4.21)$$

$$\langle P_g \rangle^g = \langle P_v \rangle^g + \langle P_a \rangle^g \qquad (4.22)$$

$$\langle \rho_g \rangle^g = \langle \rho_v \rangle^g + \langle \rho_a \rangle^g \qquad (4.23)$$

where subscript "a" stands for air and $\langle P_v \rangle^g = \frac{1}{V_g} \int_v P_v \ dv$ in accordance with

equation 4.13

$$\langle P_v \rangle^g = P^*(T) \qquad (4.24)$$

where P^* is the equilibrium pressure at the corresponding temperature.

4.4.6 INITIAL AND BOUNDARY CONDITIONS

a) Initial conditions

Initially the temperature was assumed constant everywhere and equal to the atmospheric temperature. The moisture content was also constant everywhere within the bed.

$$T(r,0) = T_{am} \qquad r_1 \leq r \leq r_3 \qquad (4.25)$$

$$\varepsilon_l(r,0) = \varepsilon_{lo} \qquad r_1 \leq r \leq r_2 \qquad (4.26)$$

b) Boundary conditions

1) On the central channel surface (r_1)

The heat and mass fluxes are continuous:

$$\langle \rho_v \rangle^g \langle v_v \rangle = h_m(\langle \rho_v \rangle^g - (\rho_v)_f) \qquad (4.27)$$

where

h_m = convective mass transfer coefficient (m/s)

$(\rho_v)_f$ = average vapour density in the convective stream (kg/m³)

$$-k_e \frac{\partial \langle T \rangle}{\partial r} = h_c (T_c - \langle T \rangle) \qquad (4.28)$$

2) On the outer surface of the bed (r_2)

The surface is impermeable to the mass flux.

$$\langle \rho_v \rangle^B \langle v_v \rangle = 0 \qquad (4.29)$$

Equations 4.2 and 4.4 were applied for the insulation region

4.4.7 PHYSICAL PROPERTIES AND COEFFICIENTS

1.Effective mass diffusivity

A literature review has been done by Kaviany(13) for the reliable formulas of effective mass diffusivity in porous media. Neale and Nader (30) have determined a formula for the effective mass diffusivity for a binary gas mixture within packed beds of impermeable spheres. The formula was derived using a geometric model and verified experimentally and given by:

$$\frac{D_{ve}}{D_v} = \frac{2\varepsilon}{3 - \varepsilon} \qquad (4.30)$$

where:

D_{ve} = effective binary mass diffusion coefficient (m^2/s)

D_v = binary mass diffusion coefficient (m^2/s)

Ryan et al (36) determined another formula for isotropic media in the

form:

$$\frac{D_{ve}}{D_v} = \frac{D_{ve}}{D_v}(\varepsilon) \qquad (4.30)$$

Both formulas are in good agreement with each other (13). Equation (4.29) was modified by Kaviany (13) to account for the presence of the liquid and takes the form:

$$\frac{D_{ve}}{D_v} = \frac{2\varepsilon}{3 - \varepsilon} (1 - S) \qquad (4.31)$$

where S is the liquid saturation, Equation (4.31) was used in this study. The following empirical equation by Brokaw is recommended by Reid et al (35) for estimating the binary mass diffusion coefficient of binary mixtures D_v for systems containing polar components:

$$D_{12} = \frac{1.858 \times 10^{-3} \; T^{3/2}\sqrt{1/M_1 + 1/M_2}}{P \; \sigma_{12}^2 \; \Omega} \qquad (4.32)$$

where:

D_{12}	=	gas diffusion coefficient (cm^2/s)
T	=	absolute temperature (K)
M_1, M_2	=	molecular weights of components 1 and 2
P	=	absolute pressure (atm)

σ_{12} = collision diameter, Å

Ω = collision integral for diffusion

Detailed calculation procedure of D_{12} is given in reference (35)

2) Effective thermal conductivity

In wet granular porous media, the liquid partially or completely displaces the gaseous phase thus increasing the effective thermal conductivity of the bed. Literature review in the area of wet porous media reveals a lack of information regarding the effective thermal conductivity. The following relation was used as given by Nield and Bejan (31)

$$k_e = \varepsilon(S_l k_l + S_g k_g) + (1-\varepsilon)k_s \qquad (4.33)$$

where:

S_l = saturation of the liquid phase

3) Convective mass transfer coefficient

Kays and Crawford (14) confirmed that if heat transfer data for the case of no blowing or suction at the surface is available ,which is usually expressed as:

$$Nu = C \, Re^a \, Pr^b \qquad (4.34)$$

then analogy of heat and mass transfer processes is possible if the mass transfer rates are small, and the mass transfer coefficient could be calculated using the following relation:

$$Sh = C \ Re^a \ Sc^b \qquad (4.35)$$

where:

Sh = Sherwood number ($h_m d/D_{12}$)

h_m = average convective mass transfer coefficient (m/s)

Sc = Schmidt number (vf/D_{12})

Other terms were defined earlier.

4. Heat transfer coefficient

The heat transfer coefficient in the case of drying was discussed by Keys (15), for the case of undersurface evaporation and small mass fluxes, the local heat transfer coefficient is given by the following relation:

$$h_c = A \ \frac{k}{x} \ Re_x^m \ Pr^q \qquad (4.36)$$

where:

h_c = convective heat transfer coefficient (W/m^2 K)

x = the distance in the direction of the convective stream (m)

A, m and q are empirical constants which depend on the physical problem. For developed laminar or turbulent flow in ducts of arbitrary geometry, the values of the constants are given by Keys (15), as follows, A=0.538, m=(2/3) and q=(1/3). In this case, the Reynolds number (Re_x) is not based upon the free stream velocity but the friction velocity which is defined as follows:

where τ_s is the shear stress at the surface. Employing the relations of the

$$u_s = \sqrt{\frac{\tau_s}{\rho}} \qquad (4.37)$$

shear stress for laminar flow in pipes (e.g. ref. 37) and with mathematical manipulation the final equation is given as follows:

$$h_c = 1.85 \, Re_d^{(\frac{1}{3})} \, Pr^{(\frac{1}{3})} \, (\frac{d}{x})^{(\frac{1}{3})} \qquad (4.38)$$

Averaging the latter equation over the length leads to equation (4.8) of the dry beds without the refining factor of the relative viscosity. In other words, the heat transfer coefficient is slightly affected in case of small mass fluxes. Hence equation 4.8 was used to calculate average heat transfer coefficient.

CHAPTER 5

DRY GRANULAR BEDS

RESULTS AND DISCUSSION

5.1 OPEN CHANNEL CONFIGURATION

It was expected that the primary mode of heat transfer within the beds with open central channel configuration is by pure conduction. This makes the open channel configuration considerably simpler to study compared to the case of beds with packed channel. The open channel configuration was studied at the beginning for the following reasons :

i.   To examine some of the available formulas for establishing the effective thermal conductivities of granular beds and to determine the formula most suitable for modelling the packed channel configuration.

ii. To provide information about the thermal characteristics and behaviour of the apparatus and estimate the essential associated heat transfer data for modelling.

iii. To study the effects of the different parameters that control the process of heat transfer in granular beds.

In order to achieve these goals, a set of experimental runs were carried out. The experimental procedure and measurement techniques outlined in chapter 3 were followed in conducting these tests. Three sizes of glass beads were used, namely, of 0.27 mm, 0.7 mm and 1.3 mm diameter. The air mass

flow rate of the electrically heated air ranged from 1.6 kg/h to 2.4 kg/h. The heating air temperature was varied from 100°C to 200°C at the inlet section. Figure 5.1 show schematically the Open Channel configuration with the location of the measured temperatures.

Figures 5.2 - 5.4 inclusive show typical temperature histories for open channel beds of different glass bead sizes and different flow conditions. The figures show the same general trend, namely, a relatively fast initial rise of temperature which gradually tends to approach the steady state conditions. This could be explained as follows: as air is introduced, the high temperature difference between the air and the bed creates a high thermal driving force that leads to high heat transfer rates and thus relatively faster temperature rise. As the bed temperature rises and the temperature difference decreases, the rate of heat transfer drops and consequently the temperature rise rate drops.

It was observed experimentally that the spacial temperature gradient in the axial direction was negligibly small (as illustrated in figure 5.5). Hence, the average temperature, defined as the arithmetic mean of the temperatures within the bed and in the direction of the flow, will be used thereafter for comparison purposes. It has to be noted that *the temperatures were measured at the mid-radii of the beds.*
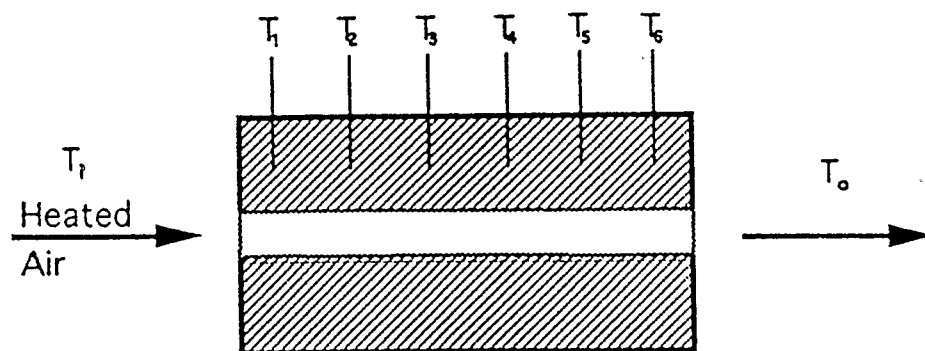
Figure 5.1   A schematic diagram of an Open Channel bed showing the location of the various thermocouples.
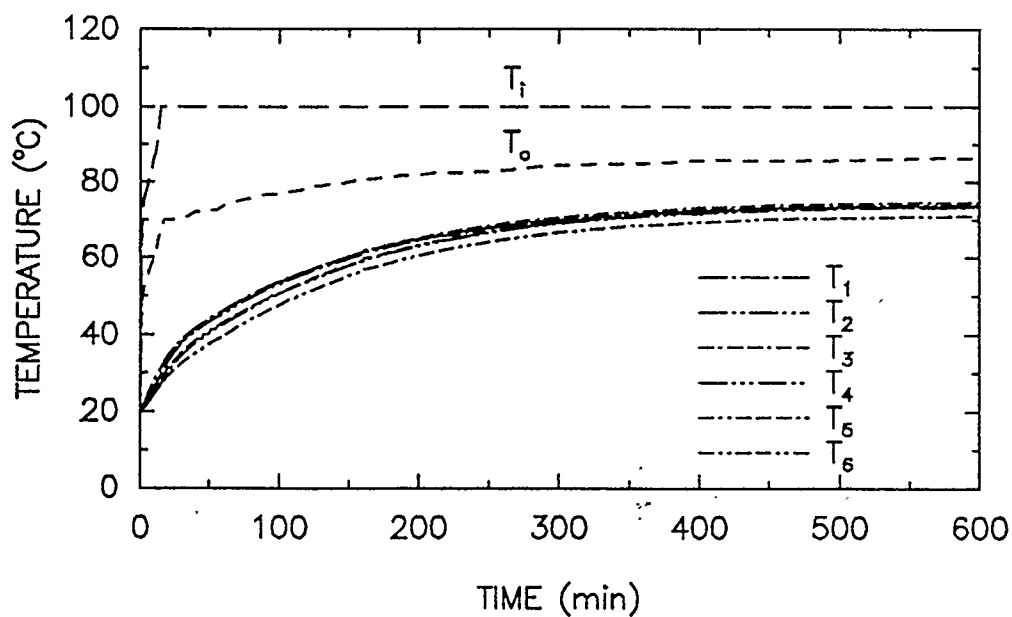
Figure 5.2   Variation of the measured temperatures with time for a dry bed Configuration: Open Channel, $d_b = 0.7$ mm, m= 1.6 kg/h
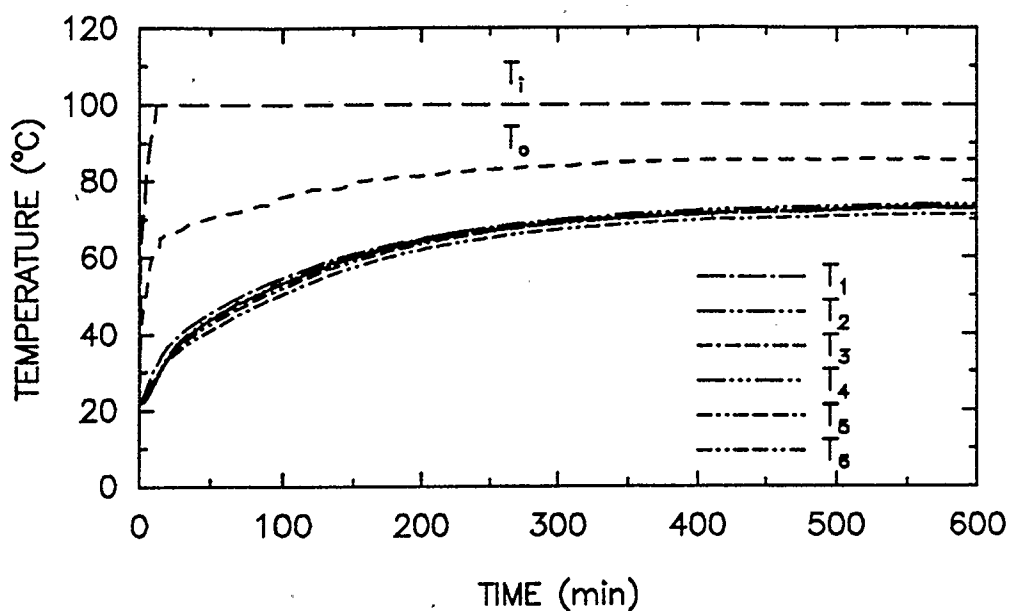
Figure 5.3   Variation of the measured temperatures with time for a dry bed
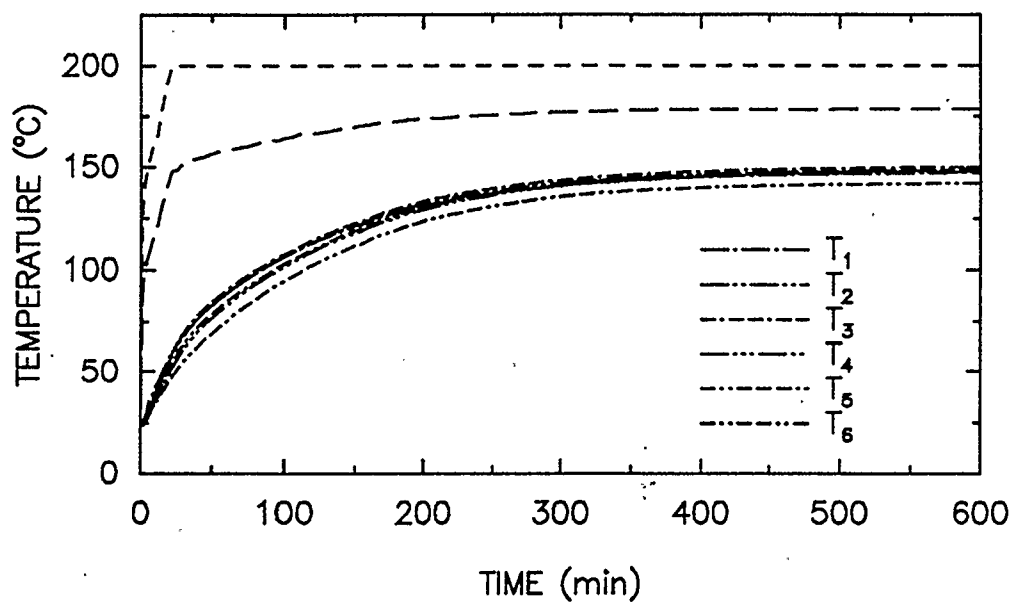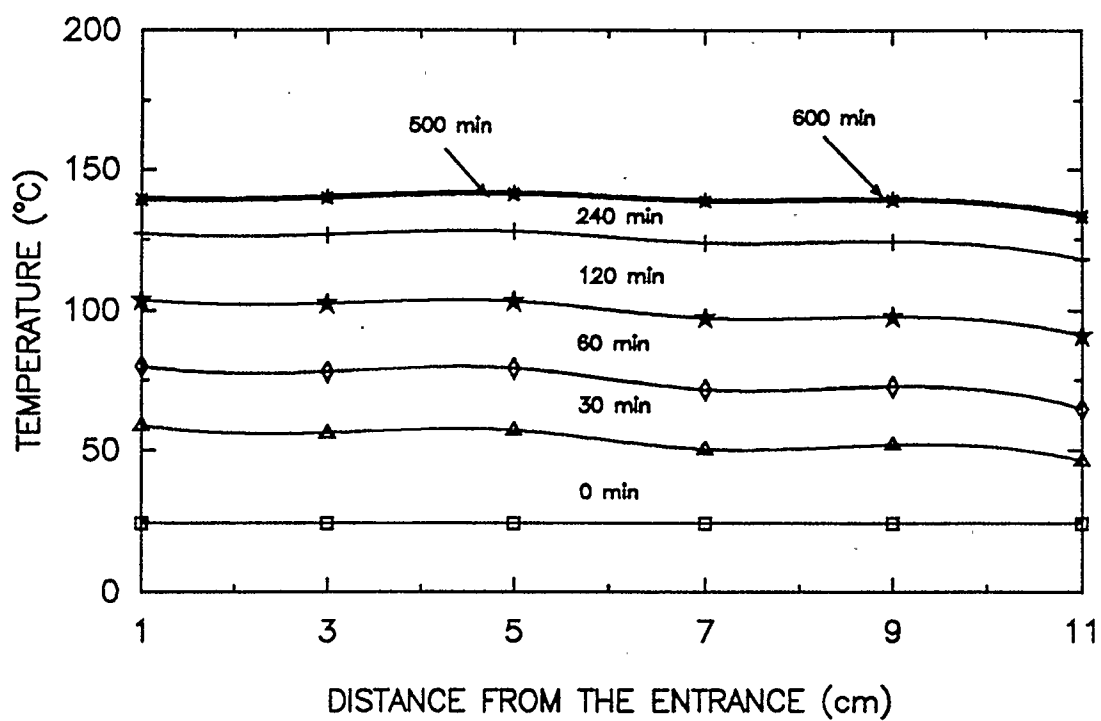Configuration: Open Channel, $d_b = 0.27$ mm, m= 1.6 kg/h

Figure 5.4   Variation of the measured temperatures with time for a dry bed
Configuration: Open Channel, $d_b =1.3$ mm, m=1.6 kg/h

Figure 5.5   Variation of the measured axial temperature profile with time for a dry bed, Configuration: Open Channel, d_b = 0.7 mm, m = 1.6 kg/h

5.1.1 EFFECT OF MASS FLOW RATE

Figure 5.6 shows the average temperature history for a bed of 0.7 mm glass beads when exposed to a heated air stream of 200°C at different mass flow rates. The graph shows that higher mass flow rates of air, in general, bring about higher temperature levels within the bed. This could be attributed to the enhanced convective heat transfer coefficient associated with higher stream velocities within the channel. This leads to higher surface temperature and heat transfer rates.

5.1.2 EFFECT OF GLASS BEAD SIZE

Figure 5.7 shows the average bed temperature history for three sizes of bed glass beads, namely, 0.27 mm, 0.7 mm and 1.3 mm diameter, when exposed to the same mass flow rate of 1.6 kg/h and T_i=200°C. It is obvious that the three temperature histories are almost identical. This implies that the glass bead size has a negligible effect on the heat transfer process. An explanation could be offered for this observation. It has been reported by many researchers in the literature review given in reference (13) that for isotropic beds of spherical particles, the effective thermal conductivity could be expressed as a function of the following factors:

1. Relative magnitude of the solid and fluid phases thermal conductivity.

2. Porosity of the bed.

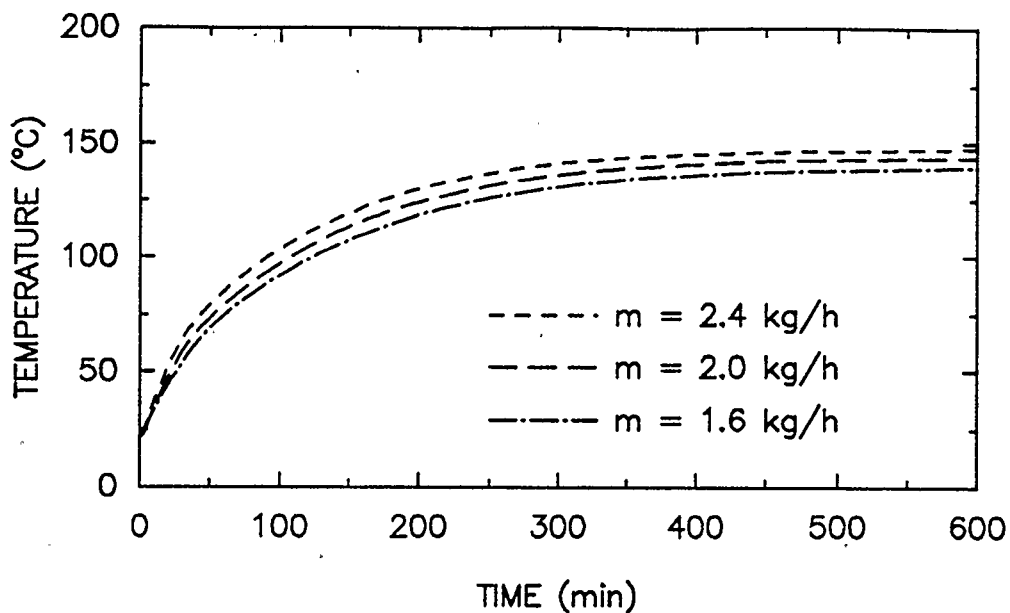Since the same combination of solid and fluid phases were used, hence

Figure 5.6 Variation of the measured temperatures with time for identical dry beds when subjected to three different mass flow rates of a heated air, Configuration: Open Channel, d_b=0.7 mm
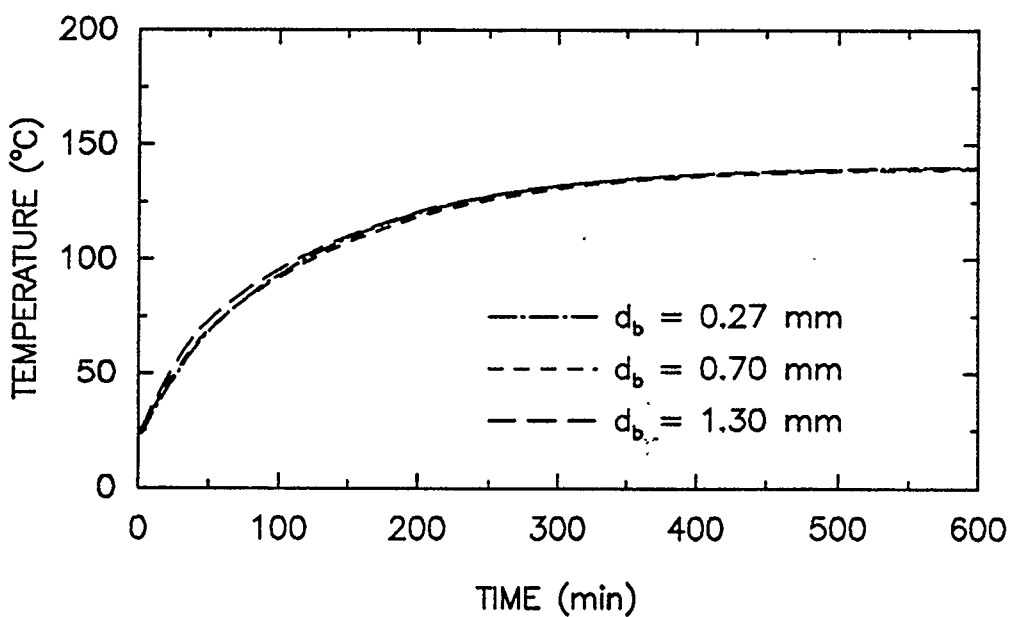

Figure 5.7 Variation of the measured temperatures with time for dry beds of different glass beads sizes, Configuration: Open Channel, m=1.6 kg/h

the first parameter was constant for all beds tested. Secondly, for random packing of spheres the value of porosity was reported to vary from 0.37 to 0.38 (13,26,15). Using these values the maximum difference in the effective thermal conductivity was found to be less than 2%.

5.1.3 COMPARISON WITH THE CONDUCTION MODEL

Figures 5.8 and 5.9 shows examples of the predicted temperature histories using the conduction model and applying the geometric mean relation to describe the effective thermal conductivity of the bed versus the experimental temperature histories. The experimental transient stream temperature was used in generating these plots to simulate the heat input exactly. As it can be seen from the graph, excellent agreement is evident. These sets of runs confirmed the validity of the model and the boundary conditions used in this model. Accordingly, it can be concluded that the conduction model and the boundary conditions appears to simulate accurately the real problem. Also, the geometric mean relation could be used with confidence in evaluating the effective thermal conductivity of these granular beds.

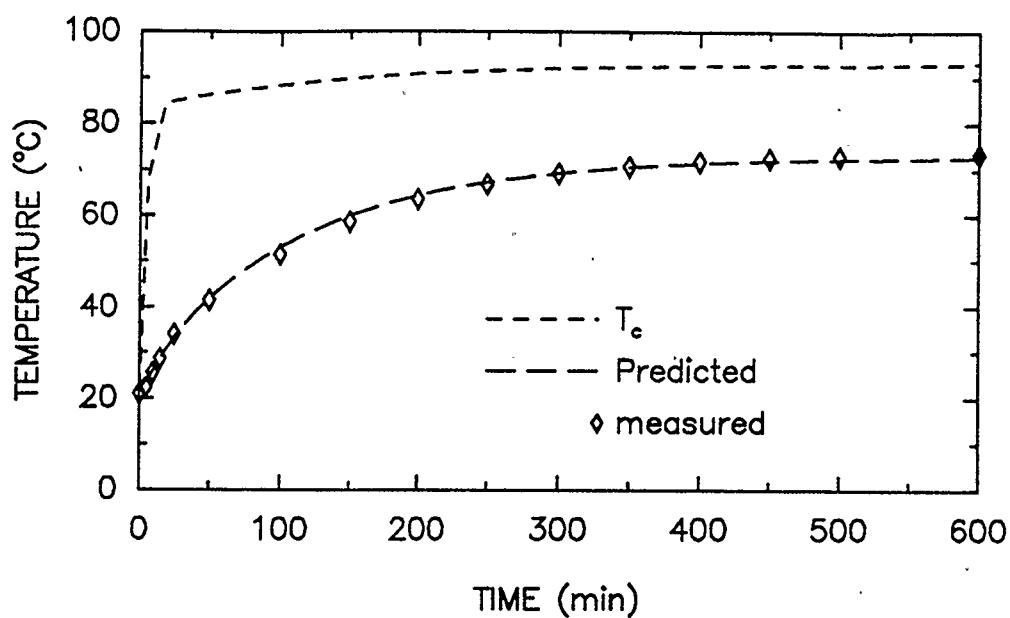Thus, the main objectives of this set of experiments were successfully achieved.

Figure 5.8 Predicted versus measured average temperature variation with time for a dry bed, Configuration: Open Channel, d_b=0.7 mm, m=1.6 kg/h
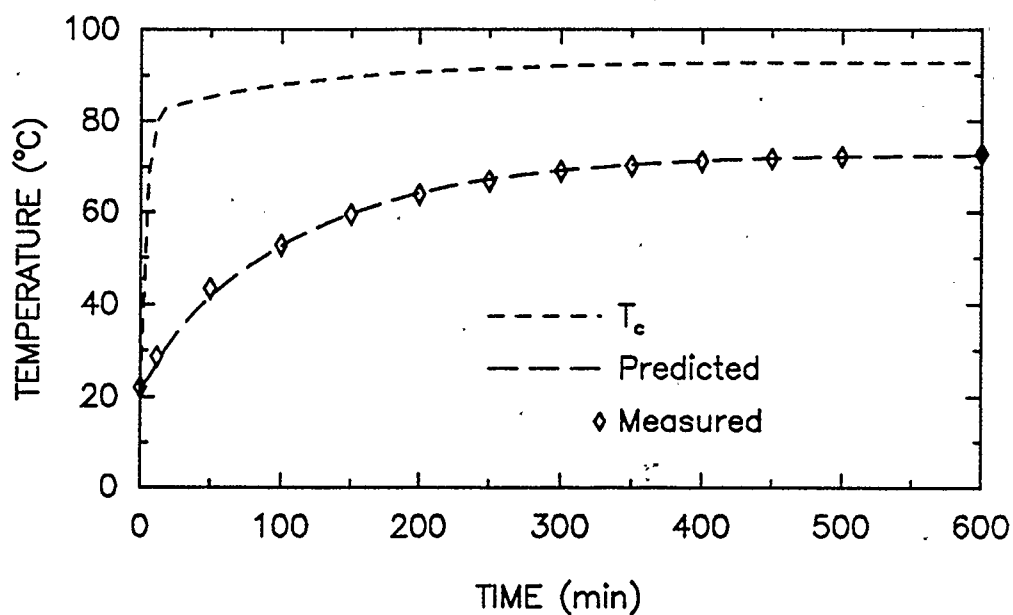

Figure 5.9 Predicted versus measured average temperature variation with time for a dry bed, Configuration: Open Channel, d_b=0.27 mm, m= 1.6 kg/h

5.2 PACKED CENTRAL CHANNEL CONFIGURATION

In the second set of runs, granular beds with the central channel filled with glass beads were examined. The main objectives of this study were:

i.   To expand the understanding of the mechanism of heat transfer in packed beds when some radial dispersion of air and internal convection are expected to occur.

ii. To determine the effect of changes in the various parameters that govern the process of heat transfer in such configuration.

iii. To estimate the extent of internal convection relative to conduction heat transfer within the beds.

iv. To provide some information about the flow of air within the bed which should help in examining the wet beds of the same configuration.

A set of runs were carried out to study the heat transfer behaviour in this configuration. Figure 5.10 shows schematically this configuration with the location of the measured temperatures. For comparative purposes; the same sizes of glass beads of the open channel configuration were used namely 0.27 mm, 0.7 mm and 1.3 mm beads. The glass beads used in the central channel were 1.3 mm and 3 mm diameter and the mass flow rate ranged from 1.6 kg/h to 2.4 kg/h.

Figures 5.11 -5.14 show typical temperature histories along the length of the bed. The graphs show that the presence of glass beads in the central channel, in general, led to higher heat transfer rates to the bed. Higher level

of temperatures could be seen within the bed when compared to the corresponding values for the open channel configuration at the same operating conditions. Also the thermal response was faster when compared to the open channel runs. The presence of glass beads within the central channel led to higher velocities which enhanced the convective heat transfer coefficient at the bed inner surface, and hence higher heat transfer rates as well as faster thermal responses. Moreover, the presence of glass beads in the channel induced some flow of hot air radially into the bed which enhanced the heat transfer; this phenomenon is known as dispersion.

In order to improve the understanding of the mechanism of heat transfer in this configuration, a parametric study was performed experimentally to investigate the effect of the various parameters that govern the heat transfer process. The results of the later investigation are presented in sections 5.2.1 to 5.2.3. Section 5.2.4 shows a comparison between the experimental results and the results obtained when using the conduction model and the convection model discussed in sections 4.2 and 4.3, respectively.

5.2.1 EFFECT OF MASS FLOW RATE

Figure 5.15 shows the effect of the mass flow rate on the temperature history at middle of the bed for 0.7 mm diameter glass beads bed with the central channel filled with 3 mm diameter glass beads. The graph shows an increase of temperature level within the bed with the increase of mass flow
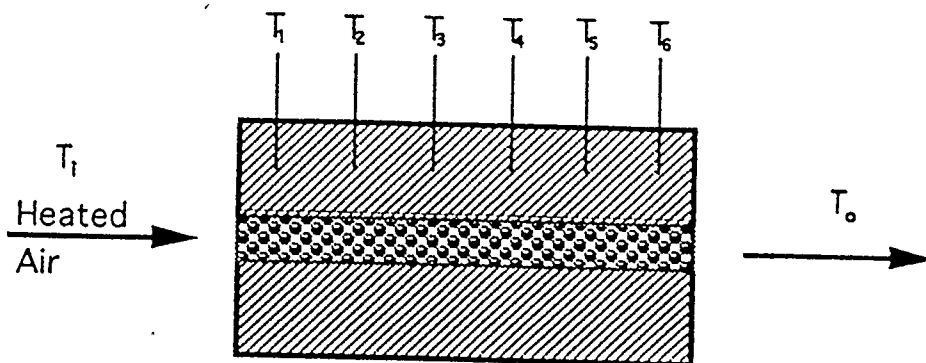
Figure 5.10 A schematic diagram of a packed Channel bed showing the location of the various temperatures.
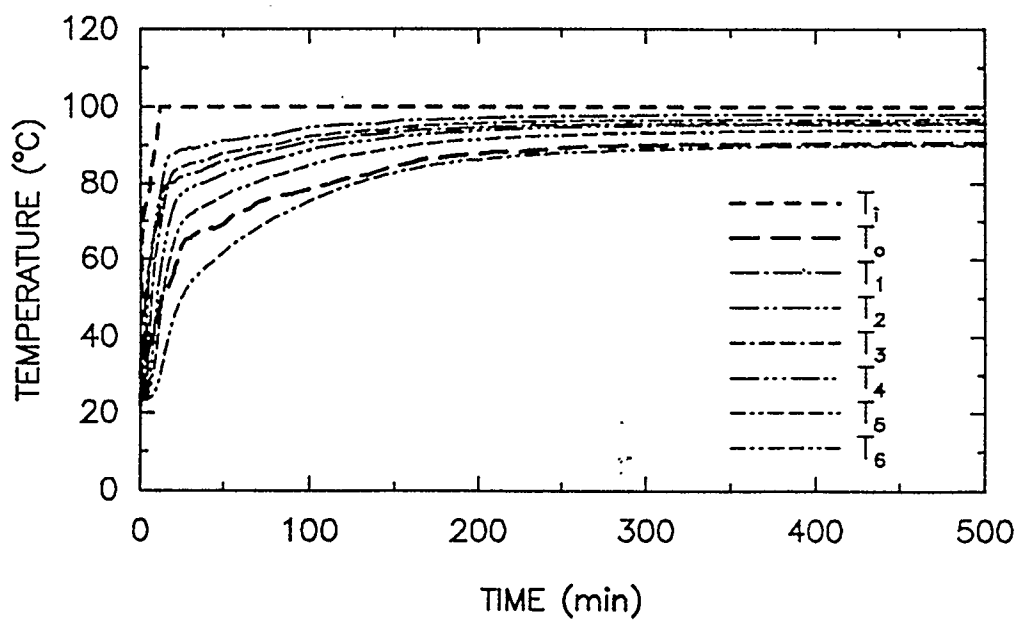

Figure 5.11 Variation of the measured temperatures with time for a dry bed Configuration: Packed Channel, d_b=0.7 mm, d_p=3.0 mm, m=2.4 kg/h
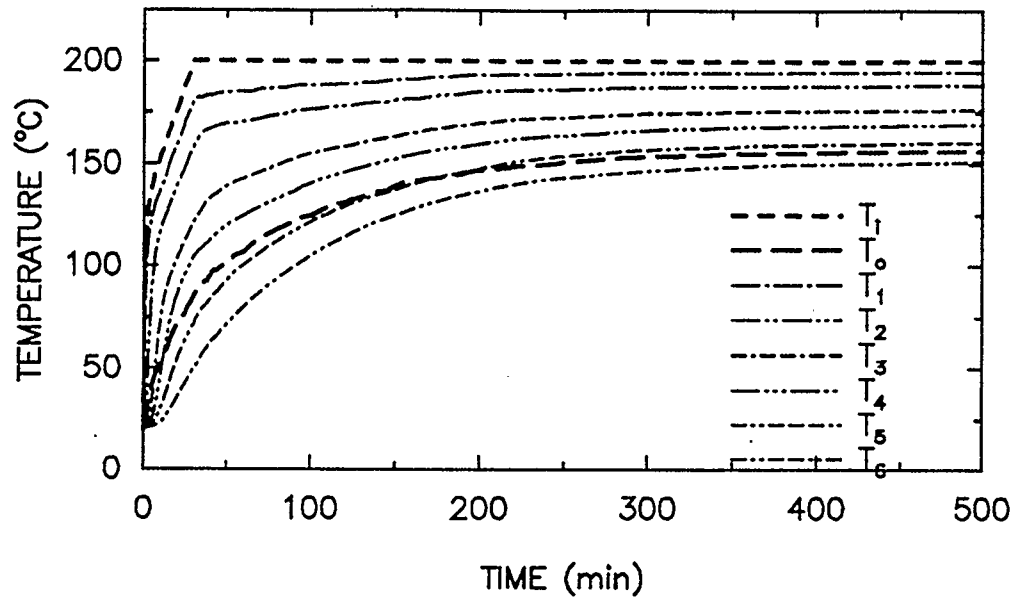
Figure 5.12 Variation of the measured temperatures with time for a dry bed
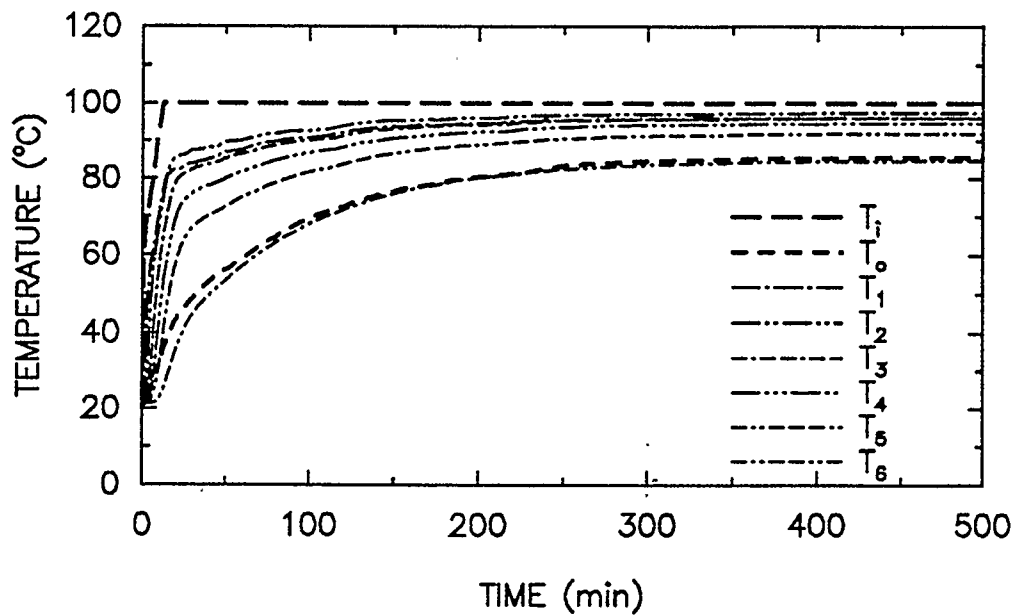Configuration : Packed Channel , d_b= 0.27 mm , d_p=3.0 mm ,
m=1.6 kg/h

Figure 5.13 Variation of the measured temperatures with time for a dry bed
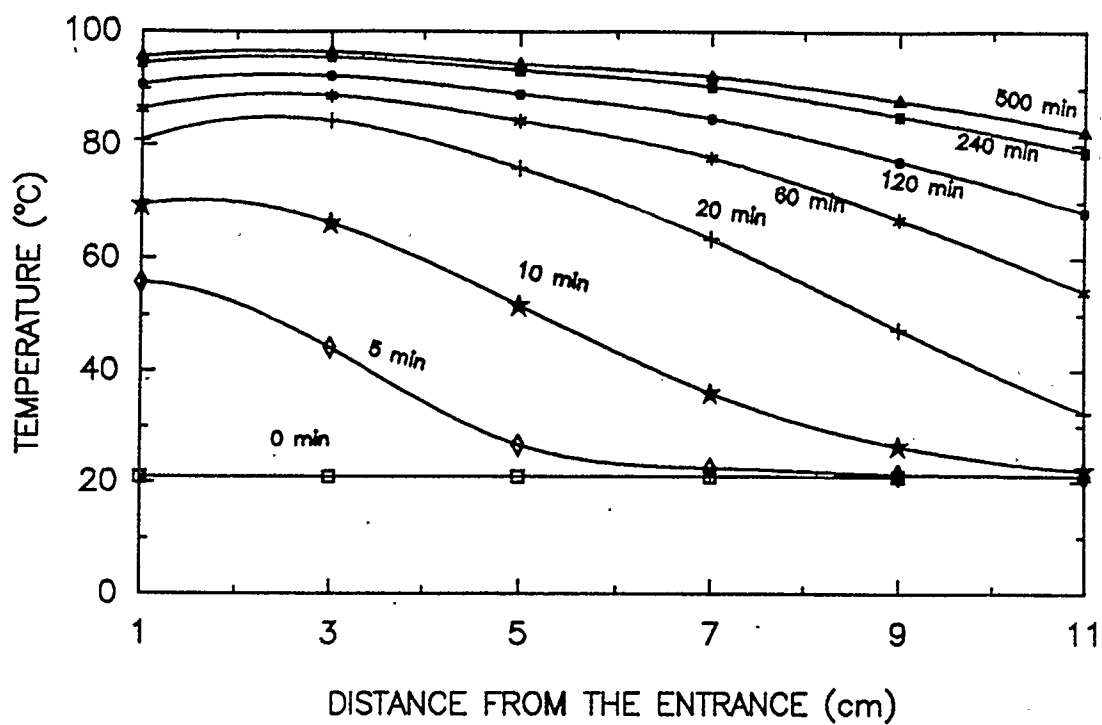Configuration : Packed Channel , d_b= 0.7 mm, d_p = 3.0 mm,
m=2.0 kg/h

Figure 5.14 Variation of the measured axial temperature with time for a dry bed, Configuration : Packed Channel, d_b = 0.7 mm, d_p = 3.0 mm, m = 1.6 kg/h

rate of the heating air. This could be attributed to the enhanced heat transfer coefficient which is associated with the higer stream velocities. Also, higher mass flow rates induces a higher rate of dispersion of air through the bed which enhances the heat transfer process.

5.2.2 EFFECT OF CHANNEL GLASS BEAD SIZE

The effect of the glass beads size of the central channel on the heat transfer rate can be seen typically in figure 5.16. Three sizes were used in the central channel, 3.0 mm, 1.6 mm and 1.3 mm for a bed of 0.7 mm diameter glass beads and at the same mass flow rate. It can be seen that finer channel beads resulted in higher heat transfer rates which is manifested in the higher temperature levels attained. The finer glass beads have almost the same porosity but they have lower permeability which represents a further restriction to the flow and induces higher radial dispersion. This may account for the higher heat transfer rates within the bed associated with finer channel beads.

5.2.3 EFFECT OF BED GLASS BEAD SIZE

Figure 5.17 shows a comparison of the temperature histories of three different glass bead sizes when the central channels was filled with 3 mm diameter glass beads. The experimental results show an increase of temperature level for beds of coarser beads. Comparing this behaviour to that

of the open channel configuration, it can be seen that the packed channel bed behaved differently. In other words, while the open channel configuration showed no significant effect of the bed glass beads size on the heat transfer rates, the packed channel configuration showed that this parameter influences the heat transfer rates. This different behaviour supports the existence of dispersion of air within the bed and emphasizes the significant role of dispersion in heat transfer for this configuration. The observed increase of heat transfer rate in beds of coarser beads could be explained as latter beds possess higher permeabilities which enhances the dispersion of air into the bed and in turn, the heat transfer rates.

5.2.4 COMPARISON WITH THE DISPERSION MODEL

As mentioned earlier in chapter 4, two models were attempted to describe the problem of heat transfer within dry beds of the packed channel configuration. The first approach was to use the conduction model along with the experimental surface temperature to predict the temperature history within the bed. In order to employ the conduction model for the packed channel configuration, an approximate technique was introduced and explained in section 4.3.1. The later technique assumes the bed to be divided in the axial direction into six segments; within each segment heat transfer occurs in the radial direction only. Figure 5.18 shows a typical comparison between the conduction model results and the corresponding experimental measurements.
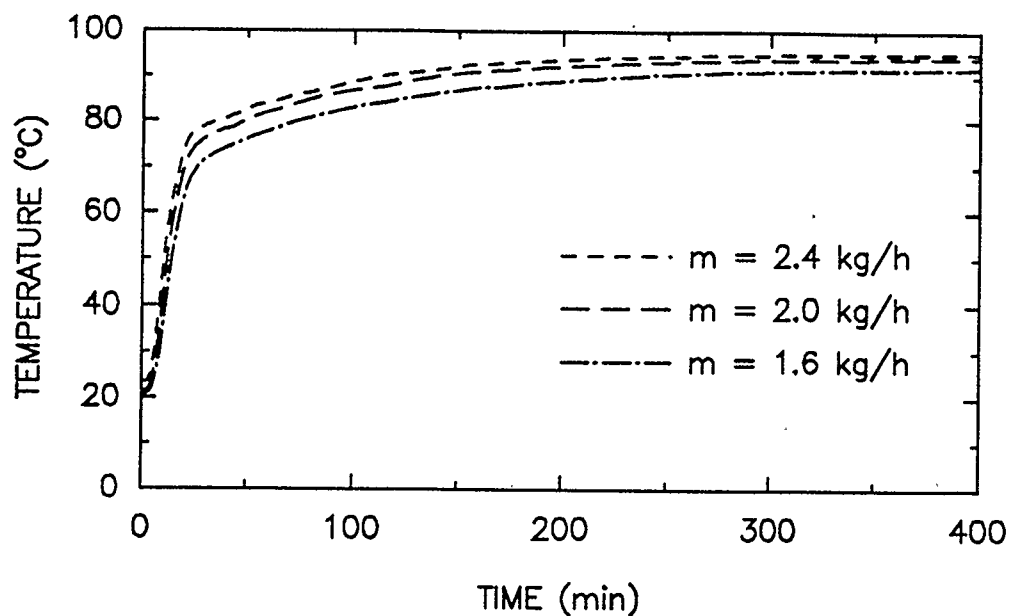
Figure 5.15 Variation of the measured temperatures with time for a dry bed when subjected to three different mass flow rates of heated air, Configuration: Packed Channel, d_b=0.7 mm, d_p=3.0 mm

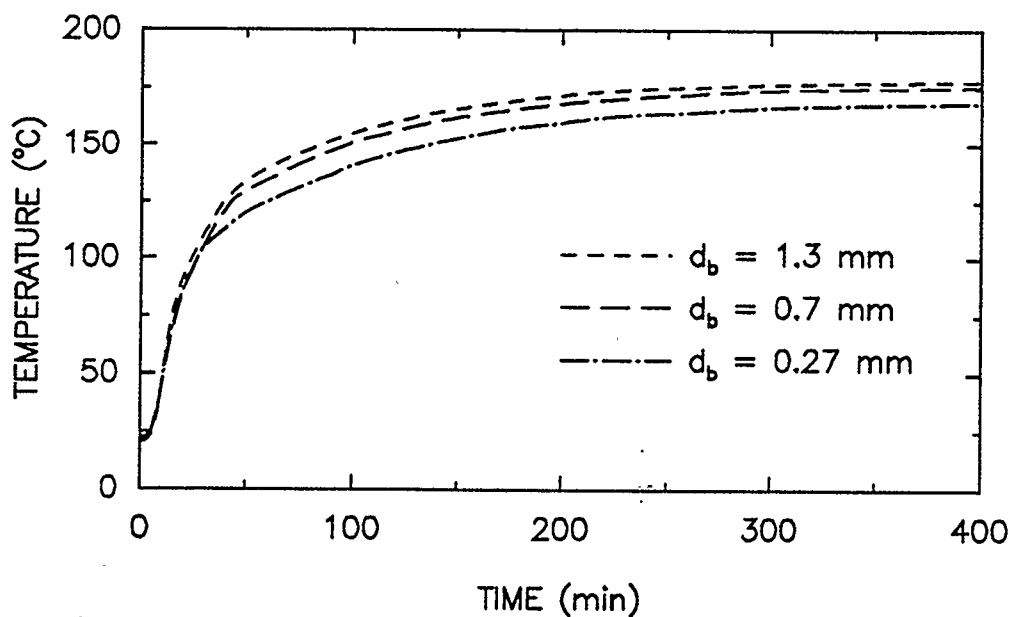Figure 5.16 Variation of the measured temperatures with time for dry beds of different glass bead sizes, Configuration: Packed Channel, d_p=3.0 mm, m = 1.6 kg/h
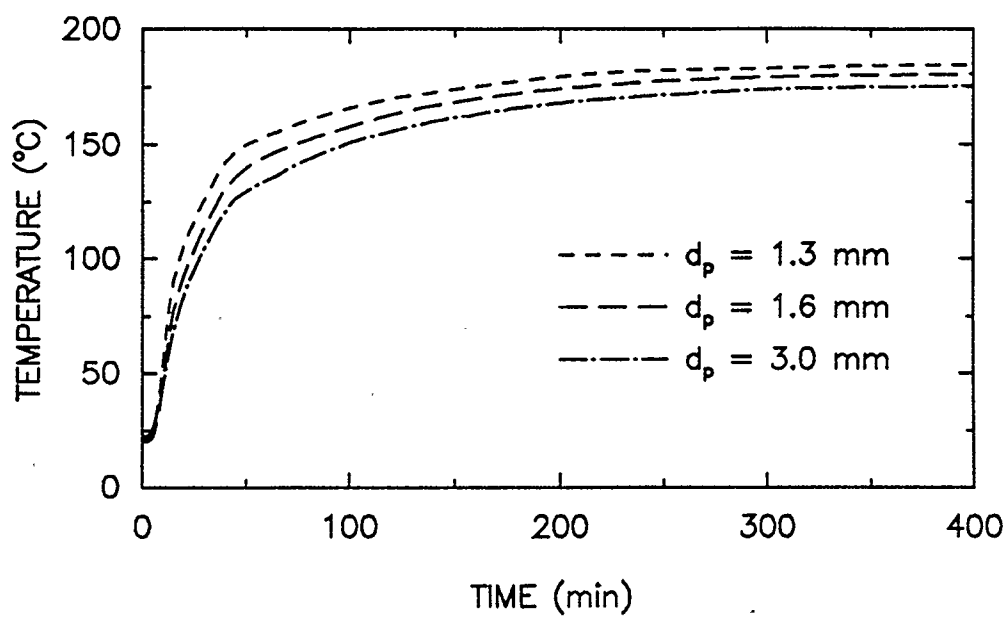
Figure 5.17 Variation of the measured temperatures with time for dry beds
with different channel glass bead sizes, Configuration: Packed
Channel, d_b = 0.7 mm, $\dot{m}$ = 1.6 kg/h

It is to be noted that the comparison was based on the temperatures at the mean radius of the bed, hence the term "temperature" if stated alone will refer to the values at the mean radius of the bed. It is obvious from figure 5.18 that predicted temperatures are consistently lower than the measured values even at the steady state. In order to estimate the extent of dispersion, the dispersion model described in section 4.3 was constructed and used. The same approximate method mentioned above was used in addition to the assumption that dispersion occurs only radially. The trial and error technique used to estimate the dispersion velocity within each segment could be described as follows:

1. A dispersion velocity at the channel surface was initially assumed.

2. Using the experimentally measured surface temperature as input to the dispersion model, the temperatures within the bed were predicted and compared to the corresponding measured one (i.e at the same radial position).

3. Steps 1 and 2 were repeated for different assumed dispersion velocities until the predicted steady state temperature was matched with the experimentally measured temperature.

The same procedure was carried out for the six segments to get the velocity distribution along the bed. Figures 5.19 - 5.21 show the final prediction of the model for the mid-radius temperature at various distances from the entrance versus the experimentally measured ones. As it can be seen, there is a

noticeable improvement of the transient results when compared to those predicted by the conduction model. To investigate the factors that affect the dispersion rate, the next subsections show the results of several runs at different conditions.

5.2.4.1 EFFECT OF MASS FLOW RATE

Figure 5.22 shows a comparison of the calculated radial dispersion velocities at the channel surface for two 0.7 mm beds at two different mass flow rates of 1.6 kg/h and 2.4 kg/h. It can be seen from the figure that the radial dispersion velocities increase by the increase of mass flow rate of air within the channel. This supports the explanation offered in section 5.2.1.

5.2.4.2 EFFECT OF CHANNEL GLASS BEADS

Figure 5.23 shows a comparison of the calculated radial dispersion velocity at the channel surface for 0.7 mm glass bead beds with the channel filled by 1.3 mm and 3 mm glass beads. The figure shows that the level of dispersion velocity increased by using finer glass beads in the channel. This also supports the explanation offered in section 5.2.2.

Finally, it is expected to have a similar trend for the effect of bed glass bead sizes.
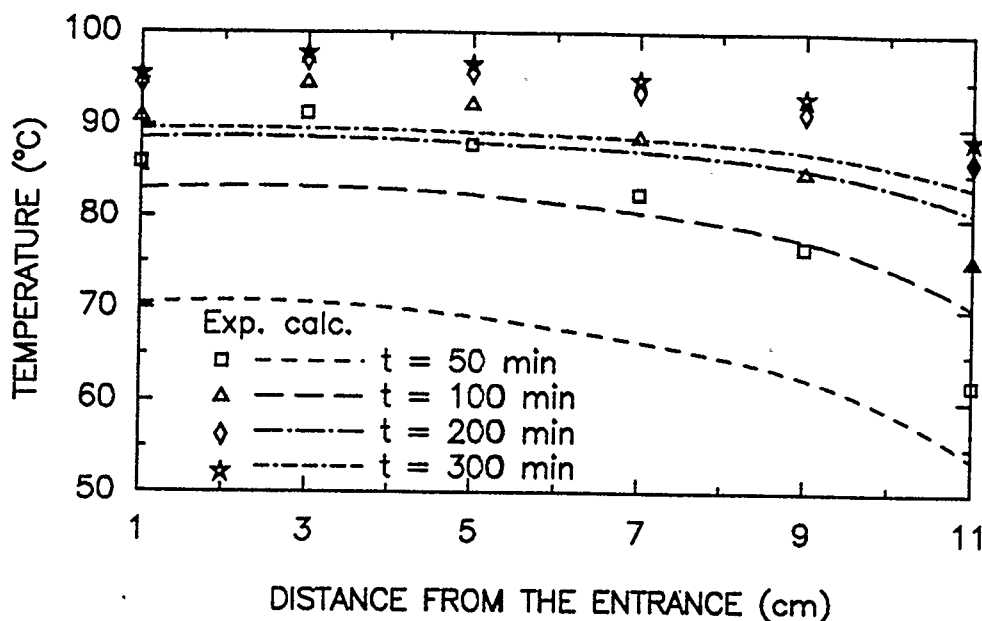
Figure 5.18 Comparison of the variation of measured temperatures in the axial direction with those predicted using the Conduction Model at different time intervals for a dry bed, Configuration: Packed Channel, d_b=0.7 mm d_p=3.0 mm, m=2.4 kg/h

Figure 5.19 Comparison of the variation of measured temperatures in the axial direction with those predicted using the Dispersion Model at different time intervals for a dry bed, Configuration: Packed Channel, d_b=0.7 mm d_p=3.0 mm, m=2.4 kg/h
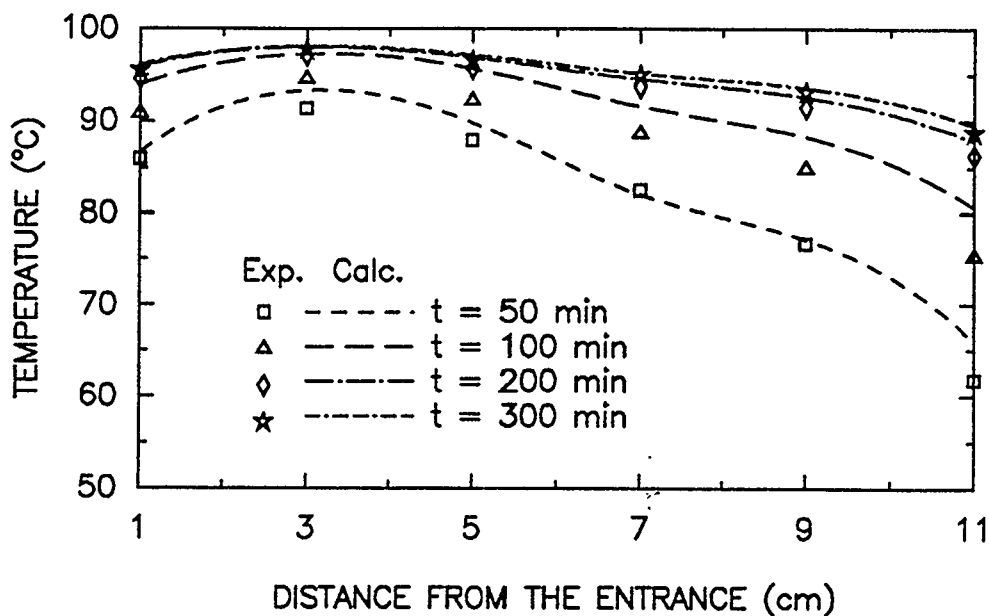
Figure 5.20 Comparison of the variation of measured temperatures in the axial direction with those predicted using the Dispersion Model at different time intervals for a dry bed, Configuration: Packed Channel, d_b=0.7 mm, d_p=3.0 mm, m=1.6 kg/h
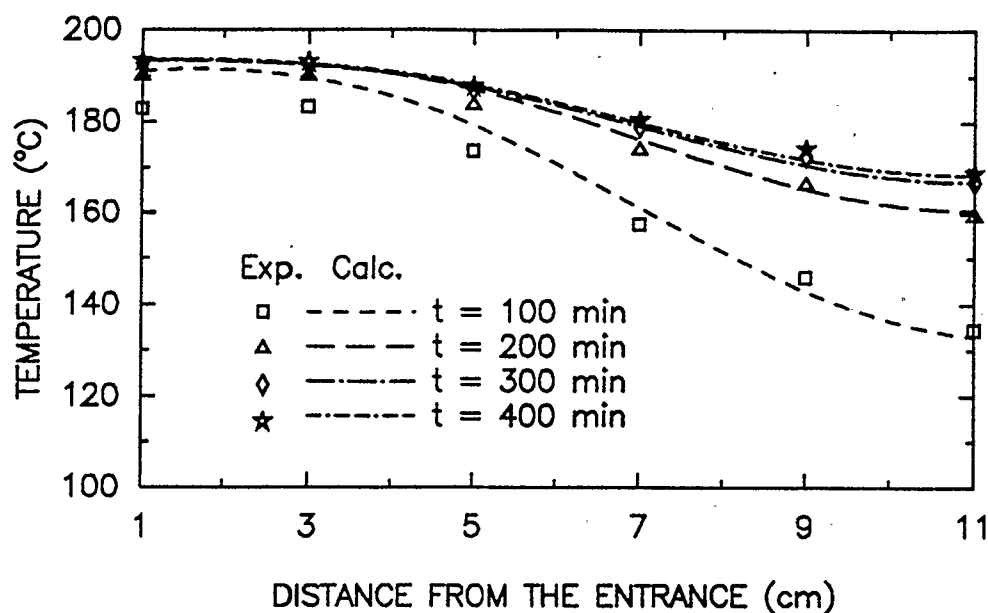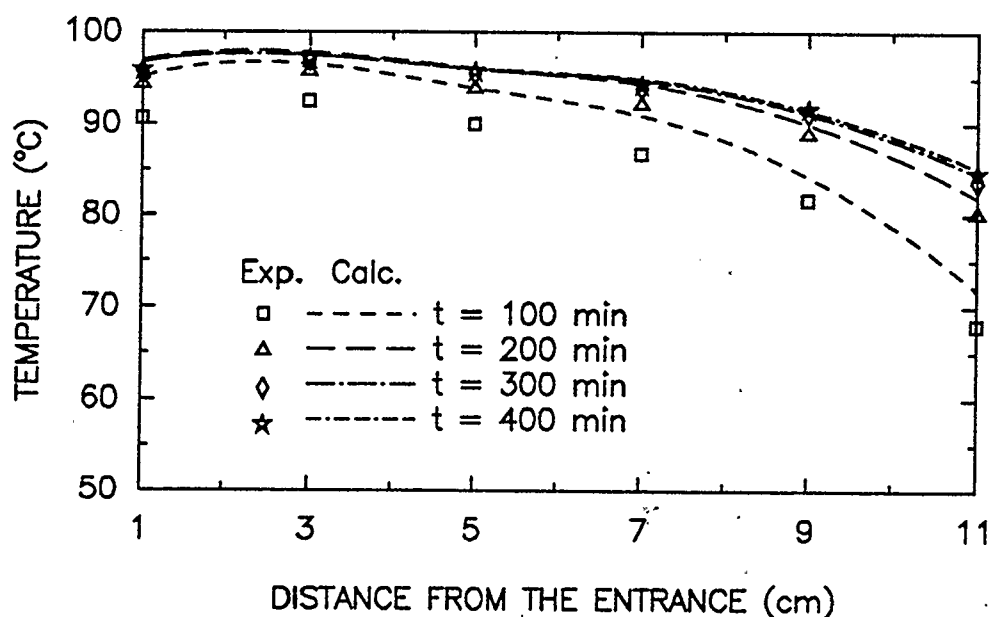

Figure 5.21 Comparison of the variation of measured temperatures in the axial direction with those predicted using the Dispersion Model at different time intervals for a dry bed, Configuration: Packed Channel, d_b=0.7 mm d_p=1.3 mm, m=1.6 kg/h

5.2.4.3 FINAL DISCUSSION OF THE MODEL

Finally, the Peclet number was calculated along the bed and used with various formulas of the effective diffusivity in order to examine the effect of dispersion on the effective diffusivity. The runs showed negligible effect on the temperature histories when using the different formulas. The reason for this could be explained as follows. It was found that the maximum Peclet number was less than 0.3 which is less than the critical value of 1.0. It was reported (13) that up till Pe=1, the molecular diffusion dominated and no significant dispersion contribution was noted on the total effective thermal diffusivity. Thus the effect of dispersion comes from the convection term (UVT). This behaviour agrees with the latter findings.

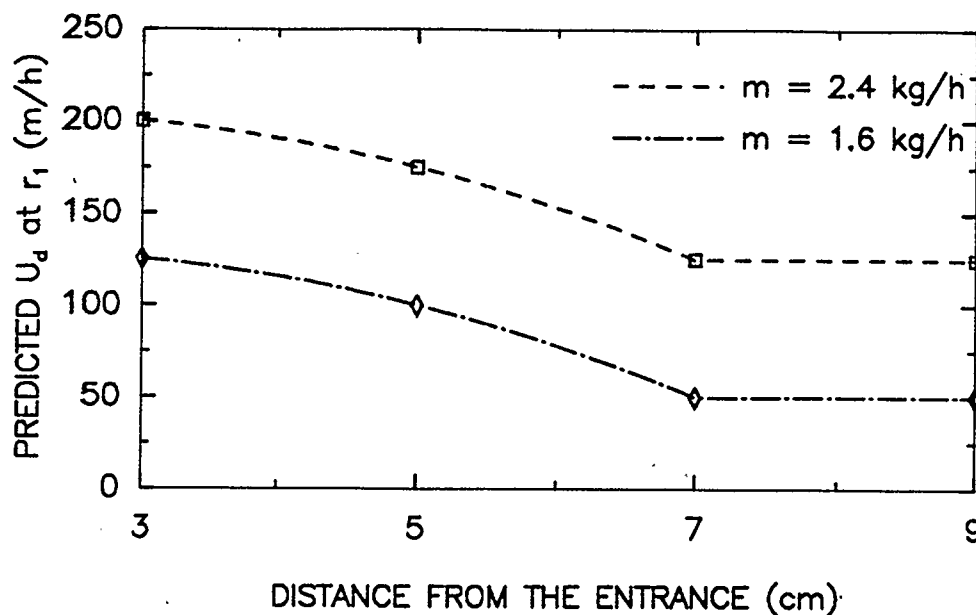Figure 5.22 Variation of the predicted dispersion velocity at the channel
surface along the length, for two different mass flow rates of air.
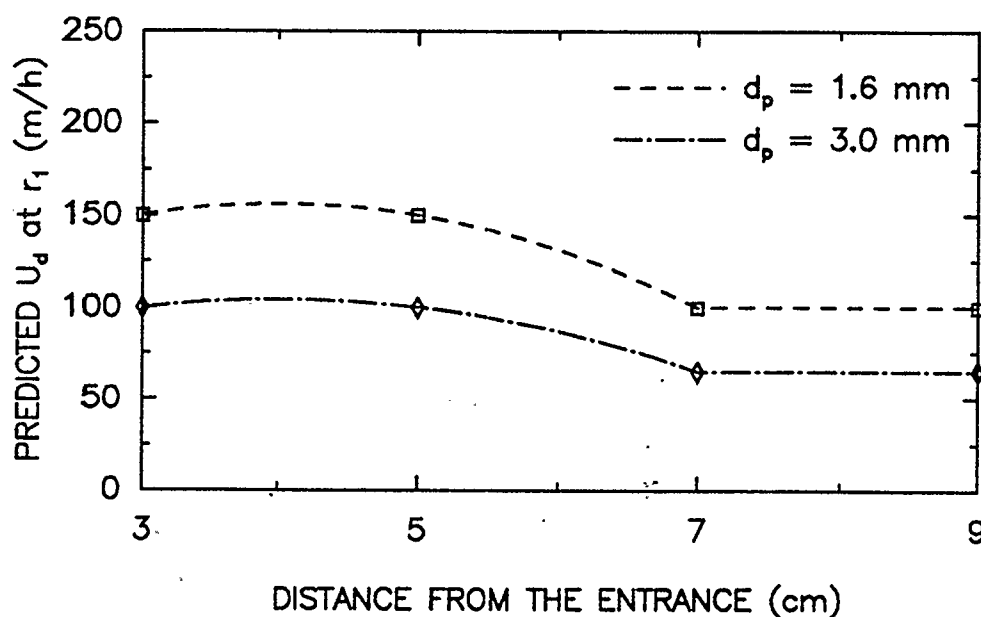Configuration: Packed Channel, d_b = 0.7 mm, d_p = 3.0 mm.

Figure 5.23 Variation of the predicted dispersion velocity at the channel
surface along the length, for two different channel glass bead
sizes. Configuration: Packed Channel, d_b = 0.7 mm, m = 1.6 kg/h

CHAPTER 6

WET GRANULAR BEDS

RESULTS AND DISCUSSION

6.1 GENERAL BACKGROUND

The introduction of a liquid phase to the dry porous media adds complexity to the analysis due to the complex nature of heat and mass transfer processes that take place simultaneously. In general, solids drying encompasses two fundamental simultaneous processes: Heat is transfered to evaporate the liquid and mass (moisture) is transfered as a liquid or as a vapour phase within the solid and as vapour from the surface. During the early stages of drying non-hygroscopic solids, the entrapped liquid is mobile (funicular state) and the liquid movement is rapid enough to maintain a saturated condition at the surface exposed to the convective stream (34). This region is characterized by a constant rate of drying, and the mechanism of moisture removal is equivalent to evaporation from a body of liquid and is essentially independent of the nature of the solid. If heat is transferred solely by convection, the surface temperature approaches the wet-bulb temperature. This period proceeds until the critical time where the falling rate period ("Pendular") starts. At the critical time, the entire evaporating surface can no longer be maintained saturated by moisture movement within the solid. After the critical time has elapsed the surface temperature starts to increase with

time and the drying rate starts to decrease. Thus, a second region of falling rate of drying starts (Pendular) in which the drying process proceeds as a combination of internal evaporation-condensation and a moving evaporation interface until the end of drying where the equilibrium moisture content is reached.
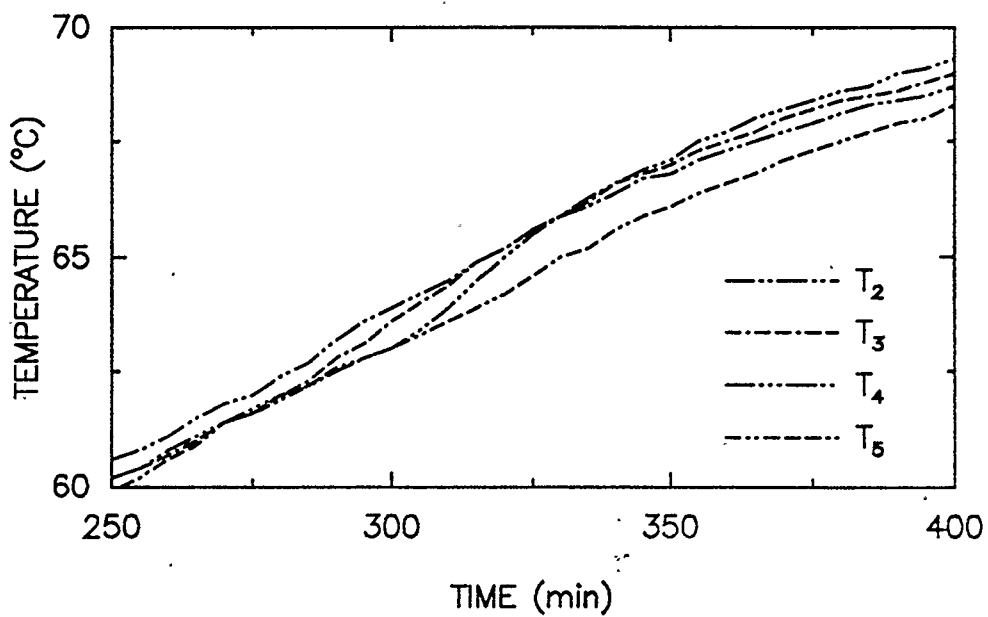
6.2 OPEN CHANNEL CONFIGURATION

The first configuration studied in the wet case was the open channel configuration. For comparison with dry bed results, the same sizes of glass beads and mass flow rates of air were used namely, 0.27 mm, 0.7 mm and 1.3 mm diameter and 1.6 kg/h to 2.4 kg/h, respectively. Exploratory tests were done to determine the maximum percentage of water saturation in order to avoid drainage of water from the bed. The result of these tests showed that the maximum percentage was around 4% by mass (i.e dry mass basis defined as kilograms of water per kilogram of dry solids). This ratio corresponds to a volumetric saturation of 16% by volume, the later value agrees with the results of Moore et al (28). Hence, two water percentages were used namely 2% and 4% by weight. Figures 6.1 - 6.4 show typical temperature histories of wet open channel beds at different flow and bed conditions. The temperatures were measured along the length of the bed and at the mean radius. In general, three regions could be identified with respect to the temperature gradient ($\partial T/\partial t$). For the first region, there was an initial relatively high gradient. This

was followed by a second region of a smaller gradient of almost constant value that ends with a sudden increase in gradient which may be disrcibed as a jump in temperature. Finally, the sudden increase of gradient soon starts to flatten until the steady state condition is reached. It was also observed that the time interval at which the temperature jump occurs increases in the direction of the air flow. For each run two graphs are provided. The first (a) shows the total temperature history while the second (b) zooms on the area of temperature jump for a closer inspection. In order to understand the later observation in light of the general background given in section 6.1, it has to be noted that the initial saturation of water used was around the critical saturation level which means that the entire drying process occurs in the falling rate period (Pendular). As hot air is introduced into the channel, temperature within the bed rises relatively rapidly due to the high temperature difference between the air streams and the bed. It was observed that this period coincides with the heating up period of the air stream where high transients exist. This probably accounts for the explanation given to the rapid rise of temperature. As a result of high temperatures persisting in the channel, rapid evaporation at the surface takes place and the surface becomes completely unsaturated (critical time). Hence an evaporation front starts to move radially outward into the bed, sweeping it in a manner similar to a combustion front. As the evaporation front approaches a location, the liquid saturation drops to the equilibrium saturation and a jump in the temperature occurs. The reason for
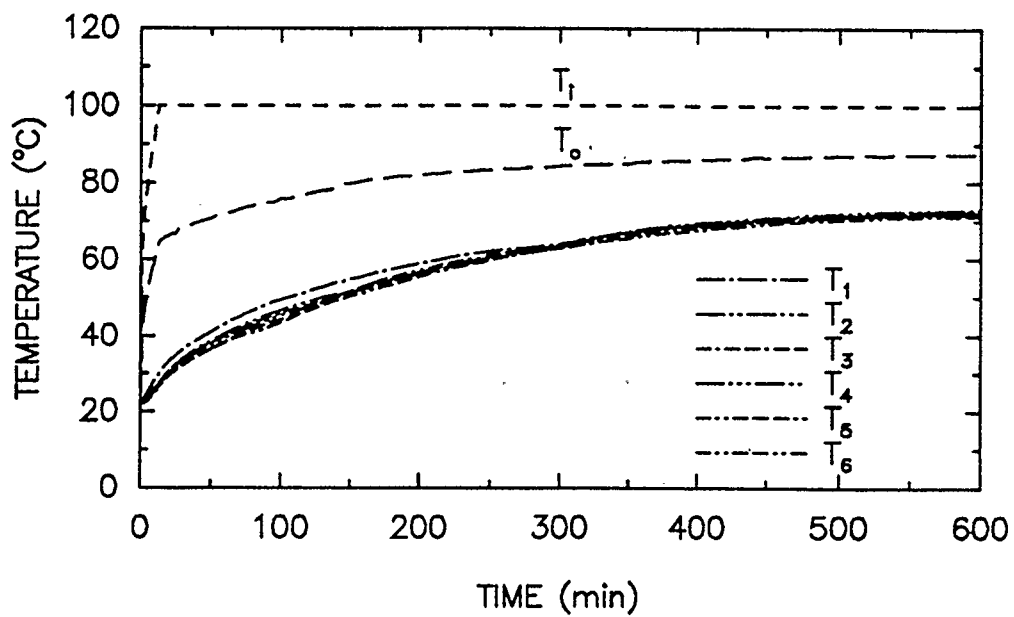
(a)

(b)

Figure 6.1 . Variation of the measured temperatures with time for a wet bed
Configuration: Open Channel, d_b=0.7 mm, m=1.6 kg/h, w= 4%

(a)

(b)

Figure 6.2   Variation of the measured temperatures with time for a wet bed
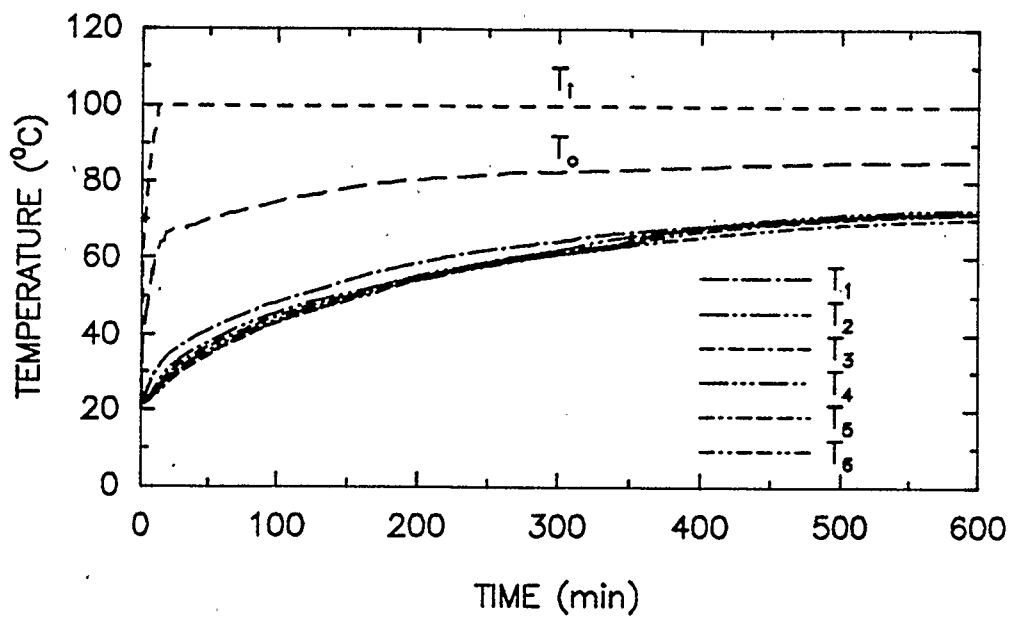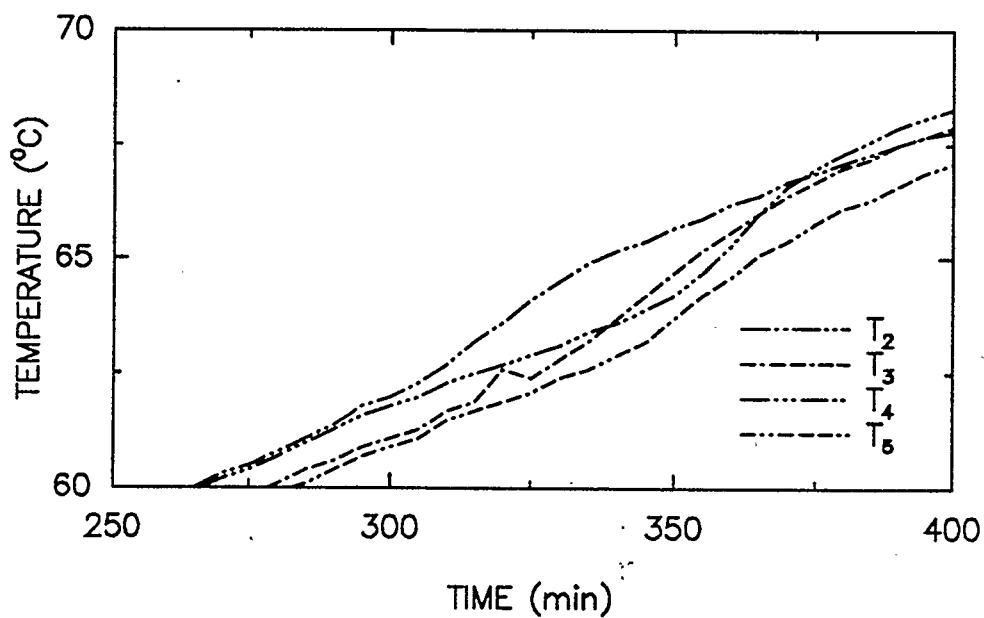Configuration: Open Channel, $d_b = 0.27$ mm, m=1.6 kg/h, w= 4%

(a)

(b)

Figure 6.3 Variation of the measured temperatures with time for a wet bed
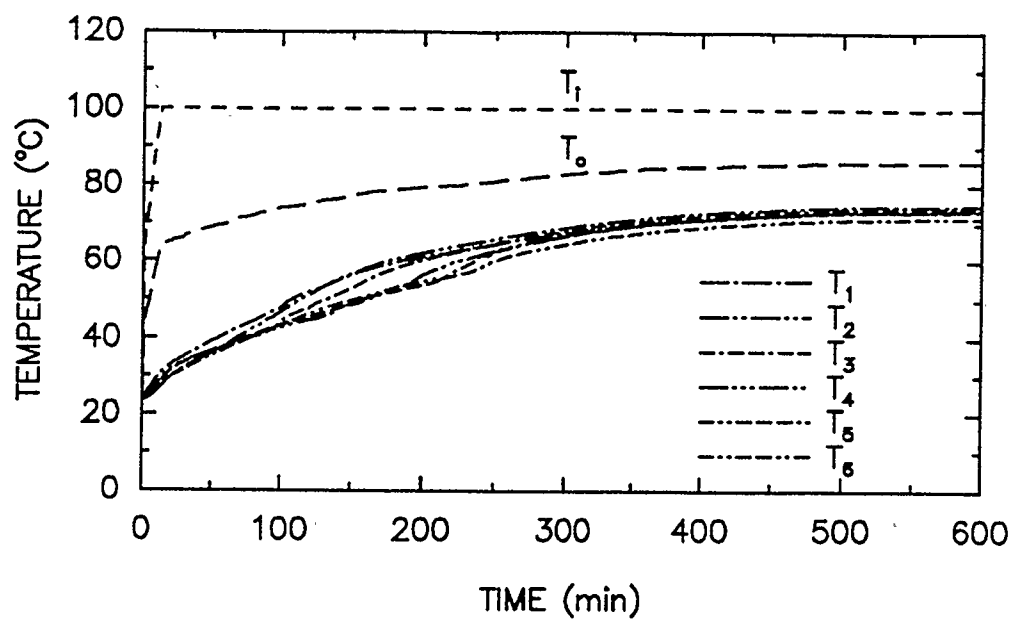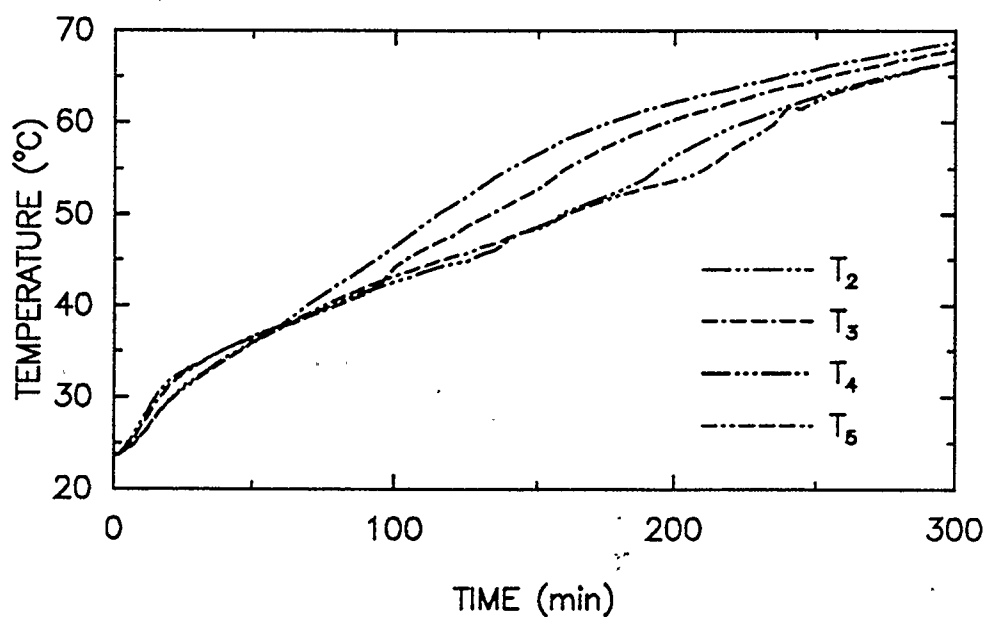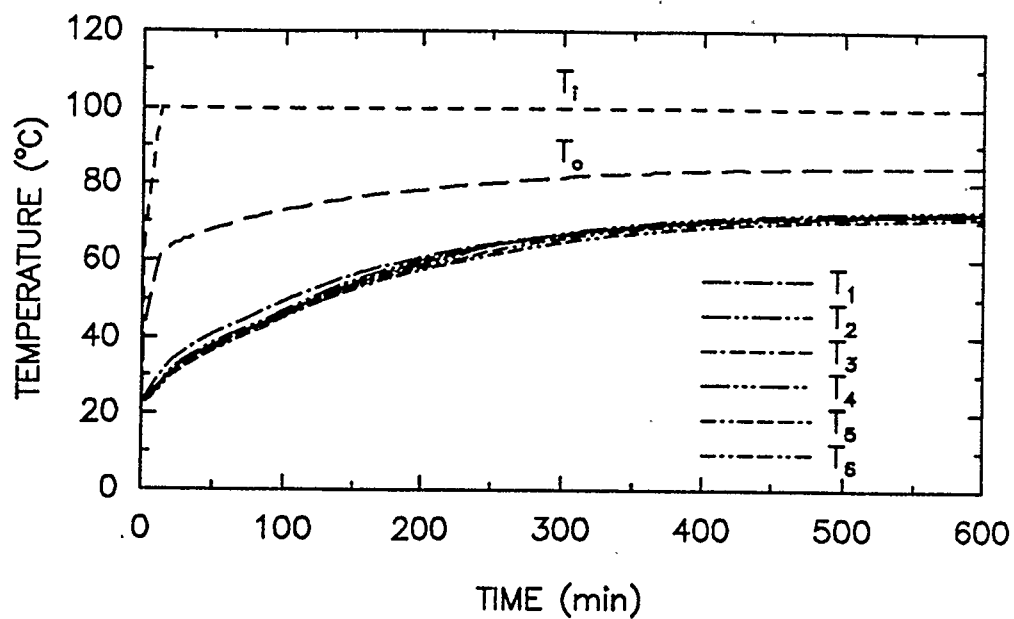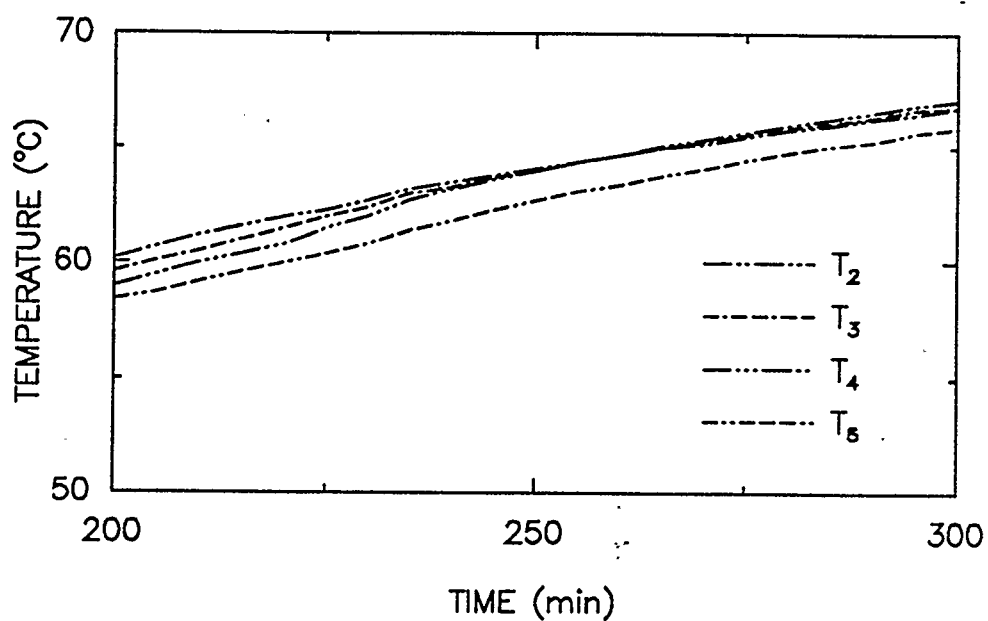Configuration: Open Channel, d_b = 1.3 mm, m=1.6 kg/h, w= 4%

(a)

(b)

Figure 6.4　Variation of the measured temperatures with time for a wet bed
Configuration: Open Channel, $d_b = 0.7$ mm, m=1.6 kg/h, w= 2%

the temperature jump could be attributed to the sudden increase in the thermal diffusivity caused by the decrease of thermal capacity of the bed. Also, the heat wasted as latent heat of evaporation is now used in heating up the bed. After the jump the heat transfer at this location resembles that of the dry conditions.

The increase of the time at which the jump takes place could be attributed to two factors:

a. a decrease of temperature in the axial direction,

b. an increase of the vapour saturation of the heating air as it flows in the channel which slightly affects the convective drying process.

6.2.1 EFFECT OF MASS FLOW RATE

Figure 6.5 shows the effect of changing the mass flow rate on the temperature history for a 0.7 mm diameter glass beads bed at an initial water saturation of 4% by mass and at 200°C inlet air temperature. The graph shows an increase in the temperature levels as well as the drying rates associated with the higher mass flow rate. The faster drying rates could be interpreted from the location of the temperature jumps on the temperature-time curve. The higher mass flow rates improved the convective heat transfer coefficient and enhanced heat transfer rates to the bed which resulted in high temperatures within the bed, as well as higher evaporation rates and enhanced diffusion of vapours. Also a higher air velocity at the channel surface helps to

entrain more vapour with its higher momentum which enhances the drying process.

6.2.2 EFFECT OF GLASS BEAD SIZE

Figure 6.6 compares the temperature histories of three different glass bead beds at the same operating conditions. Faster drying rates can be seen with beds of coarser beads. The coarser beads have larger permeabilities which enhance the diffusion of vapour through the bed and in turn speads up the drying process.

6.2.3. EFFECT OF INITIAL WATER CONTENT

Temperature histories of 2% and 4% water content runs were compared to that of a dry bed of the same glass bead size and operating conditions so as to show the effect of the initial saturation. Figure 6.7 shows that after the initial heating up period, the temperature level of wet beds becomes lower compared to that of the dry bed case, until the temperature jump occurs. After the jump the temperature approaches the steady state value. The later behaviour could be explained in a similar manner to that in sections 6.1 and 6.2. The figure also shows a faster drying for the 2% bed, depicted from the location of the jump. This is mainly due to the lower heat requirements for the evaporation of the 2% bed. Also, the lower saturation beds have a higher permeability which enhances the diffusion of vapour within the solid matrix.
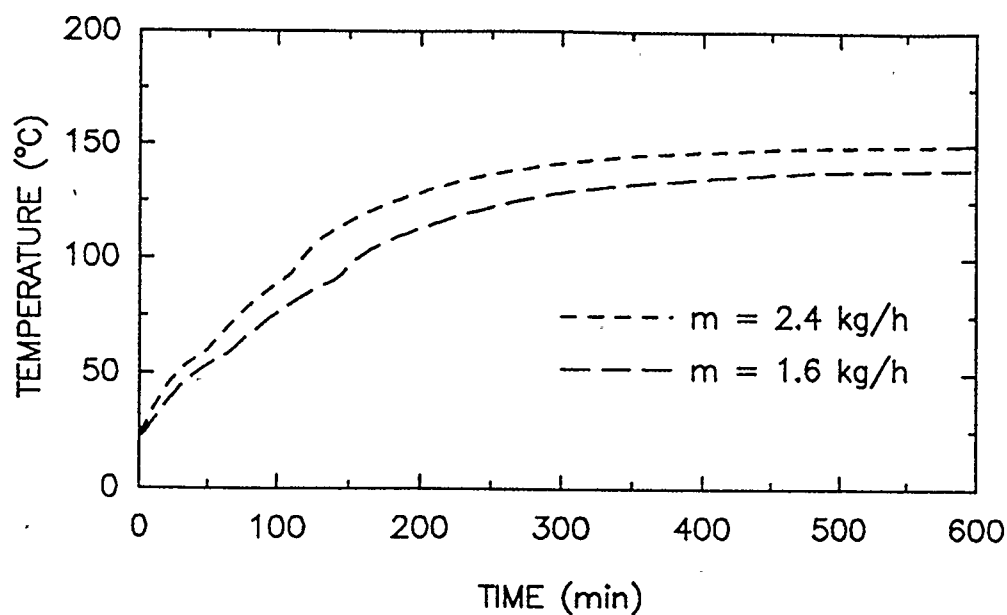
Figure 6.5 Variation of the measured temperatures with time for identical wet beds when subjected to two different mass flow rates of air, Configuration: Open Channel, d_b=0.7 mm, w= 4%.

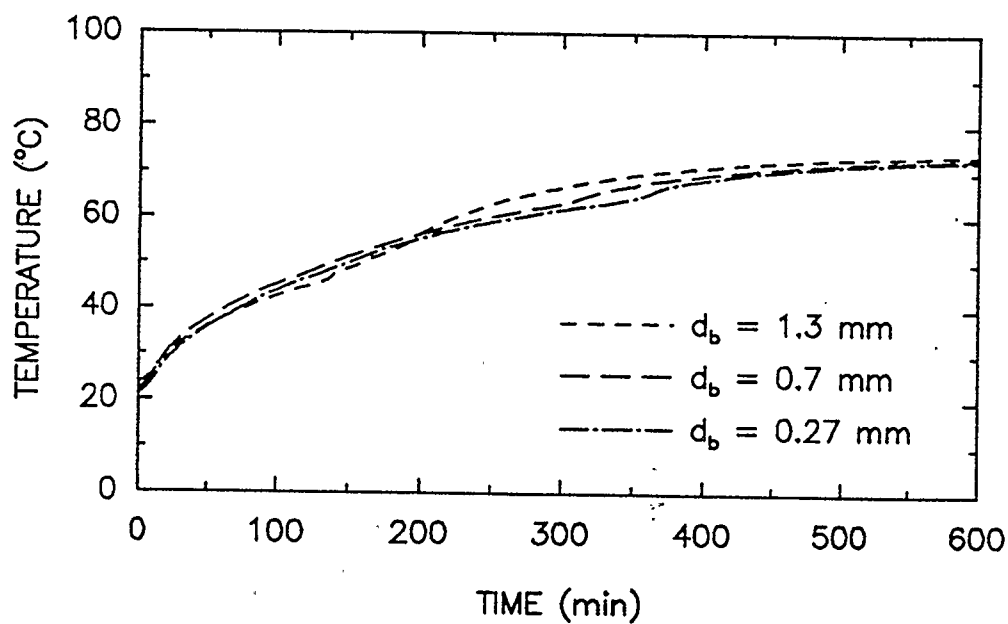Figure 6.6 Variation of the measured temperatures with time for wet beds of different glass beads sizes, Configuration: Open Channel, m=1.6 kg/h, w= 4%.
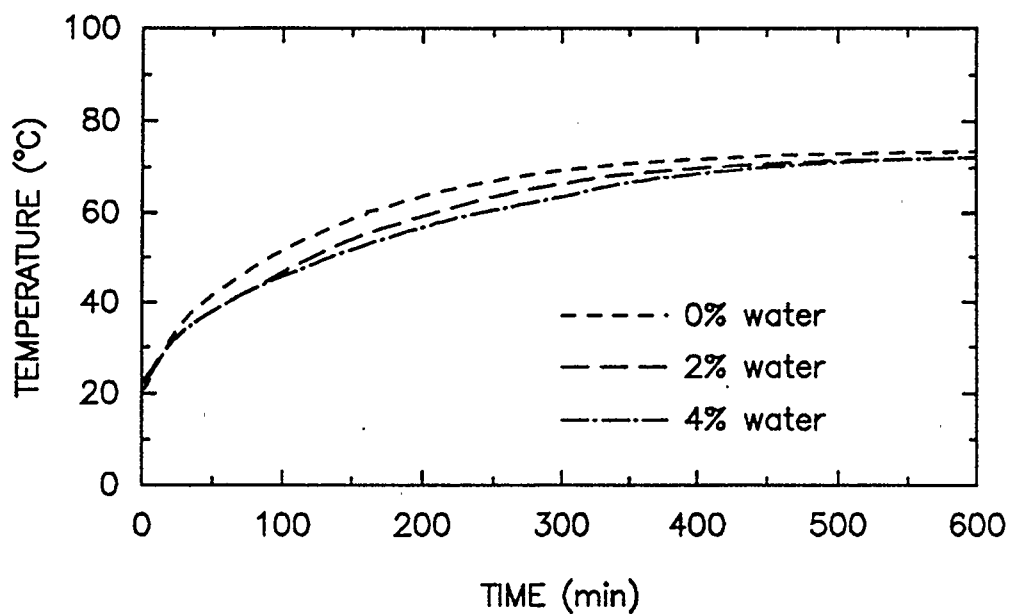
Figure 6.7   Variation of the measured temperatures with time for wet beds of different initial water content, Configuration: Open Channel, m= 1.6 kg/h, d_b=0.7 mm

6.2.4 COMPARISON WITH THE MODEL

Since no measurements were taken for the mass loss from the bed, only transient temperatures within the bed, which were measured experimentally will be the subject of comparison. Hence, the predicted temperature using the wet model described in section 4.4 will be compared to the corresponding experimental measured temperature. Typical comparative results are shown in figures 6.8 and 6.9. The experimental transient stream temperatures were used to simulate the actual heat input. Examination of these plots demonstrates a good agreement between the experimental and theoretical results in the low temperature region which was found to be less than 50°C, while a monotonic increase of deviation occurs at higher temperature levels within the bed. In order to look at the whole picture, figures 6.10 and 6.11 present the predicted transient saturation within the bed and the transient mass loss respectively for 0.7 mm glass beads bed. Figure 6.10 also shows the location of the evaporation front which is manifested in the sudden drop of saturation. The later figure illustrates that the evaporation front reached the mid-radius slightly after 200 min. Comparing this time with the experimental results shows that the later time is shorter than the experimental observation which was around 300 minutes. This may imply that the model predicts higher drying rate which is probably not the case. Examination of figure 6.9 shows that as the deviation starts to occur, an associated monotonic increase in the saturation is noticed at the impermeable surface which also implies that

a flow of vapour occurs radially outwards in addition to the mass lost by evaporation towards the channel. The reason for this could be due to the deterioration of the validity of the constant total pressure assumption which was used in the model. Hence, a total pressure build up leads to the gaseous migration towards the central channel due to the total pressure differential. Also, higher mass fluxes of vapour at the channel surface deteriorate the applicability of the assumption of heat and mass transfer analogy which appears to be valid for the first region. Moreover, the convective heat and mass transfer coefficient at the channel surface has to be evaluated at corrected air-vapour mixture in the boundary layer, as explained in (15). In summary, the previous problem could not be solved in the scope of this study since the evaporation rates were not measured. Nevertheless, apart from the fact that this model helped in understanding the processes involved, it shows that the applicability of heat and mass analogy is possible in drying processes when low evaporation rates are involved such as in the case of laminar flow at low temperature levels. It also implies that the assumption of constant total pressure could be used for the moderate sizes of particles at lower temperature levels such as those encountered in this study. However, this assumption is not likely to apply as the sizes of the pores decrease as shown by Ben Nassrallah (2). Finally the factors that could also influence this deviation is the assumption that the heating is at zero humidity in air during the whole process and the modelling is one-dimensional.
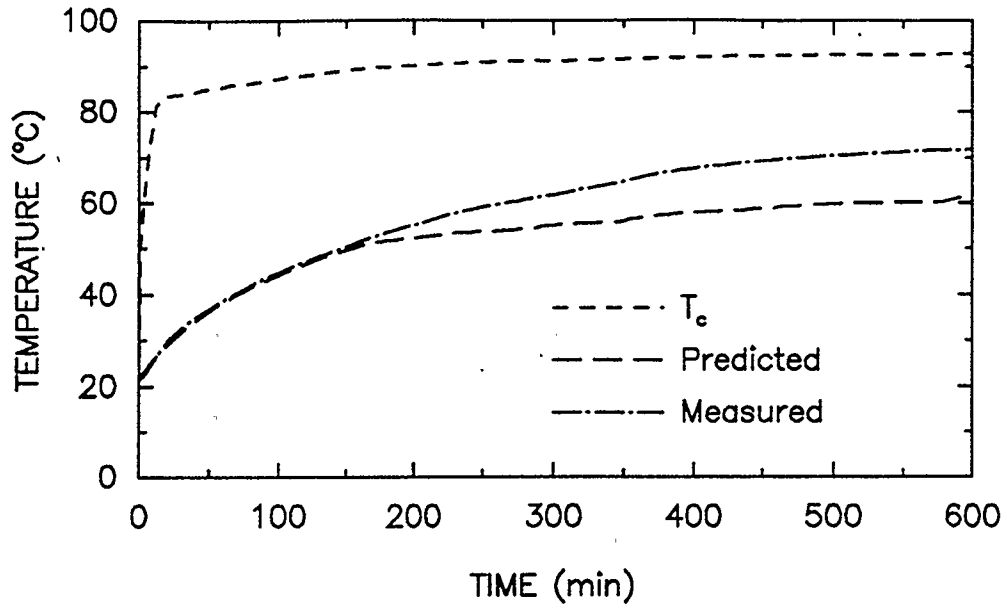
Figure 6.8   Predicted versus measured average temperature variation with
time for a wet bed, Configuration: Open Channel, $d_b = 0.27$ mm,
m=1.6 kg/h, w=4%
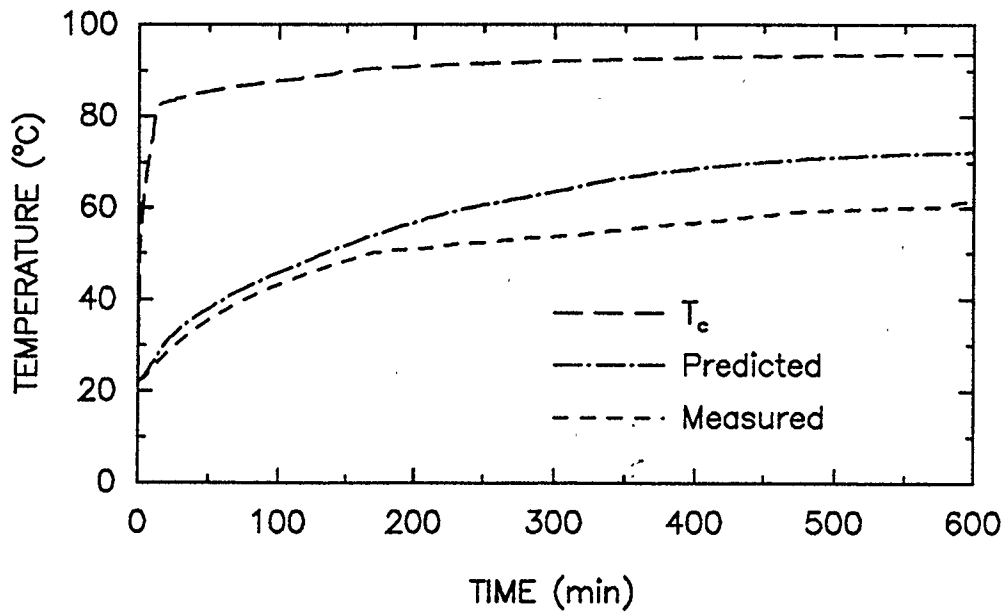
Figure 6.9   Predicted versus measured average temperature variation with
time for a wet bed, Configuration: Open Channel, $d_b = 0.7$ mm,
m=1.6 kg/h, w= 4%
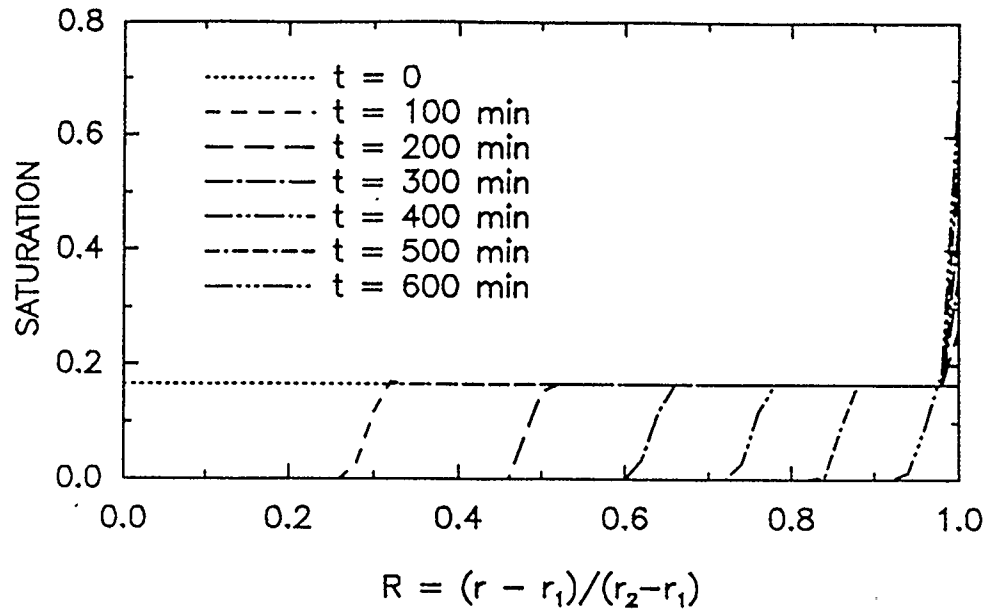
Figure 6.10 Predicted variation of water saturation with the non dimensional radial distance (R) at different time intervals for a wet bed, Configuration: Open Channel, d_b =0.7 mm, m=1.6 kg/h, w= 4%.
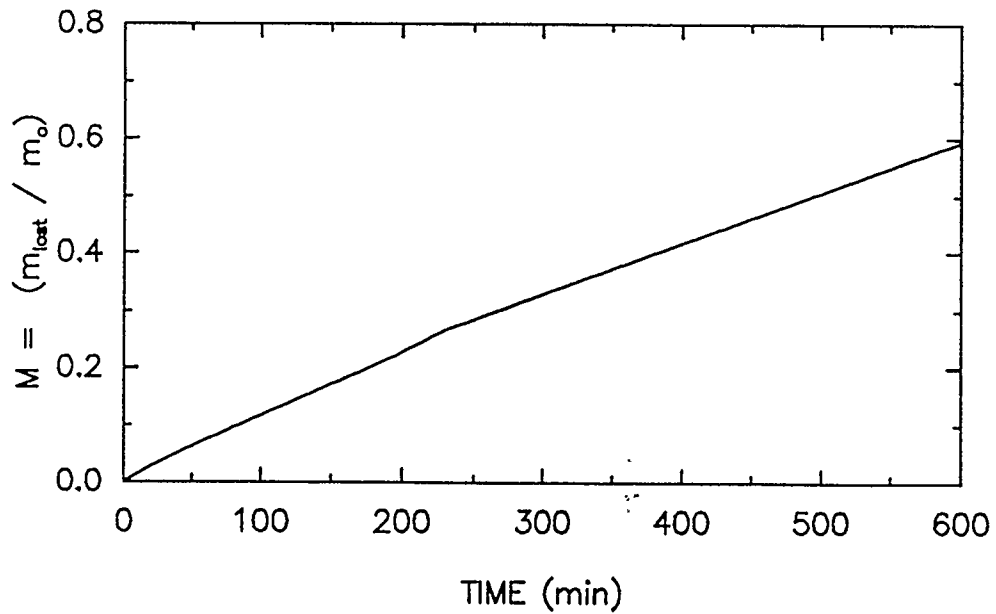
Figure 6.11 Predicted commulative mass loss fraction versus time for a wet bed, Configuration: Open Channel, d_b =0.7 mm, m=1.6 kg/h, w=4%

6.3 PACKED CHANNEL CONFIGURATION

The second set of runs involves a packed channel configuration which adds the complexity of dispersion to the wet analysis. For a comparison with the dry bed runs, the same flow parameters, glass beads and channel bead sizes were used. The moisture content employed were 2% and 4% by mass (dry mass basis). Figures 6.12 to 6.14 show typical temperature histories of wet beds with their channels filled with glass beads. The figures show three distinctive regions with respect to the temperature gradient.

Region 1: This region is characterized by only slight changes in temperature. Two cases were observed; a continuous decrease in temperature until the end of this region or the negative temperature gradient was proceeded by a period of slight increase in temperature.

Region 2: This region is characterised by very high temperature gradients similar to those of the dry beds.

Region 3: Moderate temperature gradients similar to those for the case of dry beds that decrease gradually until the steady state is reached.

It can be seen that the time interval of the first region increases in the axial direction. This could be attributed to the time required to heat up the channel glass beads and the additional higher heat requirements for evaporation within the bed.

An explanation of the temperature variation in region 1 could be suggested. At the early stages, the temperatures within the bed, as well as
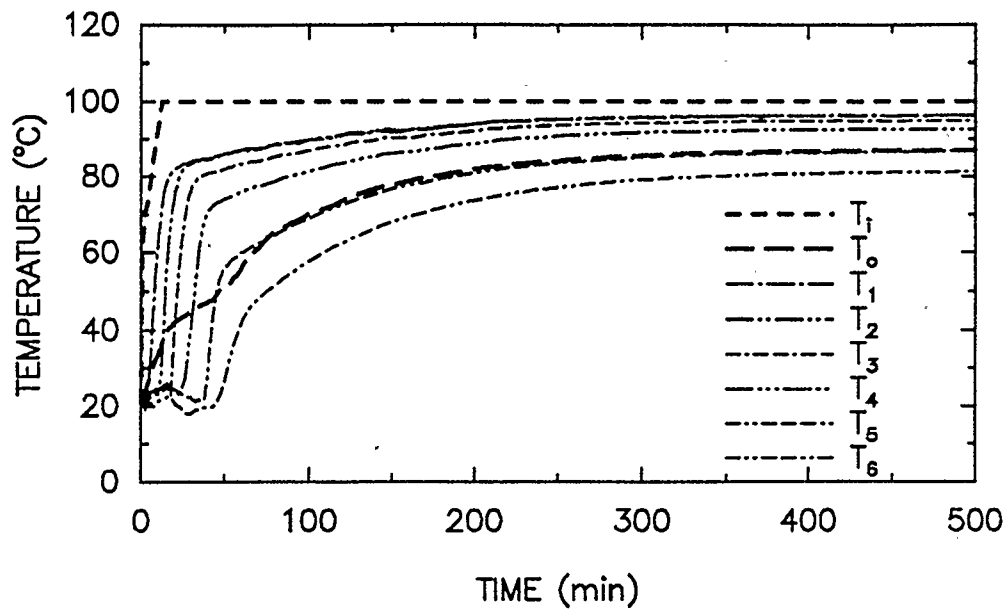
(a)
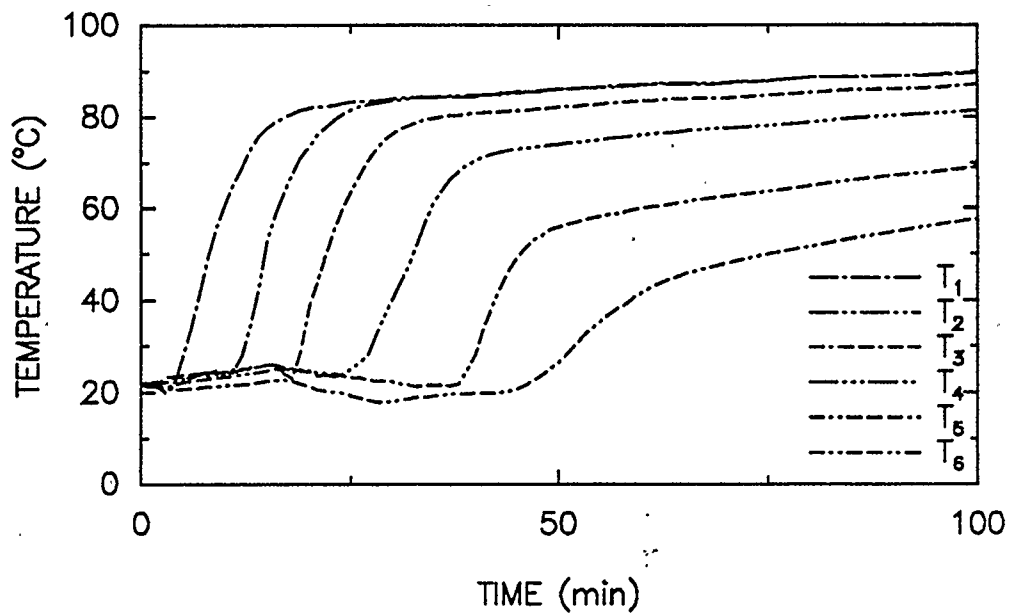
(b)

Figure 6.12 Variation of the measured temperatures with time for a wet bed
Configuration: Packed Channel, d_b=0.7 mm, d_p=3.0 mm, w= 4%,
m=1.6 kg/h
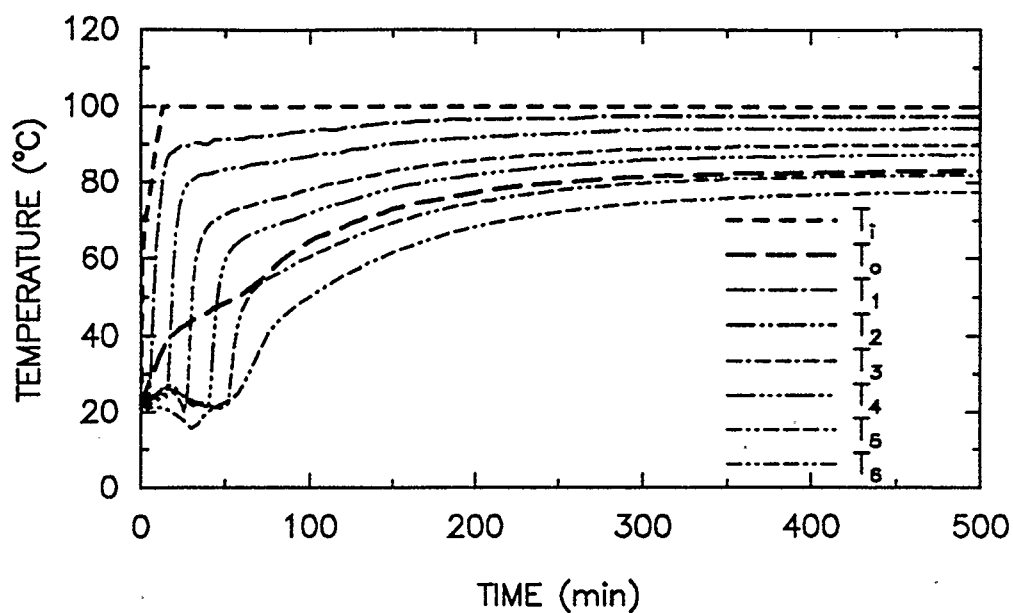
(a)
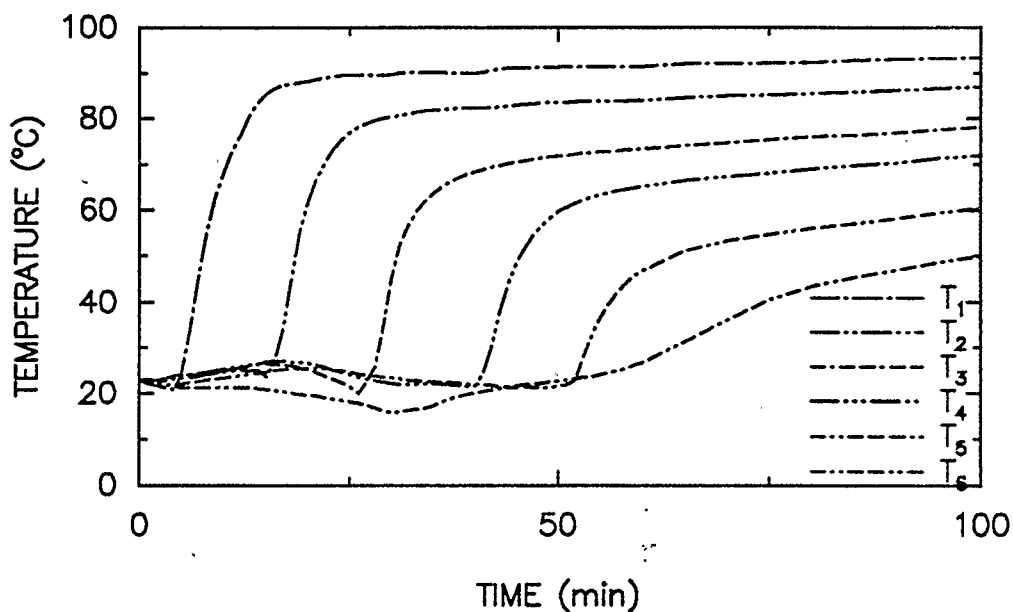
(b)

Figure 6.13 Variation of the measured temperatures with time for a wet bed
Configuration: Packed Channel, d_b =0.27 mm, d_p =3.0 mm, w= 4%,
m=1.6 kg/h
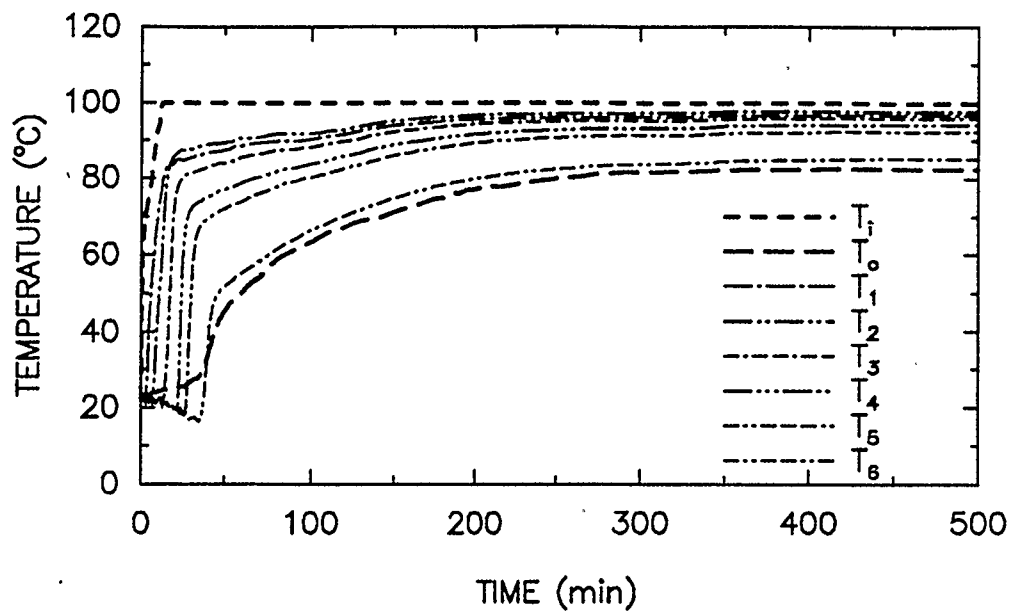
(a)
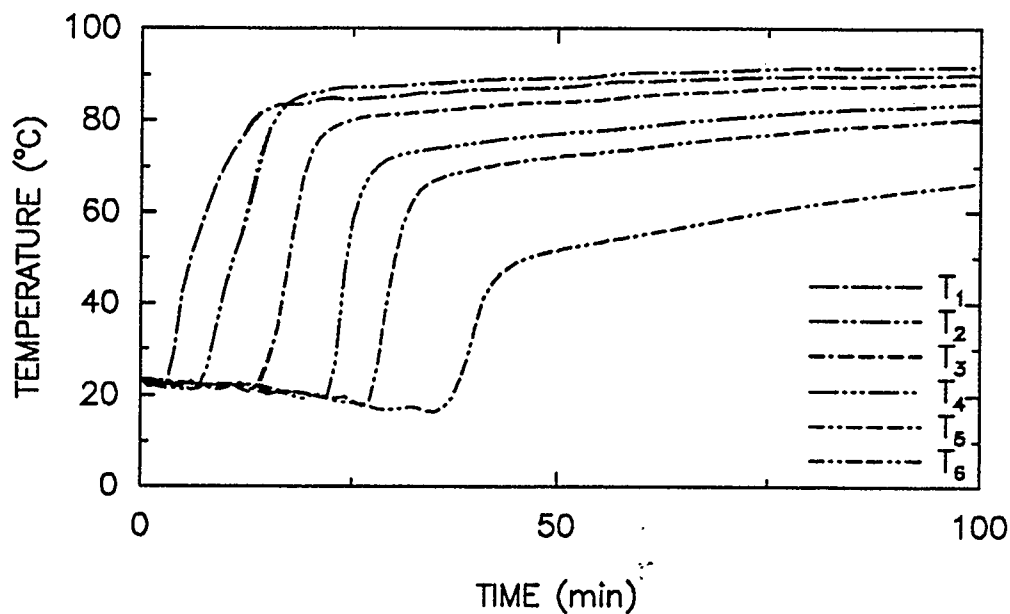
(b)

Figure 6.14 Variation of the measured temperatures with time for a wet bed
Configuration: Packed Channel, d_b =1.3 mm, d_p =3.0 mm, w= 4%,
m=1.6 kg/h

the channel are relatively low. The two modes of heat transfer, conduction and convection, compete to dominate in addition to the phase change requirements. The conduction mode tends to raise the temperature of the bed as the temperature of the air flow rises. On the other hand, the dispersion of air at relatively low temperatures within the bed tends to decrease the temperature towards the wet bulb temperature, at the corresponding dry bulb temperature and relative humidity. The magnitude of the temperature gradient and behaviour of the temperature within this region at any stage is controlled by the dominance of one regime over the other. It was noted that the period of initial rise of temperature - if any - usually ends with the end of the heating up period of the air stream. In general, when the dispersion rate is low, the effect of conduction is dominant at the very early stages and is manifested by the initial temperature rise. On the other hand, for higher rates of dispersion, the convective cooling effect of the dispersed air may override the conduction effect resulting in an entirely negative gradient of temperature. In light of the above discussion, the effect of the different parameters could be explained.

6.3.1. EFFECT OF THE BED GLASS BEAD SIZE

Figure 6.15 shows that the glass beads size of the bed has a significant effect on the temperature profile in region 1. The graph shows that for 1.3 mm glass beads, the temperature gradient in region 1 is entirely negative while for 0.7 mm and 0.27 mm, an initial temperature rise is evident. The 1.3 mm glass

beads possess the highest permeability followed by 0.7 mm and then 0.27 mm beads, hence the dispersion rate is higher for 1.3 mm and least for 0.27 mm beds. Applying the argument mentioned in section 6.3, it can be seen that it is in agreement with the trends of the experimental results.

6.3.2. EFFECT OF CHANNEL GLASS BEADS SIZE

Figure 6.16 shows the effect of the channel glass beads size on the temperature history within region 1. It can be seen that finer channel glass beads (1.3 mm diameter) bring about an entirely negative gradient while for 3 mm glass beads the two sub regions occur. As discussed in section 5.3.3 of dry beds , finer glass beads channel leads to higher rates of dispersion and hence the above explanation applies.

6.3.3. EFFECT OF MASS FLOW RATE

Figure 6.17 shows the effect of the mass flow rate on the temperature history of region 1. Alhough a higher mass flow rate has the same effect of enhancing the dispersion, it also means a higher heat input and an enhanced heat transfer rate by conduction. This may account for the relatively slight effect of mass flow rate in spite of the fact that it has a considerable effect on the dispersion.
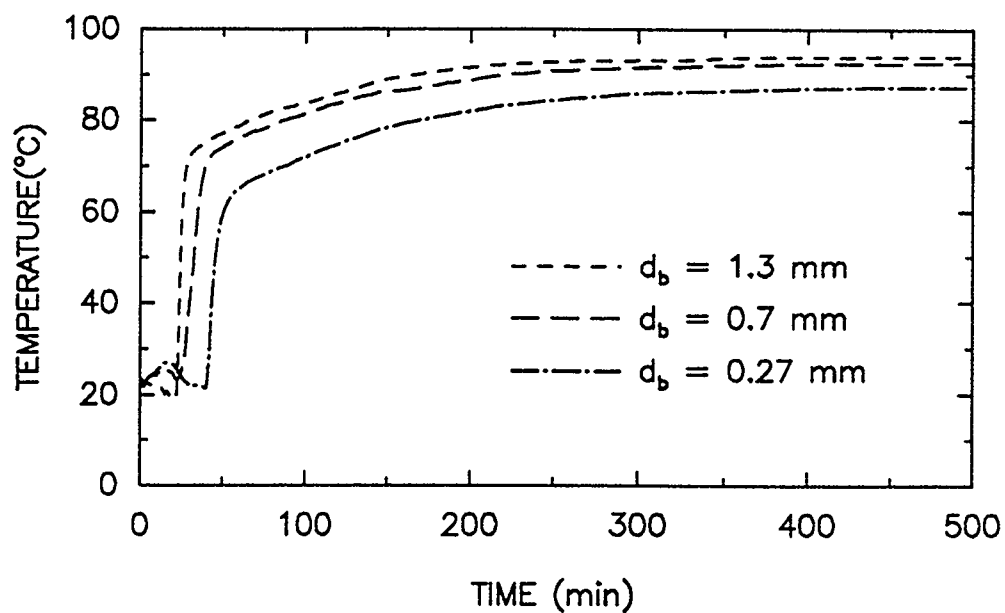
(a)
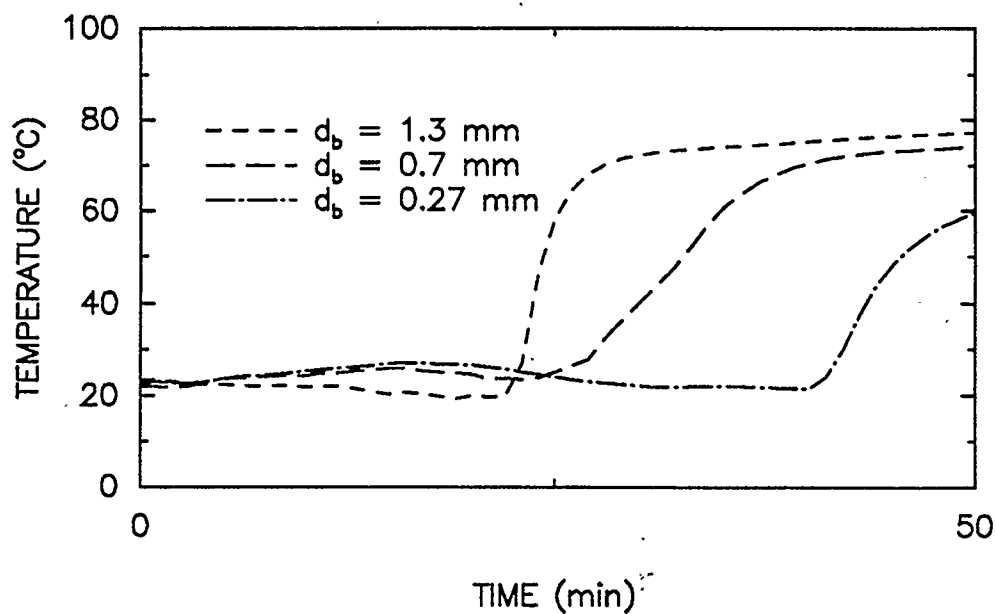
(b)

Figure 6.15 Variation of the measured temperatures with time for wet beds of different glass beads sizes, Configuration: Packed Channel, d_p=3.0 mm, m= 1.6 kg/h, w= 4%.
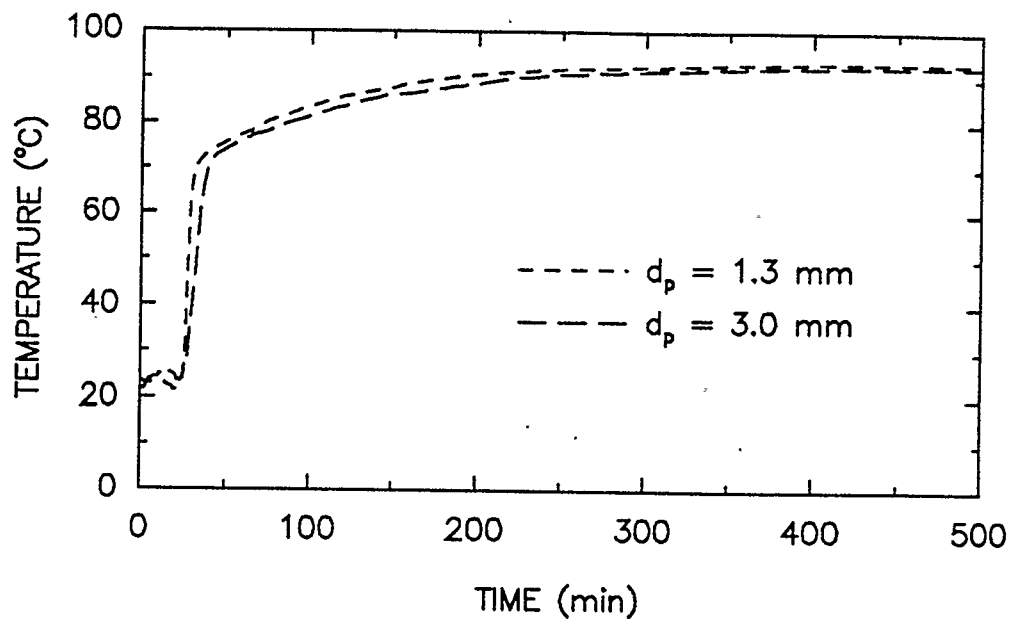
(a)
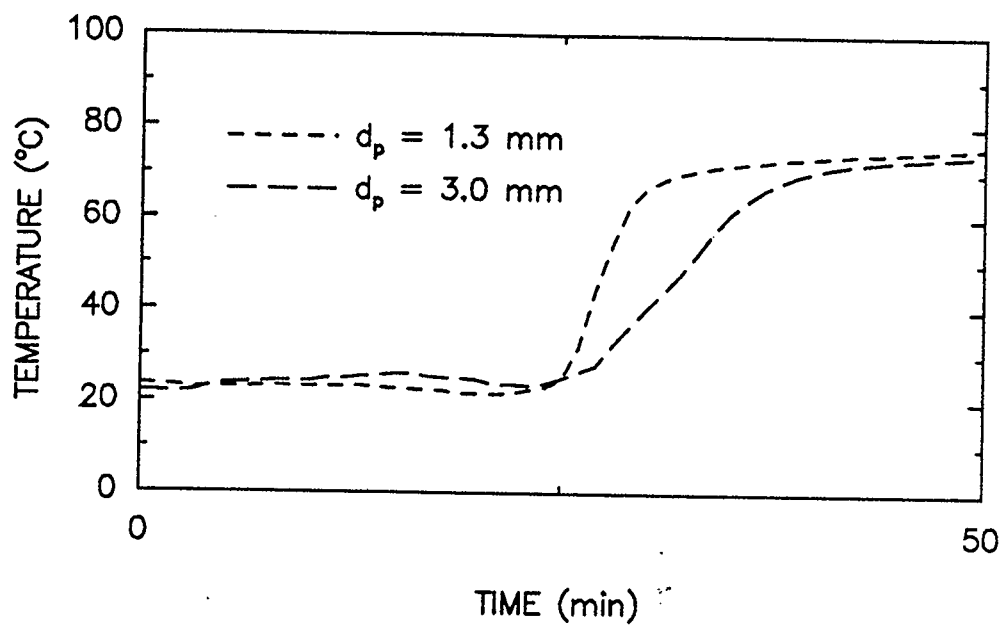
(b)

Figure 6.16 Variation of the measured temperatures with time for wet beds with two different channel glass bead sizes, Configuration: Packed Channel, d_b=0.7, m= 1.6 kg/h, w= 4%.
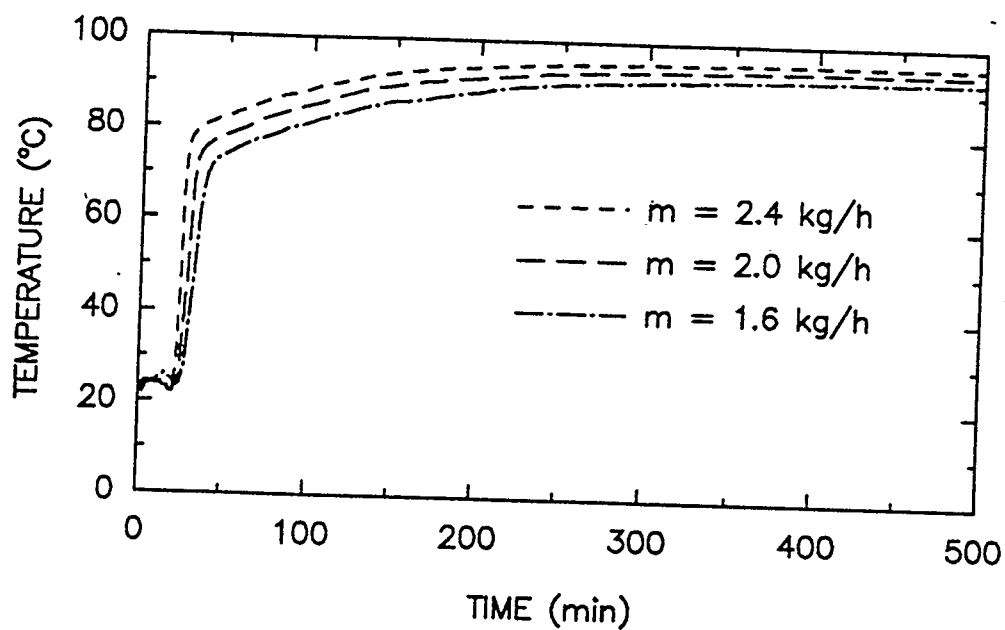
(a)
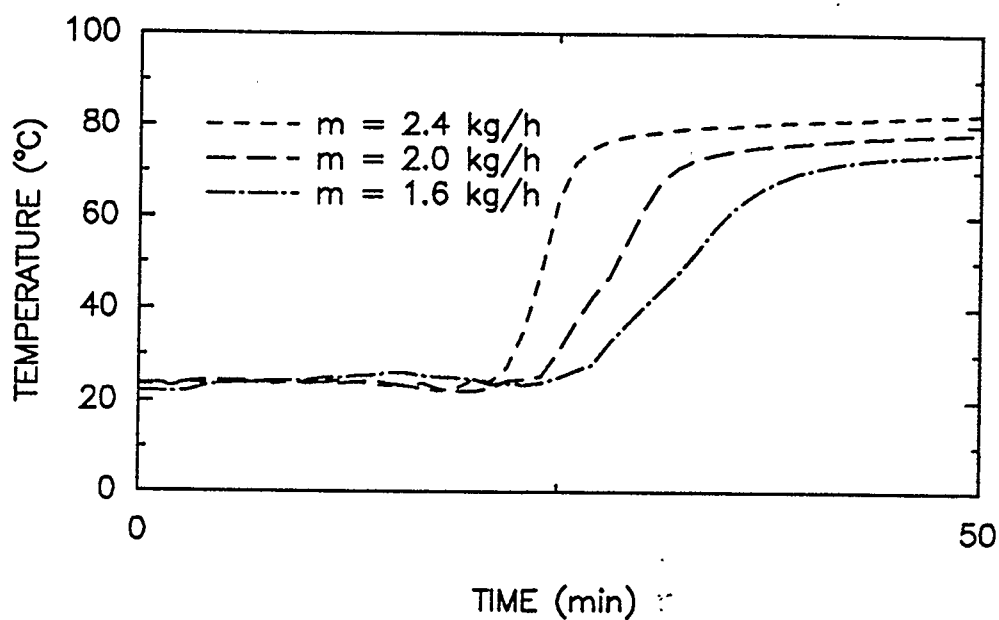
(b)

Figure 6.17 Variation of the measured temperatures with time for identical
wet beds when subjected to three different mass flow rates of air,
Configuration: Packed Channel, d_p=3.0 mm, d_b=0.7, w= 4%.

6.3.4. EFFECT OF THE INITIAL WATER CONTENT

The effect of the initial water content in region one is illustrated in figure 6.18. It shows that a lower water content (2% by weight) bed has a shorter time interval for region 1 and entirely a negative gradient of temperature. The reason is that a lower saturation is associated with lower heat requirements in evaporation which leads to higher transients within the channel. It is also associated with higher permeabilities that leads to higher dispersion rates and hence negative gradients.
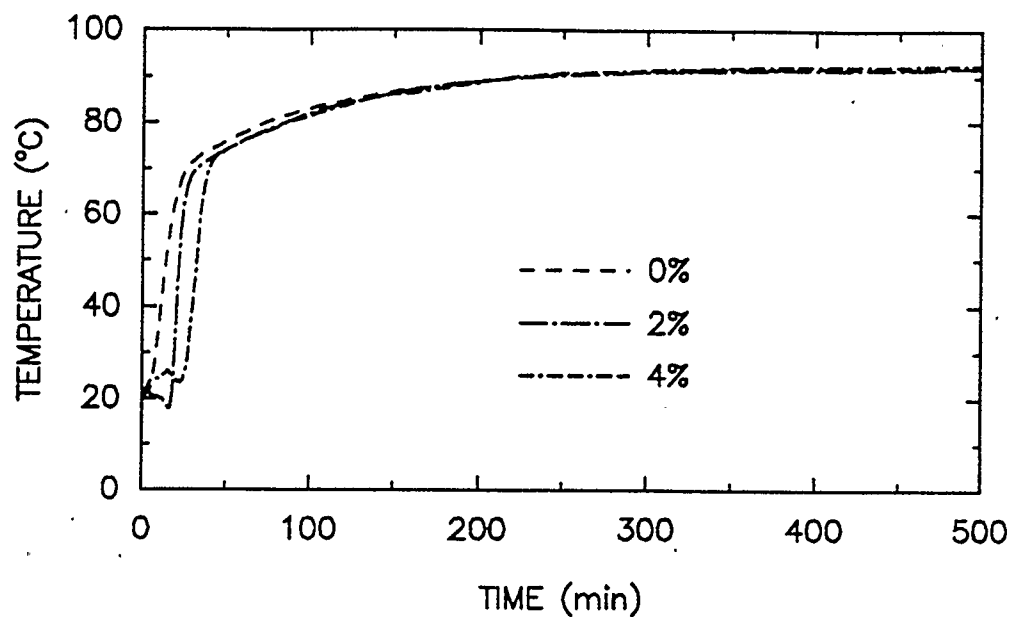
(a)
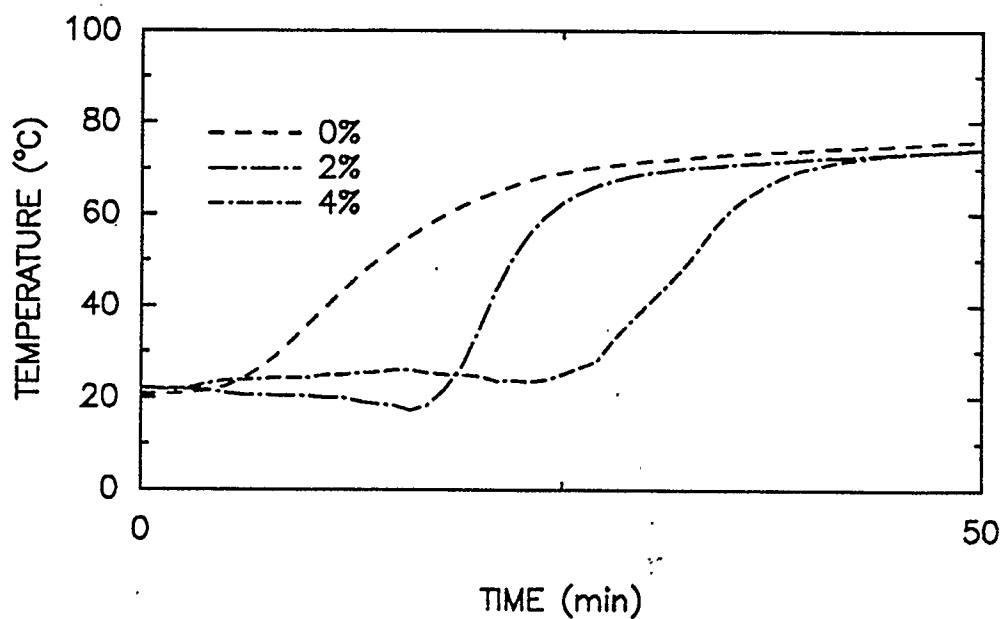
(b)

Figure 6.18 Variation of the measured temperatures with time for wet beds with different initial water content, Configuration: Packed Channel, d_b = 0.7 mm , d_p =3.0 mm, m=1.6 kg/h

CHAPTER 7

CONCLUSIONS AND RECOMMENDATIONS

7.1 CONCLUSIONS

The main results of the present investigation can be briefly summarized as follows:

i.   It was shown experimentally that the glass bead size of the bed has a negligible effect on the heat transfer rate for the range of parameters studied, while a higher mass flow rate of heating air enhances heat transfer within the beds.

ii.   Comparison between the predicted temperatures using the conduction model with the corresponding experimentally measured temperatures were found to be in excellent agreement for different beds and at different operating conditions. Thus, the conduction model with the assumed boundary conditions appeared to simulate accurately the real problem.

iii.   The experimental investigation of heat transfer within dry beds of the packed channel configuration showed that the presence of the glass beads within the channel, in general, brought about higher heat transfer rates when compared to the open channel configuration. The reason for this increase was attributed to the enhanced convective heat transfer

coefficients at the channel surface as well as the internal convective heat transfer associated with the dispersion of some of the air into the bed.

iv.   The experimental study for dry beds of the packed channel configuration showed that higher heat transfer rates were associated with higher air mass flow rates, finer channel glass beads and coarser bed glass beads.

v.   Employing the conduction based model developed to simulate the heat transfer process within dry beds of the packed channel configuration was found to be invalid both for the transient and steady states. The dispersion model which considers the simultaneous processes of heat transfer and fluid flow due to the dispersion of hot air within the bed, showed a significant improvement in the predicted temperature histories. An estimate of the dispersed air radial velocity distribution along the bed length was obtained for different runs.

vi.   Wetted beds of the open channel configuration showed three distinct regions characterized by different rates of temperature rise within the bed. An initial and relatively high temperature gradient was followed by a second region with a smaller gradient that ends with a sudden increase in the temperature (JUMP). For the third region the temperature approaches the steady state value of the corresponding dry bed case.

vii.   The experimental parametric study of the wetted granular beds of the

open channel configuration showed that faster drying rates were associated with higher mass flow rate of air, coarser beads and lower initial water saturation.

viii Comparison of the experimental and predicted results using the drying model showed good agreement at lower temperature levels while deviation occurs as the drying process proceeds.

7.2 RECOMMENDATIONS

i. Extension of the present study to other combinations of solid-liquid-gas systems is required of further understanding of the transport processes.

ii. Investigation of heat and mass transfer processes within beds saturated with various hydrocarbon fuels when subjected to streams of air heated at medium temperature ranges.

iii. Extension of the present work into higher Reynolds number range and well into the turbulent region.

iv. Extensive studies to determine the principal properties and transport coefficients of wetted porous media are crucially required to facilitate further modelling processes. The required parameters include: effective thermal conductivity, effective mass diffusivity, and convective mass transfer coefficient.

REFERENCES

1. Batchelor, G. K. and O'Brien, R. W., (1977), "Thermal or Electrical Conduction Through a Granular Material", Proceedings of the Royal Society, London, A 355, pp 313-333.

2. Ben Nasrallah, S. and Pierre, P., (1988), "Detailed Study of a Model of Heat and Mass Transfer During Convective Drying of Porous Media", International Journal of Heat and Mass Transfer, vol 31, pp 957-967.

3. Berger, D. and Pei, D., (1973), "Drying of Hygroscopic Capillary Porous Solids - A Theoretical Approach", International Journal of Heat and Mass Transfer, vol 16, pp 293-302.

4. Carbonell, R. G. and Whitaker, S., (1984), "Heat and Mass in Porous Media", in "Fundamentals of Transport Phenomenon in Porous Media" Bear and Corapcioglu, eds., Marinus Nijhoff Publishers, pp 121-198.

5. Croft, D. R. and Lilley, D. G., (1977), "Heat Transfer Calculations Using Finite Difference Equations", Applied Science Publishers Ltd.

6. Daughetry, R. L. and Franzini, J.B., (1977), "Fluid Mechanics with Engineering Applications", 8th ed., McGraw-Hill.

7. De Vries, D. A., (1958), "Simultaneous Heat and Moisture in Porous Media", Transactions of American Geophysics Union, vol 39, pp 909-916.

8. Hadley, G. R., (1986), "Thermal Conductivity of Packed Metal Powders", International Journal of Heat and Mass Transfer, vol 29, pp 909-920.

9. Hashin, Z. and Shtrikman, S., (1962), "A Variational Approach to the Theory of the Effective Magnetic Permeability of Multiphase Materials", Journal of Applied Physics, vol 33, pp 3125-3131.

10. Holman, J.P., (1968), "Heat Transfer", 2nd ed., McGraw-Hill Inc.

11. Hougen, O. A., McGauley, H. J. and Marshall, W. R., (1940), "Limitations of Diffusion Equations in Drying", American Institute of Chemical Engineers, vol 36, pp 183-210.

12. Ilic, M. and Turner, I. W., (1989), "Convective Drying of a Consolidated Slab of Wet Porous Material", International Journal of Heat and Mass Transfer, vol 32 no 12, pp 2351-2362.

13. Kaviany, M., (1991), "Principles of Heat Transfer in Porous Media", Springer-Verlag New York Inc.

14. Kays, W. M. and Grawford M. E., (1980), "Convective Heat and Mass Transfer", 2nd ed., McGraw-Hill Company.

15. Keey, R. B., (1972), "Drying Principles and Practice", Pergamon Press.

16. Koch, D. L. and Brady, J. F., (1985), "Dispersion in Fixed Beds", Journal of Fluid Mechanics, vol 154, pp 399-427.

17. Kothandaraman, C. P., Subramanyan, S., (1977), "Heat and Mass Transfer Data Book", John Wiley & Sons.

18. Krischer, O., (1940), "Heat and Mass Transfer in Drying", VDI-Forschungsh. vol 415. (cited in ref.42)

19. Krupiczka, R., (1967), "Analysis of Thermal Conductivity in Granular

Materials", International Chemical Engineering, vol 7, pp 122-144.

20. Kunii, D. and Smith J. M., (1960), "Heat Characteristics of Porous Rocks", Journal of the American Institute of Chemical Engineering, vol 6, pp 71-78.

21. Lewis, W., (1921), "The Rate of Drying of Solid Materials", The Journal of Industrial and Engineering Chemistry, vol 13, pp 427-433.

22. Luikov, A. V., (1968), "Analytical Heat Diffusion Theory", Academic Press.

23. Luikov, A. V., (1966), "Heat and Mass Transfer in Capillary-Porous Bodies", Pergamon, Oxford.

24. Maxwell, J. C., (1904), "A Treatise on Electricity and Magnetism", 3rd ed, vol 1, pp 440, Clarendon Press, Oxford.

25. McAdams, W. H., (1954), "Heat Transmission", 3rd ed., McGraw-Hill Book Company, New York.

26. Mehta, S. A., (1990), "An Examination of the Combustion and Transfer Process Within Fractured Oil Sand Beds", Ph.D. Thesis, Department of Mechanical Engineering, The University of Calgary, Calgary, Alberta, Canada.

27. Miller, M., (1969), "Bounds for Effective Electrical, Thermal and Magnetic Properties of Heterogeneous Materials", Journal of Mathematics and Physics., vol 10, pp 1988-2004.

28. Moore, R. N., Wolf, H. and Deaver, F. K., (1972), "Simultaneous Heat and Mass Transfer in Moist Porous Media", Research Report no 16,

University of Arkansas, Engineering Experiment Station.

29. Nayak, L. and Tien, C., (1978), "A Statistical Thermodynamic Theory for Coordination - Number Distribution and Effective Thermal Conductivity of Random Packed Beds", Int. J. Heat Mass Transfer, vol 21, pp 669-676.

30. Neale, G.H. and Nader, W.K., (1973), "Prediction of Transport Processes Within Homogeneous Swarm of Spherical Particles", Journal of the American Institute of Chemical Engineering, vol 19, pp 112-119.

31. Nield, D.A. and Bejan, A., (1992), "Convection in Porous Media", Springer-Verlag New York Inc.

32. Nozad, I., Carborell, R. G. and Whitaker, S., (1985), "Heat Conduction in Multiphase System I: Theory and Experiment for Two Phase Systems", Chemical Engineering Science, vol 40, pp 843-855.

33. Pepper, D. W. and Baker A. J., (1988), "Finite Differences Versus Finite Elements", in Handbook of Numerical Heat Transfer (Edited by Minkowycz, W. J., Sparrow, E. M., Schneider, G. E., and Pletcher, R.H.), John Wiley & Sons Inc.

34. Perry, R. H. and Chilton, C. H., (1973), "Chemical Engineers Handbook", 5th ed., McGraw-Hill Book Co., New York.

35. Reid, R. C., Prausnitz, J. M. and Sherwood, T. K., (1977), "The Properties of Gases and Liquids", McGraw-Hill Inc.

36. Ryan, D., Carbonell, R. G. and Whitaker, S., (1981), "Effective Diffusivities for Catalyst Pellets Under Reactive Conditions", Chemical

Engineering Science, vol 35, pp 10-16.

37. Sherwood, T. K., (1929), "The Drying of Solids-I", Industrial and Engineering Chemistry, vol 21 no 1, pp 12-16.

38. Slattery, J. C., (1981), "Momentum, Energy, and Mass Transfer in Continua", pp 406-413, R. F. Krieger Publishing Co.

39. Smith, G. D., (1978), "Numerical Solution of Partial Differential Equations: Finite Difference Method", 2nd ed., Clarendon Press, Oxford.

40. Taylor, G. I., (1953), "Dispersion of Soluble Matter in Solvent Flowing Slowly Through a Tube", Proceedings of the Royal Society, London, A 219, pp 186-203.

41. Taylor, G. I., (1954), "The Dispersion of Matter in Turbulent Flow in a Pipe", Proceedings of the Royal Society, London, A 223, pp 446-468.

42. Whitaker, S., (1977), "A Theory of Drying in Porous Media", Advances in Heat Transfer", vol 13, pp 120-203.

43. Whitaker, S., (1980), "Heat and Mass Transfer in Granular Porous Media", Advances in Drying (Edited by Mujumdar, A. S.)", vol 1, pp 23-61, Hemisphere, New York.

APPENDIX A

WHITAKER THEORETICAL APPROACH

The governing equations according to Whitaker could be written as follows:

a) Total thermal energy equation:

$$\frac{\partial}{\partial t}\langle \rho c_p T\rangle + [\rho_l (c_p)_l \langle v_l\rangle + \langle \rho_g\rangle^g \langle c_p\rangle^g \langle v_g\rangle]\cdot\nabla \langle T\rangle$$

$$+ \langle \dot{m}\rangle \Delta h_v = \nabla \cdot (k_e \cdot \nabla \langle T\rangle)+\langle\Phi\rangle \qquad (A.1)$$

where

$$\langle \rho c_p\rangle = (\varepsilon\rho c_p)_s + (\varepsilon\rho c_p)_l + \varepsilon_g \langle \rho_v\rangle^g (c_p)_v + \varepsilon_g\langle\rho_a\rangle^g(c_p)_a \qquad .$$

b)Liquid phase continuity equation:

$$\frac{\partial}{\partial t}(\rho_l \ \varepsilon_l) + \nabla.(\rho_l\langle v_l\rangle) + \langle \dot{m}\rangle = 0 \qquad (A.2)$$

c) Liquid phase equation of motion:

$$\langle v_l\rangle = -\frac{K_l}{\mu_l}.(\nabla \langle p_l\rangle^l - \rho_l g) \qquad (A.3)$$

d) Gas phase continuity equation:

$$\frac{\partial}{\partial t}(\varepsilon_g\langle\rho_g\rangle^g)+ \nabla.(\langle\rho_g\rangle^g\langle v_g\rangle) - \langle \dot{m}\rangle = 0 \qquad (A.4)$$

e) Gas phase continuity equation:

$$\langle v_g \rangle = - \frac{K_g}{\mu_g} \cdot (\nabla \langle P_g \rangle^g - \rho_g g) \qquad\qquad (A.5)$$

f) Gas phase diffusion equation:

$$\frac{\partial}{\partial t}(\varepsilon_g \langle \rho_v \rangle^g) + \nabla \cdot (\langle \rho_v \rangle^g \langle v_v \rangle) - \langle \dot{m} \rangle = 0 \qquad\qquad (A.6)$$

where

$$\langle \rho_v \rangle^g \langle v_v \rangle = \langle \rho_v \rangle^g \langle v_g \rangle - \nabla \cdot (\langle \rho_g \rangle^g D_{ve} \cdot \nabla \frac{\langle \rho_v \rangle^g}{\langle \rho_g \rangle^g}) \qquad\qquad (A.7)$$

g) Volume constraint:

$$\varepsilon_s + \varepsilon_l(t) + \varepsilon_g(t) = 1 \qquad\qquad (A.8)$$

h) Thermodynamic relations:

$$\langle P_v \rangle^g = \langle \rho_v \rangle^g R_v \langle T \rangle \qquad\qquad (A.9)$$

$$\langle P_a \rangle^g = \langle \rho_a \rangle^g R_a \langle T \rangle \qquad\qquad (A.10)$$

$$\langle P_g \rangle^g = \langle P_v \rangle^g + \langle P_a \rangle^g \qquad (A.11)$$

$$\langle \rho_g \rangle^g = \langle \rho_v \rangle^g + \langle \rho_a \rangle^g \qquad (A.12)$$

$$\langle P_v \rangle^g = \overset{\circ}{P}_v \exp(\frac{A}{T_o} - \frac{B}{\langle T \rangle}) \qquad (A.13)$$

The above are 12 governing equations in 12 unknowns. The main draw back of these equations according to Whitaker was the complexity of the formulation and the insufficiency of boundary conditions for the transport equations. For the latter reason he carried some manipulations to simplify the model. The relevant simplification was that the dry air flux is often weak compared to the vapour flux. Taking ($\rho_a v_a = 0$) equation (A.7) could be written as:

$$\langle \rho_v \rangle^g \langle v_v \rangle = - \frac{\langle \rho_g \rangle^g D_{ve}}{1 - \langle \rho_v \rangle^g / \langle \rho_g \rangle^g} \cdot \nabla (\frac{\langle \rho_v \rangle^g}{\langle \rho_g \rangle^g}) \qquad (A.14)$$

Where:

T : temperature

t : time

v : averaged velocity

ρ : density

c_p : specific heat at constant pressure

k_e : effective thermal conductivity tensor

Δh_v : enthalpy of vaporization per unit mass

$\dot{m}$: mass rate of evaporation per unit volume

g : gravity vector

ε_i : volume fraction of i_{th} phase, V_i/V

P_i : partial pressure of i_{th} phase

K_i : phase permeability

R_i : gas constant for the i_{th} phase

Φ : rate of heat generation

suffix:

s : solid phase

l : liquid phase

g : gas phase
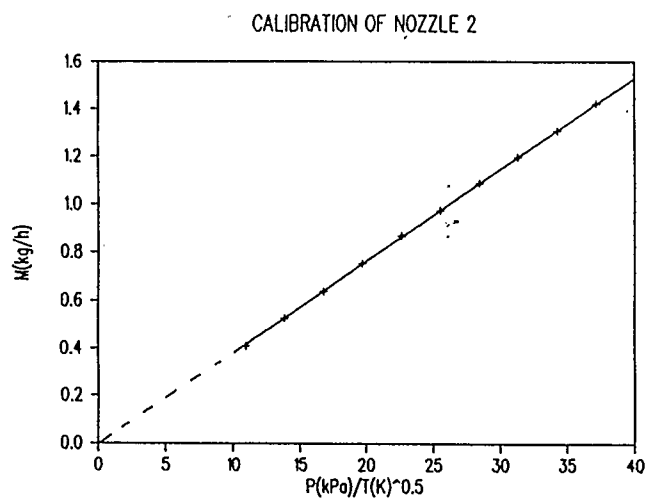
v : vapour

a : air

APPENDIX B

CALIBRATION CHARTS FOR CHOKED NOZZLES

The following are the calibration curves of the choked nozzles employed for the compressed air. These were calibrated against a wet test meter.

CALIBRATION OF NOZZLE 1

CALIBRATION OF NOZZLE 2

CALIBRATION OF NOZZLE 3

CALIBRATION OF NOZZLE 4
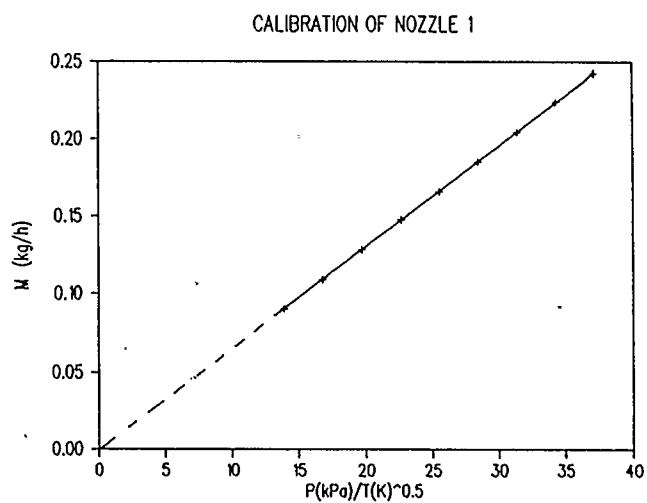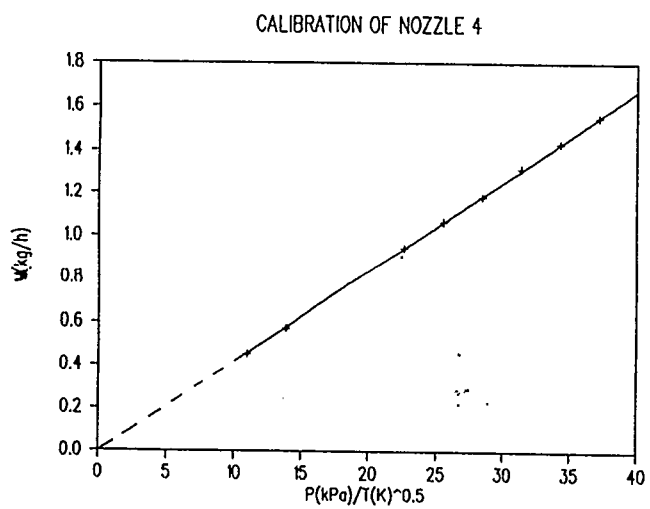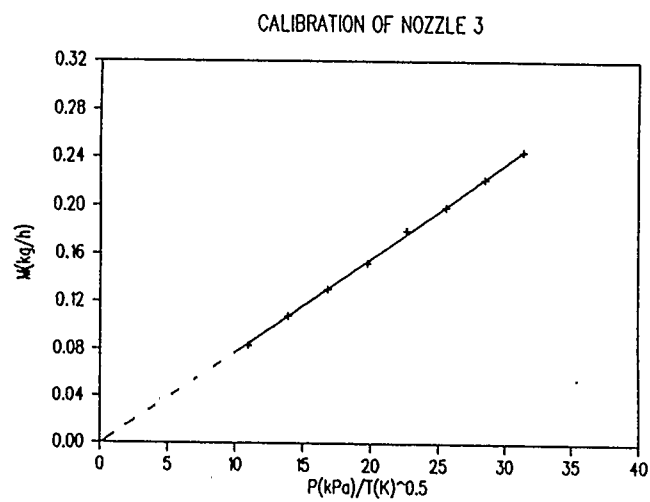
APPENDIX C

LIST OF COMPUTER PROGRAMS

```
c   CONDUCTION MODEL
c   TRANSIENT TEMPERATURES WITHIN CYLINDRICAL DRY GRANULAR
c   BEDS OF THE OPEN CHANNEL CONFIGURATION

c   This program was devloped to solve the heat conduction problem within
c   dry granular beds mentioned in chapter 4 of this thesis.
c
c   ao-a5  are the coefficients determined experimentally for
c          the mean air stream temperature
c   ta  = ambient air temperature (c)
c   rou = average density of the granular bed (kg/m3)
c   cp  = average specific heat of the granular bed (kcal/kg c)
c   rkc = thermal conductivity of the insulation (kcal/h m c)
c   roc = density of the insulation (kg/h m c)
c   cc  = specific heat of the insulation (kcal/kg c)
c   EPSF = porosity of the bed
c   q   = mass flow rate of air (kg/h)
c   ro  = inner radius of the bed (radius of the channel) (m)
c   roo = outer radius of the bed
c   --------------------------------------------------
      dimension at(121),bt(121),ct(121),dt(121),temp(121),fo(121)
      dimension r(121),rk(121),zz(121)
      open(38,FILE='MINA1')
      open(9,FILE='MINA2')
      read(38,*) ao,a1,a2,a3,a4,a5,bo,b1,b2,b3,b4,b5,ta,rou,cp
     &,rkc,roc,cc,EPSF,q
      ro=.006
      roo=.03
      k=31
      n=121
      dr=(roo-ro)/(k-1.0)
      tau=.001
      do 9 i=1,n
      r(i)=ro+(i-1)*dr
9     continue
      ra1=r(k-1)+0.5*dr
      ra2=r(k+1)-0.5*dr
c   solution of the finit difference equtions
      do 3 j=1,10000
      time=j*tau*60
      ss=j
      sf=ss/100
      l=j/100
      sr=sf-l
      if(j.eq.1) go to 63
      templ=temp(n)
c   calculation of the mean temperature of the hot stream of air from the
```

```
c   experimental data
      tg=ao1+a1*time-a2*time**2.0+a3*time**3.0-a4*time**4.0+a5*time**5.0
92    do 5 i=1,n
      if(i.eq.1) go to 33
      if(i.eq.k) go to 66
      if(i.gt.k) go to 55
      fo(i)=(rk(i)*tau)/((rou*cp)*(dr**2.0))
      zz(i)=(rk(i+1)-rk(i-1))*tau/(4.0*(dr**2.0)*rou*cp)
      ct(i)=-.5*fo(i)
      at(i)=fo(i)+1.0
      bt(i)=-.5*fo(i)
      dt(i)=(.5*fo(i)-(.5*fo(i))*(dr/r(i))-zz(i))*temp(i-1)
     &+(1.0-fo(i))*temp(i)
     &+((+.5*fo(i))*(dr/r(i))+.5*fo(i)+zz(i))*temp(i+1)
      go to 5
33    fo(i)=rk(i)*tau/((dr**2.0)*rou*cp)
      zz(i)=(rk(i+1)-rk(i))*tau/(2.0*(dr**2.0)*rou*cp)
      Bi=hg*dr/rk(i)
      ct(i)=0.0
      at(i)=1.0+fo(i)+Bi*fo(i)
      bt(i)= -1.0*fo(i)
      dt(i)=(1.0-fo(i)-Bi*fo(i)+(Bi*fo(i))*(dr/r(i)))
     &+2.0*Bi*zz(i))*temp(i)+(2.0*Bi*fo(i)+(-Bi*fo(i))
     &*(dr/r(i))-2.0*Bi*zz(i))*tg+fo(i)*temp(i+1)
      go to 5
66    rcv=(ra1*rou*cp+ra2*roc*cc)/(2*r(i))
      fo(i)=(rk(i)*tau)/(rcv*dr**2.0)
      zz(i)=(rk(i+1)-rk(i-1))*tau/(2.0*(dr**2.0)*rcv)
      ct(i)=-.5*fo(i)
      at(i)=fo(i)+1.0
      bt(i)=-.5*fo(i)
      dt(i)=(.5*fo(i)-.5*fo(i)*(dr/r(i))-zz(i))*temp(i-1)
     &+(1.0-fo(i))*temp(i)
     &+(.5*fo(i)+.5*fo(i)*(dr/r(i))+zz(i))*temp(i+1)
      go to 5
55    if(i.eq.n) go to 44
      fo(i)=rk(i)*tau/((dr**2.0)*roc*cc)
      ct(i)=-.5*fo(i)
      at(i)=fo(i)+1.0
      bt(i)=-.5*fo(i)
      dt(i)=(.5*fo(i)-.5*fo(i)*(dr/r(i)))*temp(i-1)
     &+(1.0-fo(i))*temp(i)
     &+(.5*fo(i)+.5*fo(i)*(dr/r(i)))*temp(i+1)
      go to 5
44    fo(i)=rk(i)*tau/((dr**2.0)*roc*cc)
      Bi=h*dr/rk(i)
      ct(i)=-1*fo(i)*(.5)
      at(i)=(1/2)+fo(i)*.5+Bi*fo(i)*.5
```

```
      bt(i)=0.0
      dt(i)=fo(i)*(.5)*temp(i-1)
     &+((1/2)-(.5)*fo(i)-Bi*fo(i)*(.5)-Bi*(0.5*fo(i))*(dr/r(i)))
     &*temp(i)
     &+((fo(i)*.5*Bi)+Bi*(fo(i)/2.0)*(dr/r(i))+Bi*fo(i)*(.5))*ta
5     continue
      call thomas (at,bt,ct,dt,temp,n)
      go to 8
c     Initial conditions
63    do 21 i=1,n
      temp(i)=ta
21    continue
      tg=ta
      temp1=temp(n)
c     Calculation of the thermal conductivity at the different radii
8     do 27 i=1,n
      if(i.gt.k)go to 34
      if(i.lt.k)go to 35
      if(i.eq.k)go to 36
34    rk(i)=rkc
      go to 27
35    rk(i)=((0.65)**(1.0-EPSF))*(.024**EPSF)
      go to 27
36    rk(i)=0.0
27    continue
      ds(k)=rk(k)+((ra1*rk(k-1)+ra2*rk(k+1))/(2.0*r(k)))
c     calculation of the convective heat transfer coefficient (h) at
c     the outer surface of the insulation
      tempm=(temp1+temp(n))/2.0
      tm=(tempm+ta)/2.0
      rx=tempm-ta
      rka=0.20670349E-01+0.90727888E-04*tm-0.51470522E-06*tm**2.0
     &+0.30219847E-08*tm**3.0
      v=0.47762390E-01+0.31292057E-03*tm+0.48599242E-06*tm**2.0
      pr=.7
      if(rx.lt.0)go to 51
      gr=(9.81*(3600**2.0))*(tempm-ta)*(.18**3.0)
     &/((tm+273)*(v**2.0))
      go to 52
51    gr=0.0
52     ra=gr*pr
      if(ra.gt.2.0E+07)go to 42
      rn1=.54*((ra)**.25)
      rn2=.27*((ra)**.25)
      go to 43
42    rn1=.135*(ra**.25)
      rn2=.27*(ra**.25)
43    h=((3*rn1+rn2)*rka/4.0)*7.0/(22*2.0*r(n))
```

```
c     calculation of the convective heat transfer coefficient (hg)
c     at the channel surface
22    t1=(tg+temp(1))/2
      if(t1.gt.90.0)go to 23
      pka=-0.53062148E-01+0.40799766E-02*t1-0.67647692E-04*t1**2.0
     &+0.35930429E-06*t1**3.0
      v1=0.62262084E-01+0.13870765E-03*t1+0.88462286E-06*t1**2.0
     &-0.62456973E-08*t1**3.0
      go to 24
23    pka=0.21593280E-01+0.57795198E-04*t1+0.16187775E-07*t1**2.0
      v1=0.59344769E-01+0.22031754E-03*t1-0.24555476E-06*t1**2.0
c     pr=0.70670944E+00-0.23322942E-03*t1+0.49920823E-06*t1**2.0
24    if(temp(1).gt.90)go to 71
      vs=0.62262084E-01+0.13870765E-03*temp(1)
     &+0.88462286E-06*temp(1)**2.0-0.62456973E-08*temp(1)**3.0
      go to 72
71    vs=0.59344769E-01+0.22031754E-03*temp(1)
     &-0.24555476E-06*temp(1)**2.0
72    re=(7*q)/(11*ro*v1)
      hg=1.86*(pka/(2*ro))*((2*re*pr*ro/.12)**.33)*((v1/vs)**.14)
      if(j.eq.1) go to 83
      if(sr.gt.0.0)go to 3
83    write(9,*)time,tg,temp(1),temp(16),temp(k)
3     continue
      stop
      end


      subroutine thomas(a,b,c,d,x,n)
      dimension a(1),b(1),c(1),d(1),x(1),q(3000),g(3000)
      wi=a(1)
      g(1)=d(1)/wi
      do 1 i=2,n
      q(i-1)=b(i-1)/wi
      wi=a(i)-c(i)*q(i-1)
1     g(i)=(d(i)-c(i)*g(i-1))/wi
      x(n)=g(n)
      do 20 i=2,n
      j=n-i+1
20    x(j)=g(j)-q(j)*x(j+1)
      return
      end
```

```
c   DISPERSION MODEL
c   TRANSIENT TEMPERATURES WITHIN CYLINDRICAL DRY GRANULAR BEDS
c   OF THE PACKED CHANNEL CONFIGURATION
c
c   This program was devloped to solve the heat conduction problem within
c   dry granular beds mentioned in chapter 4 of this thesis.
c
c   ao-a5 are the coefficients determined experimentally for
c        the mean air stream surfacetemperature
c   u    = assumed Darcean velocity (m/h)
c   rp   = diameter of the glass bead
c   ta   = ambient air temperature (c)
c   rou  = average density of the granular bed (kg/m3)
c   cp   = average specific heat of the granular bed (kcal/kg c)
c   rkc  = thermal conductivity of the insulation (kcal/h m c)
c   roc  = density of the insulation (kg/h m c)
c   cc   = specific heat of the insulation (kcal/kg c)
c   cf   = specific heat of air
c   rf   = density of air
c   rkf  = thermal conductivity of air
c   EPSF = porosity of the bed
c   q    = mass flow rate of air (kg/h)
c   ro   = inner radius of the bed (radius of the channel) (m)
c   roo  = outer radius of the bed
c   -----------------------------------------------------
c   -----------------------------------------------------
      dimension at(121),bt(121),ct(121),dt(121),temp(121),fo(121)
      dimension r(121),ds(121),pe(121),xt(121),rk(121)
      dimension zz(121)
      open(38,FILE='trall')
      open(9,FILE='mfaiklrl')
      read(38,*) ta,u,rou,cp,rp,rkf,rof,cf
     &,rkc,roc,cc,EPSF,q
      ro=.006
      roo=.03
      k=31
      n=121
      dr=(roo-ro)/(k-1.0)
      tau=.001
      EPSF=0.363
      do 9 i=1,n
      r(i)=ro+(i-1)*dr
9     continue
      ra1=r(k-1)+0.5*dr
      ra2=r(k+1)-0.5*dr
c   solution of the finit difference equtions
```

```
      do 3 j=1,10000
      time=j*tau*60
      ss=j
      sf=ss/100
      l=j/100
      sr=sf-l
      if(j.eq.1) go to 63
      temp1=temp(n)
c   calculation of the surface temperature of t from the
c   Experimental Data
      t1=ao1+a1*time-a2*time**2.0+a3*time**3.0-a4*time**4.0+a5*time**5.0
92    do 5 i=1,n
      if(i.eq.1) go to 33
      if(i.eq.k) go to 66
      if(i.gt.k) go to 55
      B=rof*cf*u*ro*tau/((2.0*rou*cp)*(dr**2.0))
      fo(i)=(ds(i)*tau)/((rou*cp)*(dr**2.0))
      zz(i)=(ds(i+1)-ds(i-1))*tau/(4.0*(dr**2.0)*rou*cp)
      ct(i)=-.5*fo(i)
      at(i)=fo(i)+1.0
      bt(i)=-.5*fo(i)
      dt(i)=(.5*fo(i)-(-1.0*B+.5*fo(i))*(dr/r(i))-zz(i))*temp(i-1)
     &+(1.0-fo(i))*temp(i)
     &+((-1.0*B+.5*fo(i))*(dr/r(i))+.5*fo(i)+zz(i))*temp(i+1)
      go to 5
33    ct(i)=0.0
      at(i)=1.0
      bt(i)=0.0
      dt(i)=t1
      go to 5
66    rcv=(ra1*rou*cp+ra2*roc*cc)/(2*r(i))
      B=rof*cf*u*ro*tau/((2.0*rcv)*(dr**2.0))
      fo(i)=(ds(i)*tau)/(rcv*dr**2.0)
      zz(i)=(ds(i+1)-ds(i-1))*tau/(2.0*(dr**2.0)*rcv)
      ct(i)=-.5*fo(i)
      at(i)=fo(i)+1.0
      bt(i)=-.5*fo(i)
      dt(i)=(.5*fo(i)-.5*fo(i)*(dr/r(i))-zz(i))*temp(i-1)
     &+(1.0-fo(i))*temp(i)
     &+(.5*fo(i)+.5*fo(i)*(dr/r(i))+zz(i))*temp(i+1)
      go to 5
55    if(i.eq.n) go to 44
      fo(i)=ds(i)*tau/((dr**2.0)*roc*cc)
      ct(i)=-.5*fo(i)
      at(i)=fo(i)+1.0
      bt(i)=-.5*fo(i)
      dt(i)=(.5*fo(i)-.5*fo(i)*(dr/r(i)))*temp(i-1)
     &+(1.0-fo(i))*temp(i)
```

```fortran
     &+(.5*fo(i)+.5*fo(i)*(dr/r(i)))*temp(i+1)
       go to 5
44     fo(i)=ds(i)*tau/((dr**2.0)*roc*cc)
       Bi=h*dr/ds(i)
       ct(i)=-1*fo(i)*(.5)
       at(i)=(1/2)+fo(i)*.5+Bi*fo(i)*.5
       bt(i)=0.0
       dt(i)=fo(i)*(.5)*temp(i-1)
     &+((1/2)-(.5)*fo(i)-Bi*fo(i)*(.5)-Bi*(0.5*fo(i))*(dr/r(i)))
     &*temp(i)
     &+((fo(i)*.5*Bi)+Bi*(fo(i)/2.0)*(dr/r(i)))+Bi*fo(i)*(.5))*ta
5      continue
       call thomas (at,bt,ct,dt,temp,n)
       go to 8
c
c      Initial conditions
63     do 21 i=1,n
       temp(i)=ta
21     continue
       t1=ta
       temp1=temp(n)
c
c      calculation of the dispersion component ( D* cf*rf)
8      do 27 i=1,n
       if(i.gt.k)go to 34
       if(i.lt.k)go to 35
       if(i.eq.k)go to 36
34     rk(i)=rkc
       ds(i)=rk(i)
       go to 27
35     if(u.eq.0)go to 38
       rk(i)=aa*temp(i)+bb
       pe(i)=u*ro*rp*rof*cf/(rkf*r(i))
       xt(i)=.75*pe(i)+(1/6)*((22/7)**2.0)*(1.0-rE)*pe(i)*log(pe(i))
       ds(i)=rk(i)+rE*rkf*xt(i)
       go to 27
38     rk(i)=((0.65)**(1.0-EPSF))*(.024**EPSF)
       ds(i)=rk(i)
       go to 27
36     rk(i)=0.0
       ds(i)=0.0
27     continue
       ds(k)=ds(k)+((ra1*ds(k-1)+ra2*ds(k+1))/(2.0*r(k)))
c
c      calculation of the convective heat transfer coefficient (h) at
c      the outer surface of the insulation
       tempm=(temp1+temp(n))/2.0
       tm=(tempm+ta)/2.0

       rx=tempm-ta
       rka=0.20670349E-01+0.90727888E-04*tm-0.51470522E-06*tm**2.0
     &+0.30219847E-08*tm**3.0
       v=0.47762390E-01+0.31292057E-03*tm+0.48599242E-06*tm**2.0
c      pr=0.70721436-0.22792489E-03*tm+0.72370256E-06*tm**2.0
       pr=.7
       if(rx.lt.0)go to 51
       gr=(9.81*(3600**2.0))*(tempm-ta)*(.18**3.0)
     &/((tm+273)*(v**2.0))
       go to 52
51     gr=0.0
52     ra=gr*pr
       if(ra.gt.2.0E+07)go to 42
       rn1=.54*((ra)**.25)
       rn2=.27*((ra)**.25)
       go to 43
42     rn1=.135*(ra**.25)
       rn2=.27*(ra**.25)
43     h=((3*rn1+rn2)*rka/4.0)*7.0/(22*2.0*r(n))
       if(j.eq.1) go to 83
       if(sr.gt.0.0)go to 3
83     write(9,53)time,temp(1),temp(16)
53     format(F6.2,1x,F6.2,1x,F6.2)
3      continue
       stop
       end

       subroutine thomas(a,b,c,d,x,n)
       dimension a(1),b(1),c(1),d(1),x(1),q(3000),g(3000)
       wi=a(1)
       g(1)=d(1)/wi
       do 1 i=2,n
       q(i-1)=b(i-1)/wi
       wi=a(i)-c(i)*q(i-1)
1      g(i)=(d(i)-c(i)*g(i-1))/wi
       x(n)=g(n)
       do 20 i=2,n
       j=n-i+1
20     x(j)=g(j)-q(j)*x(j+1)
       return
       end
```

```
c   DRYING MODEL
c   TRANSIENT TEMPERATURES WITHIN CYLINDRICAL WET GRANULAR BEDS
OF        THE OPEN CHANNEL CONFIGURATION
c
c     This program was devloped to solve the heat and mass transfer
c     problem withind wet granular beds mentioned in chapter 4
c     of this thesis.
c
c     ao-a5   are the coefficients determined experimentally for
c             the mean air stream temperature
c     ta  = ambient air temperature (c)
c     rkc = thermal conductivity of the insulation (kcal/h m c)
c     roc = density of the insulation (kg/h m c)
c     cc  = specific heat of the insulation (kcal/kg c)
c     EPSF = porosity of the bed
c     EPSO = initial volume fraction of air (Va/V)
c     q    = mass flow rate of air (kg/h)
c     ro   = inner radius of the bed (radius of the channel) (m)
c     roo  = outer radius of the bed
c     --------------------------------------------------
      dimension at(201),bt(201),ct(201),dt(201),temp(201),fo(201)
      dimension r(201),ds(201),pvg(51),rvg(51),qv(51),tempf(51)
      dimension EPSG(51),EPSG1(51),dm(51),EVAP(51),zz(51),CONV(51)
      dimension rvg1(51),rgg(51),tempk(51),rgg1(51),SAT(51)
      dimension deff(51),ar(51),tgr(51),rcp(51),rcp1(51),CR(51)
      dimension dp(51),VAP(51)
      open(38,FILE='MINA')
      open(9,FILE='CYRIL')
      open(40,FILE='CYRIL1 ')
      open(41,FILE='CYRIL2')
      open(42,FILE='CYRIL3')
      open(43,FILE='CYRIL4')
      open(10,FILE='MARK1')
      open(11,FILE='MARK2')
      open(12,FILE='MARK3')
      open(13,FILE='MARK4')
      open(14,FILE='MARK5')
      open(15,FILE='MARK6')
      open(16,FILE='MARK7')
      open(17,FILE='MARK8')
      open(18,FilE='MARK9')
      open(19,FilE='MARK10')
      open(20,FilE='MARK11')
      open(21,FilE='MARK12')
      open(22,FilE='MARK13')
      rewind(9)
      rewind(10)
      rewind(11)
      rewind(12)
      rewind(13)
      rewind(14)
      rewind(15)
      rewind(16)
      rewind(17)
      rewind(18)
      rewind(19)
      rewind(20)
      rewind(21)
      rewind(22)
      rewind(40)
      rewind(41)
      rewind(42)
      rewind(43)
      read(38,*),ta,EPSO,EPSF,rkc,roc,cc,q
      ro=.006
      roo=.03
      k=51
      n=201
      dr=(roo-ro)/(k-1.0)
      tau=.000001
      do 9 i=1,n
      r(i)=ro+(i-1)*dr
9     continue
      ra1=r(k-1)+0.5*dr
      ra2=r(k+1)-0.5*dr
      Rv=461.52
      pgg=101300.0
      rMa=28.97
      rMv=18.015
      ROUL=980.0
      cpv=.477
      do 3 j=1,10000000
      time=j*tau*60.0
      ss=j
      sf=ss/83333
      l=j/83333
      sr=sf-l
c     calculation of the mean temperature of the hot stream of air from the
c     experimental data
      tg=ao1+a1*time-a2*time**2.0+a3*time**3.0-a4*time**4.0+a5*time**5.0
123   if(j.eq.1) go to 63
      temp1=temp(n)
c     Calculation of the latent heat of vaporization and vapour
c     partial pressure
      do 12 i=1,k
```

```
        VAP(i)=2504806.0-2457.059*tempk(i)
        pvg(i)=638.39+40.888*tempk(i)+(1.5924*(tempk(i))**2.0)
        &+(0.023538*(tempk(i))**3.0)+(0.00030608*(tempk(i))**4.0)
        &+(2.6552e-06*(tempk(i))**5.0)
12      continue
c       Calculation of the effective mass diffusivity at various radii
        do 540 i=1,k
        ar(i)=(tempk(i)+273.0)/(262.0)
        tgr(i)=((1.06036/(ar(i)**.1561))+(.19300/exp(.47635*ar(i)))
        &+(1.03587/exp(1.52996*ar(i)))
        &+(1.76474/exp(3.89411*ar(i))))
        deff(i)=(5.68973E-09*((273.0+tempk(i))**1.5)/tgr(i))
        &*(2.0*EPSF/(3.0-EPSF))*(1.0-SAT(i))
540     continue
c       Calculation of the partial vapor density and total density
        do 635 i=1,k
        if(EPSG1(i).GE.EPSF)go to 631
        go to 638
631     if(i.EQ.1)go to 633
        rvg(i)=rvg1(i)-tau*3600.0*(r(i+1)*qv(i+1)-r(i-1)*qv(i-1))/
        &(EPSF*r(i)*2.0*dr)
        go to 636
633     rvg(i)=rvg1(i)-tau*3600.0*(r(i+1)*qv(i+1)-r(i)*qv(i))/
        &(EPSF*r(i)*dr)
        go to 636
638     rvg(i)=pvg(i)/(Rv*(273.0+tempk(i)))
636     rgg(i)=pgg*rMa/(8314.0*(tempk(i)+273.0))+rvg(i)*(1.0-rMa/rMv)
635     continue
c       calculation of the vapour flux (density * velocity)
        qv(1)=-1*BETA*rvg(1)
        qv(k)=0
        do 14 i=2,k-1
        qv(i)=-1*deff(i)*((rgg(i)**2.0)/(rgg(i)-rvg(i)))*
        &((rvg(i+1)/rgg(i+1))-(rvg(i-1)/rgg(i-1)))/(2.0*dr)
14      continue
c       Calculation of the volume fraction of gaseous phase
        EPSG(1)=EPSG1(1)*((ROUL-rvg1(1))/(ROUL-rvg(1)))
        &+tau*3600.0*(r(2)*qv(2)-r(1)*qv(1))/(dr*r(1)
        &*(ROUL-rvg(1)))
        EPSG(k)=EPSG1(k)*((ROUL-rvg1(k))/(ROUL-rvg(k)))
        &+tau*3600*(r(k)*qv(k)-r(k-1)*qv(k-1))/(dr*r(k)
        &*(ROUL-rvg(k)))
        do 79 i=2,k-1
        EPSG(i)=EPSG1(i)*((ROUL-rvg1(i))/(ROUL-rvg(i)))
        &+tau*1800.0*(r(i+1)*qv(i+1)-r(i-1)*qv(i-1))/(dr*r(i)
        &*(ROUL-rvg(i)))
79      continue
        do 97 i=1,k
```

```
        if(EPSG1(i).GE.EPSF) go to 100
        go to 97
100     EPSG(i)=EPSF
        EPSG1(i)=EPSG(i)
97      continue
c       Calculation of the ( density * specific heat) of the bed
c       at the various radii
        do 745 i=1,k
        rcp(i)=(EPSF-EPSG(i))*ROUL+EPSG(i)*(rvg(i)*.447
        &+(rgg(i)-rvg(i))*.24)+(1.0-EPSF)*2450.0*.2
745     continue
        rcp(k)=(ra1*rcp(k-1)+ra2*roc*cc)/(2.0*r(k))
c       Calculation of the mass rate of evaporation per unit volume
c       at the various radii
        do 73 i=1,k
        dm(i)=ROUL*(EPSG(i)-EPSG1(i))/tau
73      continue
        if(EPSG1(k).GE.EPSF)go to 811
815     do 74 i=1,k
        CONV(i)=qv(i)*cpv*tau*3600.0/(2.0*dr)
        EVAP(i)=dm(i)*(VAP(i)*239E-06+0.5*tempk(i))*tau
74      continue
        go to 92
811     do 812 i=1,k
        qv(i)=0.0
        CONV(i)=0.0
        EVAP(i)=0.0
        rcp(i)=1560.0*.2
        rcp1(i)=1560.0*.2
812     continue
92      do 5 i=1,n
        COND=tau/(2*dr)
        if(i.eq.1) go to 33
        if(i.eq.k) go to 66
        if(i.gt.k) go to 55
        fo(i)=(ds(i)*tau)/(dr**2.0)
        zz(i)=(ds(i+1)-ds(i-1))/(2.0*dr)
        ct(i)=-.5*fo(i)
        at(i)=fo(i)+rcp(i)
        bt(i)=-.5*fo(i)
        dt(i)=(.5*fo(i)-.5*fo(i)*dr/r(i)+CONV(i)-COND*zz(i))
        &*temp(i-1)+(rcp1(i)-fo(i)-CR(i))*temp(i)
        &+(-1.0*CONV(i)+.5*fo(i)*(dr/r(i))+.5*fo(i)+COND*zz(i))
        &*temp(i+1)-EVAP(i)
        go to 5
33      fo(i)=ds(i)*tau/(dr**2.0)
        zz(i)=(ds(i+1)-ds(i))/dr
        Bi=hg*dr/ds(i)
```

```
      ct(i)=0.0
      at(i)=rcp(i)*fo(i)+Bi*fo(i)
      bt(i)=-1.0*fo(i)
      dt(i)=(rcp1(i)-fo(i)-Bi*fo(i)+Bi*fo(i)*(dr/r(i))+
     &2.0*Bi*COND*zz(i)-2.0*Bi*CONV(i)-CR(i))*temp(i)-EVAP(i)
     &+(2.0*Bi*fo(i)-Bi*fo(i)*(dr/r(i))+2.0*Bi*CONV(i)-2.0*Bi
     &*COND*zz(i))*tg+fo(i)*temp(i+1)
      go to 5
66    fo(i)=(ds(i)*tau)/(dr**2.0)
      zz(i)=(ds(i+1)-dsm)/(dr)
      ct(i)=-.5*fo(i)
      at(i)=fo(i)+rcp(i)
      bt(i)=-.5*fo(i)
      dt(i)=(.5*fo(i)-.5*fo(i)*(dr/r(i))-COND*zz(i))*temp(i-1)
     &+(rcp1(i)-fo(i)))*temp(i)-EVAP(i)
     &+(.5*fo(i)+.5*fo(i)*(dr/r(i))+COND*zz(i))*temp(i+1)
      go to 5
55    if(i.eq.n) go to 44
      fo(i)=ds(i)*tau/((dr**2.0)*roc*cc)
      ct(i)=-.5*fo(i)
      at(i)=fo(i)+1.0
      bt(i)=-.5*fo(i)
      dt(i)=(.5*fo(i)-.5*fo(i)*(dr/r(i)))*temp(i-1)
     &+(1.0-fo(i))*temp(i)
     &+(.5*fo(i)+.5*fo(i)*(dr/r(i)))*temp(i+1)
      go to 5
44    fo(i)=ds(i)*tau/((dr**2.0)*roc*cc)
      Bi=h*dr/ds(i)
      ct(i)=-1*fo(i)*(.5)
      at(i)=(.5)+fo(i)*.5+Bi*fo(i)*.5
      bt(i)=0.0
      dt(i)=fo(i)*(.5)*temp(i-1)
     &+((.5)-(.5)*fo(i)-Bi*fo(i)*(.5)-Bi*(0.5*fo(i))*(dr/r(i)))
     &*temp(i)
     &+((fo(i)*.5*Bi)+Bi*(fo(i)/2.0)*(dr/r(i))+Bi*fo(i)*(.5))*ta
5     continue
      call thomas (at,bt,ct,dt,temp,n)
      go to 8
c     Initial conditions
63    do 21 i=1,k
      EPSG(i)=EPSO
      tempf(i)=ta
      tempk(i)=ta
21    continue
      do 199 i=1,n
      temp(i)=ta
199   continue
      do 99 i=1,k
      VAP(i)=2504806.0-2457.059*tempk(i)
      pvg(i)=638.39+40.888*tempk(i)+(1.5924*(tempk(i))**2.0)
     &+(0.023538*(tempk(i))**3.0)+(0.00030608*(tempk(i))**4.0)
     &+(2.6552e-06*(tempk(i))**5.0)
      rvg(i)=pvg(i)/(Rv*(273.0+tempk(i)))
      rgg(i)=pgg*rMa/(8314.0*(tempk(i)+273.0))+rvg(i)*(1.0-rMa/rMv)
99    continue
      temp1=temp(n)
      dmt=0.0
      do 432 i=1,k-1
      rcp(i)=(EPSF-EPSG(i))*ROUL+EPSG(i)*(rvg(i)*.447
     &+(rgg(i)-rvg(i))*.24)+(1.0-EPSF)*2450.0*.2
432   continue
      rcp(k)=(ra1*rcp(k-1)+ra2*roc*cc)/(2.0*r(k))
8     do 28 i=1,k
      EPSG1(i)=EPSG(i)
      rvg1(i)=rvg(i)
      rgg1(i)=rgg(i)
      rcp1(i)=rcp(i)
28    continue
      do 107 i=1,k
      tempk(i)=(tempf(i)+temp(i))/2
107   continue
      do 108 i=1,k
      tempf(i)=temp(i)
108   continue
c     Calculation of the thermal conductivity
      do 27 i=1,n
      if(i.gt.k)go to 34
      if(i.le.k)go to 35
c     if(i.eq.k)go to 36
34    ds(i)=rkc
      go to 27
35    SAT(i)=abs((EPSF-EPSG(i))/EPSF)
      ds(i)=((0.65)**(1.0-EPSF))*((0.55)**(EPSF-EPSG(i)))
     &*(.024**(EPSG(i)))
c35   ds(i)=EPSG(i)*0.024+(EPSF-EPSG(i))*0.55+0.65*(1.0-EPSF)
27    continue
      dsm=(ds(k)+ds(k-1))/2.0
      ds(k)=((ra1*dsm+ra2*ds(k+1))/(2.0*r(k)))
c     Calculation of the convective heat  and mass transfer
c     coefficients
      tempm=(temp1+temp(n))/2.0
      tm=(tempm+ta)/2.0
      rx=tempm-ta
      rka=0.20670349E-01+0.90727888E-04*tm-0.51470522E-06*tm**2.0
     &+0.30219847E-08*tm**3.0
      v=0.47762390E-01+0.31292057E-03*tm+0.48599242E-06*tm**2.0
```

```fortran
c     pr=0.70721436-0.22792489E-03*tm+0.72370256E-06*tm**2.0
      pr=.7
      if(rx.lt.0)go to 51
      gr=(9.81*(3600**2.0))*(tempm-ta)*(.18**3.0)
     &/((tm+273)*(v**2.0))
      go to 52
51    gr=0.0
52    ra=gr*pr
      if(ra.gt.2.0E+07)go to 42
      rn1=.54*((ra)**.25)
      rn2=.27*((ra)**.25)
      go to 43
42    rn1=.135*(ra**.25)
      rn2=.27*(ra**.25)
43    h=((3*rn1+rn2)*rka/4.0)*7.0/(22.0*2.0*r(n))
22    t1=(tg+temp(1))/2.0
      if(t1.gt.90.0)go to 23
      pka=-0.53062148E-01+0.40799766E-02*t1-0.67647692E-04*t1**2.0
     &+0.35930429E-06*t1**3.0
      v1=0.62262084E-01+0.13870765E-03*t1+0.88462286E-06*t1**2.0
     &-0.62456973E-08*t1**3.0
c     pr=0.70731604E+00-0.24950225E-03*t1+0.17305322E-05*t1**2.0
c     &-0.12299538E-07*t1**3.0
      go to 24
23    pka=0.21593280E-01+0.57795198E-04*t1+0.16187775E-07*t1**2.0
      v1=0.59344769E-01+0.22031754E-03*t1-0.24555476E-06*t1**2.0
c     pr=0.70670944E+00-0.23322942E-03*t1+0.49920823E-06*t1**2.0
24    if(temp(1).gt.90)go to 71
      vs=0.62262084E-01+0.13870765E-03*temp(1)
     &+0.88462286E-06*temp(1)**2.0-0.62456973E-08*temp(1)**3.0
      go to 72
71    vs=0.59344769E-01+0.22031754E-03*temp(1)
     &-0.24555476E-06*temp(1)**2.0
72    re=(7*q)/(11*ro*v1)
      hg=1.86*(pka/(2*ro))*((2*re*pr*ro/.12)**.33)*((v1/vs)**.14)
c     &*(1.074)**(re/1000)
      BETA=1.86*(deff(1)/(2*ro))*((2*re*.6*ro/.12)**.33)
     &*((v1/vs)**.14)
      dmt=dmt+abs(qv(1))*tau*3600.0
      if(j.eq.1) go to 83
      if(sr.gt.0.0)go to 3
      if(sr.eq.0.0)go to 83
83    write(9,*)time,tg,temp(1),temp(26),dmt
      write(40,*)time,temp(1),temp(5),temp(8),temp(11)
      write(41,*)time,temp(14),temp(17),temp(20),temp(23)
      write(42,*)time,temp(26),temp(29),temp(32),temp(35)
      write(43,*)time,temp(38),temp(41),temp(44),temp(47),temp(50)
      write(10,*)time,SAT(1),SAT(2),SAT(3),SAT(4)
      write(11,*)time,SAT(5),SAT(6),SAT(7),SAT(8)
      write(12,*)time,SAT(9),SAT(10),SAT(11),SAT(12)
      write(13,*)time,SAT(13),SAT(14),SAT(15),SAT(16)
      write(14,*)time,SAT(17),SAT(18),SAT(19),SAT(20)
      write(15,*)time,SAT(21),SAT(22),SAT(23),SAT(24)
      write(16,*)time,SAT(25),SAT(26),SAT(27),SAT(28)
      write(17,*)time,SAT(29),SAT(30),SAT(31),SAT(32)
      write(18,*)time,SAT(33),SAT(34),SAT(35),SAT(36)
      write(19,*)time,SAT(37),SAT(38),SAT(39),SAT(40)
      write(20,*)time,SAT(41),SAT(42),SAT(43),SAT(44)
      write(21,*)time,SAT(45),SAT(46),SAT(47),SAT(48)
      write(22,*)time,SAT(49),SAT(50),SAT(51),temp(201)
3     continue
      close(38)
      close(9)
      close(10)
      close(11)
      close(12)
      close(13)
      close(14)
      close(15)
      close(16)
      close(17)
      close(18)
      close(19)
      close(20)
      close(21)
      close(22)
      close(40)
      close(41)
      close(42)
      stop
      end

      subroutine thomas(a,b,c,d,x,n)
      dimension a(1),b(1),c(1),d(1),x(1),q(3000),g(3000)
      wi=a(1)
      g(1)=d(1)/wi
      do 1 i=2,n
      q(i-1)=b(i-1)/wi
      wi=a(i)-c(i)*q(i-1)
1     g(i)=(d(i)-c(i)*g(i-1))/wi
      x(n)=g(n)
      do 20 i=2,n
      j=n-i+1
20    x(j)=g(j)-q(j)*x(j+1)
      return
      end
```